

Hycal
ENERGY RESEARCH LABORATORIES LTD.

EXTRA COPY

**PARAMOUNT RESOURCES LTD.
CAMERON HILLS KEG RIVER
NUMERICAL SIMULATION STUDY**

9211-P33-4-2

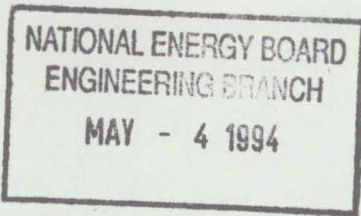
Prepared for

Paramount Resources Ltd.

Prepared by

Hycal Energy Research Laboratories Ltd.

April 12, 1994



93-044

TABLE OF CONTENTS

	Page
TABLE OF CONTENTS	i
LIST OF TABLES	iii
LIST OF FIGURES	iv
INTRODUCTION	1
GEOLOGICAL MODEL	4
NUMERICAL SIMULATOR	6
SIMULATOR INPUT	10
FLUID PROPERTIES	11
ROCK PROPERTIES	12
HISTORY MATCH	13
PREDICTIONS	15
Run 1	15
Run 2	15
Run 3	15
Run 4	16
Run 5	16
Run 6	16
Run 7	16
Run 8	17
Run 9	17
Run 10	17
Run 11	17
Run 12	18
Run 13	18
COMPARISON OF RUNS	19
Run 1 and Run 3	19
Run 2 and Run 4	19
Run 1 and Run 2	19
Run 3 and Run 4	19

TABLE OF CONTENTS (cont'd)

Run 2 and Run 5	19
Run 6 and Run 7	21
Run 8 and Run 9	21
Run 10 and Run 11	23
Run 11 and Run 12	23
Run 6 and Run 13	24
 PREDICTION LIMITATIONS	26
 CONCLUSIONS	28

LIST OF TABLES

TABLE	1:	Prediction No. 1
TABLE	2:	Prediction No. 2
TABLE	3:	Prediction No. 3
TABLE	4:	Prediction No. 4
TABLE	5:	Prediction No. 5
TABLE	6:	Prediction No. 6
TABLE	7:	Prediction No. 7
TABLE	8:	Prediction No. 8
TABLE	9:	Prediction No. 9
TABLE	10:	HOR 1 Results
TABLE	11:	HOR 2 Results
TABLE	12:	HOR 3 Results
TABLE	13:	Vertical Well With Connected Aquifer

LIST OF FIGURES

FIGURE 1: Well L47 Porosity vs Depth - Metres

FIGURE 2: PVT Properties - Oil Formation Volume Factor

FIGURE 3: PVT Properties - Solution Gas-Oil Ratio

FIGURE 4: PVT Properties - Gas Compressibility Factor

FIGURE 5: PVT Properties - Oil Viscosity

FIGURE 6: PVT Properties - Gas Viscosity

FIGURE 7: Matrix Relative Permeability vs Water Saturation

FIGURE 8: Matrix Relative Capillary Pressure vs Water Saturation

FIGURE 9: Matrix Relative Permeability vs Gas Saturation

FIGURE 10: Fracture Relative Permeability vs Water Saturation

FIGURE 11: Fracture Relative Capillary Pressure vs Water Saturation

FIGURE 12: Matrix Relative Permeability vs Gas Saturation

FIGURE 13: History Match GOR

FIGURE 14: History Match Water Cut

FIGURE 15: Matrix Pressure - 28 Days

FIGURE 16: Fracture Pressure - 28 Days

FIGURE 17: Matrix Gas Saturation - 28 Days

FIGURE 18: Fracture Gas Saturation - 28 Days

FIGURE 19: Matrix Water Saturation - 28 Days

FIGURE 20: Fracture Water Saturation - 28 Days

FIGURE 21: Fracture Water Saturation - 46 Days

LIST OF FIGURES (Cont'd)

FIGURE 22: Fracture Water Saturation - 127 Days

FIGURE 23: Fracture Water Saturation - 410 Days

FIGURE 24: Fracture Water Saturation - 866 Days

FIGURE 25: Fracture Water Saturation - 1067 Days

FIGURE 26: Comparison of Oil Rates vs Cuml Oil

FIGURE 27: Comparison of Oil Rates vs Time - Days

FIGURE 28: Comparison of Producing Gas-Oil Ratios vs Cuml Oil

FIGURE 29: Comparison of Producing Gas-Oil Ratios vs Time - Days

FIGURE 30: Comparison of Water Cut vs Cuml Oil

FIGURE 31: Comparison of Water Cut vs Time - Days

FIGURE 32: Comparison of Cumulative Oil vs Time - Days

FIGURE 33: Comparison of Oil Rates vs Time - Days

FIGURE 34: Comparison of Cuml Oil Rates vs Time - Days

FIGURE 35: Comparison of Oil Rates - Prediction 6 and 7

FIGURE 36: Comparison of Producing Gas Oil Ratios - Predictions 6 and 7

FIGURE 37: Comparison of Water Cuts - Predictions 6 and 7

FIGURE 38: Comparisons of Cumulative Oil - Predictions 6 and 7

FIGURE 39: Comparisons of Cumulative Oil - Predictions 8 and 9

FIGURE 40: Water Saturation Fracture - Prediction 9 - 0 Days

FIGURE 41: Water Saturation Matrix - Prediction 9 - 0 Days

FIGURE 42: Gas Saturation Fracture - Prediction 9 - 0 Days

LIST OF FIGURES (Cont'd)

FIGURE 43: Gas Saturation Matrix - Prediction 9 - 0 Days

FIGURE 44: Water Saturation Fracture - Prediction 9 - 90 Days

FIGURE 45: Water Saturation Matrix - Prediction 9 - 90 Days

FIGURE 46: Gas Saturation Fracture - Prediction 9 - 90 Days

FIGURE 47: Gas Saturation Matrix - Prediction 9 - 90 Days

FIGURE 48: Water Saturation Fracture - Prediction 9 - 365 Days

FIGURE 49: Water Saturation Matrix - Prediction 9 - 365 Days

FIGURE 50: Gas Saturation Fracture - Prediction 9 - 365 Days

FIGURE 51: Gas Saturation Matrix - Prediction 9 - 365 Days

FIGURE 52: Water Saturation Matrix - Prediction 9 - 853 Days

FIGURE 53: Gas Saturation Matrix - Prediction 9 - 853 Days

FIGURE 54: Gas Saturation Fracture - Prediction 9 - 853 Days

FIGURE 55: Gas Saturation Matrix - Prediction 9 - 1492 Days

FIGURE 56: Comparison of Cumulative Oil - HOR 1 and 2

FIGURE 57: Comparison of Cumulative Oil - HOR 2 and 3

FIGURE 58: Comparison of Producing Gas Oil Ratios - HOR 2 and 3

FIGURE 59: Comparison of Water Cut - HOR 2 and 3

FIGURE 60: Water Saturation Fracture - HOR2 472 Days

FIGURE 61: Water Saturation Matrix - HOR2 472 Days

FIGURE 62: Gas Saturation Fracture - HOR2 472 Days

FIGURE 63: Gas Saturation Matrix - HOR2 472 Days

LIST OF FIGURES (Cont'd)

FIGURE 64: Water Saturation Fracture - HOR3 477 Days

FIGURE 65: Water Saturation Matrix - HOR3 477 Days

FIGURE 66: Gas Saturation Fracture - HOR3 477 Days

FIGURE 67: Gas Saturation Fracture - HOR3 477 Days

FIGURE 68: Water Saturation Fracture - HOR2 729 Days

FIGURE 69: Water Saturation Matrix - HOR2 729 Days

FIGURE 70: Gas Saturation Fracture - HOR2 729 Days

FIGURE 71: Gas Saturation Matrix - HOR2 729 Days

FIGURE 72: Water Saturation Fracture - HOR3 729 Days

FIGURE 73: Water Saturation Matrix - HOR3 729 Days

FIGURE 74: Gas Saturation Fracture - HOR3 729 Days

FIGURE 75: Comparison of Oil Rates - Prediction 6 and 10

FIGURE 76: Comparison of Water Cut - HOR 3 and Prediction 10

FIGURE 77: Comparison of Oil Rates - HOR 3 and Prediction 10

INTRODUCTION

This study was requested by Paramount Resources Ltd. to evaluate the optimal method to produce well L47 in the Cameron Hills Keg River Reservoir. Paramount supplied well logs, petrophysical, petrographic, core analyses, PVT, relative permeability, capillary pressure and pressure data.

A single well numerical simulation study was conducted using the Computer Modelling Group Black Oil Simulator (IMEX). The model was used in the dual porosity, dual permeability mode. Two field production tests were conducted, one in 1990 and another in 1993. These two production tests were used to tune the simulator. Once the simulator was tuned thirteen predictive runs were made. These are tabulated below:

1. Lower set of perforations (1496.5 - 1499.0 m), open initial rate - 10 m³/day, minimum bottomhole pressure - 2500 kPa.
2. Lower set of perforations (1496.5 - 1499.0 m), open initial rate - 10 m³/day, minimum bottomhole pressure - 5000 kPa.
3. Lower and upper sets of perforation (1496.5 - 1499 m), (1487 - 1488.5 m) open; initial rate - 10 m³/day, minimum bottomhole pressure - 2500 kPa.
4. Lower and upper sets of perforations (1496.5 - 1499.0 m), (1487 - 1488.5 m) open initial rate - 10 m³/day, minimum bottomhole pressure - 5000 kPa
5. Lower perforations (1496.5 - 1499.0 m) open, initial rate - 20 m³/day, minimum bottomhole pressure - 5000 kPa.
6. Lower and upper sets of perforations (1406.5 - 1499 m), 1487 - 1488.5 m open. No restriction on rate, but there was a minimum bottomhole constraint of 2500 kPa.
7. Same as Run 6 except only the lower set of perforations were open.
8. Same as Run 6 except the well was only produced from January 1 to April 1 each year.
9. Same as Run 8 except only the lower set of perforations was open.

The next three sets of predictions were performed for the horizontal wells. They are referred to as HOR 1, HOR 2, and HOR 3. For each of these predictions a 400 x 400 m area was used. The horizontal well was drilled for a length of 400 m through this reservoir. It had exactly the same stratification as was used for the previous predictions. The horizontal well was drilled in Zone 4. The gascap thickness was increased to 2 m. Vertically there were eight layers, one layer for the gascap and layers for each of the zones.

10. On all graphs this is referred to as HOR1. It was run to test the effects of grid size, a 9 x 7 x 8 grid system was used with no aquifer.
11. On all graphs this is referred to as HOR2. It was run on a grid size of 11 x 11 x 9 to compare with Run 9. It had no aquifer.
12. This run was the same as 11 except a strong aquifer was attached to the reservoir.
13. Same as Run 6 except an active aquifer was attached to the reservoir.

Runs 1 and 2 were to compare the effects of producing the well at a low initial rate and varying the minimum bottomhole pressure to determine if the lower rates would affect water and gas coning.

Runs 3 and 4 were run at the same low rates and bottom hole pressures but the higher set of perforations were included. Run 5 was made to study the effects of a higher initial rate and a minimum bottomhole pressure of 5000 kPa. This run can be compared with run 2.

Runs 6 and 7 were made to compare perforation interval. The only difference between the two runs was the zone perforated.

Runs 8 and 9 were made to compare perforation interval and cyclic production.

Runs 10, 11 and 12 were made to compare the effects of grid size, oil and active aquifer.

Run 13 was made to compare the effects of adding an active aquifer on a vertical well and to compare it with Run 12, a horizontal well with an active aquifer.

The report gives a description of the geological model used, the history matching, numerical simulation and predictions. Conclusions, recommendations and results of the predictions are also discussed.

GEOLOGICAL MODEL

GEOLOGICAL MODEL

Paramount supplied only a brief description of the geology of the Cameron Hills pool. This is reproduced here. The pool consists of cycles of open marine platform deposits shallowing upward to peritidal mudstones and packstones. Dolomitization obliterates a significant amount of the original depositional fabric. Reservoir quality appears to be controlled by depositional/diagenetic facies, ie., high energy mudstones are of excellent reservoir quality while peritidal mudstones are virtually impermeable. Porosity types include moldic vuggy, intercrystalline, and fracture porosity. Excellent leached fossil vuggy porosity occurs in high energy depositional facies. Minor intercrystalline and fracture porosity enhances the reservoir in these zones. Dolomitic peritidal mudstone and packstone facies exhibit minor intercrystalline porosity. Permeability and storage capacity are controlled by solution-enlarged fractures which are often vertically oriented. There are at least three basic rock facies: a) micritic mudstone and packstone, b) coral and stroma topographic rudstone, and c) open marine floatstones.

The micritic mudstones with packstone laminations are comprised of a very tight network of anhedral replacement dolomite cemented with a later euhedral to subhedral zoned, dolomite cement. The tightly interlocking matrix has very little storage capacity besides fractures, although whole core analysis recognizes up to 4 or 5% porosity in places.

Relicts of original biota within the rudstone/packstone facies suggest ostracods, oncolites, algae and other restricted (stressed) biota dominate the assemblage. Pyrite is commonly found associated with this rock type.

The dolomitized coral/stromatoporoid mudstones are characterized by their leached fossil porosity. Porosity is in the order of 8 to 12 percent. The open marine floatstones contain abundant fine amphipods, euryamphipods, molluscs, brachiopods, dendroid corals and algae in a micritic matrix. Porosity is in the order of 6 to 8 percent.

The diagenetic events include but are not limited to:

1. dolomitization of the original matrix;
2. leaching of fossiliferous material where matrix porosity was high enough to allow the influx of fluids for dissolution;
3. dolomite cementation - several episodes, as euhedral dolomite crystals are zoned (hydrothermal saddle dolomite?);
4. oil emplacement and biodegradation - preserved as bitumen lining large vugs;
5. pyritization;
6. emplacement and trapping of existing hydrocarbon accumulations.

The well log calculated porosity from well L47 supplied by Paramount was plotted to obtain the zonation for the well. Figure 1 provides this plot. The well was divided into seven zones. From the well log calculations average porosities were calculated for each layer. Permeabilities were obtained from the porosity permeability relationship for well J37. Tabulated below are the properties for each layer:

Layer	Thickness meters	Porosity	Permeability mD
1	6.2	0.030	0.7
2	3.7	0.033	0.8
3	8.6	0.054	1.0
4	9.5	0.019	0.01
5	18.4	0.023	0.3
6	14.3	0.029	0.07
7	6.5	0.029	0.07

The well was assigned a drainage radius of 205 meters. The water-oil contact was assigned a depth of 1540 meters KB for the well.

NUMERICAL SIMULATOR

NUMERICAL SIMULATOR

CMG's Black Oil Simulator was used for this study in the dual porosity - dual permeability mode. This mode was utilized because the reservoir is fractured with relatively little permeability in the matrix. A 23 x 1 x 19 radial grid model was used for the vertical well simulation. A single wellbore in the centre of the cylindrical system was used. A 11 x 11 x 8 grid was used for the horizontal well cases. Properties in each layer in the matrix in the radial direction were kept constant. Tabulated below are the properties for each layer for the matrix for the vertical well model.:

Layer	Zone	Porosity (Fraction)	Permeability mD	Thickness (m)
1	1	0.03	0.7	0.5
2	1	0.03	0.7	3.0
3	1	0.03	0.7	2.7
4	2	0.033	0.8	3.7
5	3	0.054	1.0	3.0
6	3	0.054	1.0	3.0
7	3	0.054	1.0	2.6
8	4	0.019	0.01	3.0
9	4	0.019	0.01	3.0
10	4	0.019	0.01	3.5
11	5	0.023	0.3	3.0
12	5	0.023	0.3	3.0
13	5	0.023	0.3	3.0
14	5	0.023	0.3	3.0
15	5	0.023	0.3	3.0
16	5	0.023	0.3	3.4
17	6	0.029	0.7	7.0
18	6	0.029	0.7	7.3
19	7	0.029	0.7	6.5

The spacing of the grid blocks in the radial direction were as follows:

Grid Block Number in Radial Direction	Length Metres
1	1.0
2	2.0
3	4.0
4	8.0
5	10.0
6	10.0
7	10.0
8	10.0
9	10.0
10	10.0
11	10.0
12	10.0
13	10.0
14	10.0
15	10.0
16	10.0
17	10.0
18	10.0
19	10.0
20	10.0
21	10.0
22	10.0
23	10.0

The above configuration yields a drainage radius of 205 meters for the producing well.

Initially the fracture system was defined in a uniform manner for the entire reservoir. During the history match it was found that a large connected fracture system could not match the production data, so a more limited system was utilized. The following table provides the properties of the fracture system used in the radial direction.

Grid Block Number Radius Direction	Permeability Radius - Direction mD	Permeability Direction mD	Permeability Z-Direction mD
1	2000	3000	3000
2	2000	3000	3000
3	2000	3000	3000
4	2000	3000	3000
5	2000	3000	3000
6	100	100	100
7	1.0	1.0	1.0
8	1.0	1.0	1.0
9	1.0	1.0	1.0
10	1.0	1.0	1.0
11	1.0	1.0	1.0
12	1.0	1.0	1.0
13	1.0	1.0	1.0
14	1.0	1.0	1.0
15	1.0	1.0	1.0
16	1.0	1.0	1.0
17	1.0	1.0	1.0
18	1.0	1.0	1.0
19	1.0	1.0	1.0
20	1.0	1.0	1.0
21	1.0	1.0	1.0
22	1.0	1.0	1.0
23	1.0	1.0	1.0

The above configuration gave a fracture system with a drainable volume which matched the production history. The fractures were given a porosity of 1 percent.

For the 400 x 400 m square area used for the horizontal wells each grid block was 36.36 m square with variable thickness. Tabulated below is the thickness of each layer:

Layer	Thickness - m
1	2.0
2	5.7
3	3.7
4	8.6
5	9.5
6	18.4
7	14.3
8	6.5

The permeability and porosity of each layer is tabulated below:

Layer	Porosity	Permeability mD
1	0.1	0.7
2	0.03	0.7
3	0.033	0.8
4	0.054	1.0
5	0.019	0.1
6	0.023	0.7
7	0.029	0.7
8	0.029	0.7

The fracture porosity was 0.01 and the fracture permeability was 10 mD. It was difficult to know the exact permeability to give the fractures. The value of 10 mD was chosen arbitrarily and has no field evidence to support it. From the single well test there was indication of a poorly connected fracture system in the oil zone. It showed there is likely an area of higher permeability connected to the aquifer, but not highly connected through the oil zone. Therefore a relatively low fracture permeability was assigned to the overall fracture system.

SIMULATOR INPUT

SIMULATOR INPUT

The geological model described in the geological and numerical simulator sections was inputted in addition to this data. It was also necessary to input fluid, relative permeability, and capillary pressure data. PVT data was available for the field and special core studies were available for three different rock types.

FLUID PROPERTIES

A subsurface sample of reservoir fluid was collected and a PVT analysis available. The bubblepoint pressure was 10190 kPa and the solution gas-oil ratio was 56.11 m³/m³, the bubblepoint oil formation volume factor was 1.148 and the oil viscosity at the bubblepoint was 2.18 mPa.s. Figure 2 illustrates the oil formation volume factor, Figure 3 the solution gas-oil ratio, Figure 4 the oil viscosity, Figure 5 the gas compressibility factor and Figure 6 the gas viscosity. Since the numerical simulator is a multi-bubblepoint simulator, these curves have been extended. This allows gas to be forced back into solution if the pressure increases. The saturation pressure is near the original reservoir pressure indicating the reservoir fluid is saturated.

ROCK PROPERTIES

ROCK PROPERTIES

The matrix in well L47 has very low porosity and permeability so the low permeability rock type special core data was utilized for it. Gas-oil capillary pressure was assumed to be zero. The high permeability special core data were utilized for the fracture system. The high permeability fracture system most likely consists of fractures and permeable vuggy type rocks. The gas-oil capillary pressure was assumed to be zero in this system also.

The relative permeability curves indicate the rock tends to be oil-wet. This will result in minimal imbibition of water into the tight matrix. Figure 7 shows the water-oil relative permeability for the matrix, Figure 8 the water-oil capillary pressure, and Figure 9 the gas-oil relative permeability data. Figures 10 to 12 show the same data for the fractures. Some of these curves show uneven extensions as saturations approach 1.0. They have been extended to a value of 1.0 to meet simulator requests. In actual practice these saturations are never reached because zero permeability to the other phase is reached at the residual flooding saturation, preventing a further reduction in saturation for the current phase.

HISTORY MATCH

HISTORY MATCH

Initially no gascap and a uniform fracture system were employed. When these properties were employed the producing gas-oil ratio could not be matched, nor could water breakthrough time and the water cut be matched. To match the reservoir performance a gascap had to be placed in the reservoir. No gas was placed over the well but away from the well a gascap is present and the highly connected fracture system extent was limited to a radius of about 35 meters around the wellbore. With this limited fracture system and a gascap it was possible to match the production test data.

Figure 13 shows the GOR match and Figure 14 shows the water-cut match. The GOR match follows the trend observed in the field. The water-cut slightly over predicts water cut for the 1990 test, matches water cut for the 1993 test prior to reperforation and slightly under predicts water-cut after reperforation. Overall it was believed that the match was satisfactory.

A number of vertical cross-section contours of saturations and pressures were generated to display what was actually happening in the reservoir. These are all for the 1990 test, (the ones for the other test are similar). Figure 15 shows the pressure distribution at 28 days in the matrix. The pressure is the highest in the low permeability streak and the aquifer blocks around the wellbore. The pressure has been reduced to about 7500 kPa around the wellbore. Figure 16 shows the pressure distribution at the end of the 1990 test at 28 days in the fracture. The pressure distribution is relatively uniform in the radial direction. One would expect this with such a highly permeable system around the wellbore.

Figure 17 shows the gas saturation in the matrix at the end of the test. This figure shows that gas has moved down through the matrix a small amount. Figure 18 shows the gas saturation in the fractures at the end of the test. Gas has coned through the fractures and built up a gas saturation around the top of the well. In this test the well is perforated in layers 5 to 7. Layer 5 is showing a gas saturation around the wellbore.

Figure 19 shows the water saturation in the matrix at the conclusion of the test. Water has not invaded the matrix; all that exists is a transition zone at the oil-water contact. Figure 20 shows the water saturation in the fracture system. Water has coned up through the fractures into the perforations. Away from the highly permeable fracture system there has only been a slight movement of water up through the fractures.

Water saturation profiles were generated after the well was shut in to see how quickly the water cone would dissipate. The well was shut in at the start of day 29. Figure 21 shows the water saturation profile at day 46 or 17 days after the well was shut in. Comparing this with Figure 20 it can be seen that the cone has dropped about 10 meters. Figure 22 shows the profile at 127 days having dropped about 18 meters. Figure 23 shows the profile at 410 days. It has dropped about 26 meters. Figures 24 and 25 show the profile at 863 and 1067 days. At each of these later times the cone has not receded any further.

The oil, free gas and solution gas-in-place in the vertical well simulation are as follows:

Oil	$1.81183 \times 10^5 \text{ m}^3$
Free gas	$6.39271 \times 10^5 \text{ m}^3$
Solution gas	$1.01662 \times 10^7 \text{ m}^3$

The oil, free gas and solution gas-in-place in the horizontal simulations are:

Oil	$2.46852 \times 10^5 \text{ m}^3$
Free Gas	$3.14771 \times 10^6 \text{ m}^3$
Solution Gas	$1.38508 \times 10^7 \text{ m}^3$

PREDICTIONS

PREDICTIONS

Once the history match was completed thirteen predictive runs were made. These runs were made to determine the effect of completion interval, production rate, bottomhole pressure, water influx and well type on recovery of oil. Each of these predictive runs will be discussed, and then a comparison will be made between the individual runs.

Run 1

The set of perforations at 1496.5 to 1499.0 metres was utilized. An initial oil rate of 10 m³/d was used and the bottomhole pressure was allowed to go to 2500 kPa. Once a flowing bottomhole pressure of 2500 kPa was reached, the rate was reduced to maintain the pressure. Table 1 gives a tabulation of results of this prediction. The simulation was stopped when an oil rate of about 1.0 m³/day was obtained. The well produced for 1882 days and produced a total of 10422 m³ of oil. The GOR reached a high of 1017 m³/m³ and the water cut reached a high of 66 percent.

Run 2

The only difference between Run 1 and Run 2 was that in Run 2 the bottomhole pressure was not allowed to go below 5000 kPa. This well produced for 1477 days and had a cumulative oil production of 7726 m³. The GOR reached a high of 826 m³/m³ and the maximum water cut was 63 percent. Table 2 presents the results of the run.

Run 3

In this run an additional interval (1487 - 1488.5) was perforated. The well produced at an initial rate of 10 m³/day until the bottomhole pressure of 2500 kPa was reached; the rate was then reduced to maintain a bottomhole pressure of 2500 kPa. The well produced for 2120 days

and had a cumulative oil production of 10577 m³. The maximum GOR was 1092 and the maximum water cut was 70 percent. Table 3 presents the results of this run.

Run 4

All of the parameters in this run were the same as in Run 3 except the minimum bottomhole pressure was 5000 kPa. The well produced for 1526 days and had a cumulative oil recovery of 7871 m³. The maximum GOR was 765 m³/m³ and the maximum water cut was 64 percent. Table 4 presents the results of this run.

Run 5

This run was the same as Run 2 except the initial oil production rate was 20 m³/d instead of 10 m³/d. The well produced for 1327 days had a cumulative oil production of 7937 m³. The maximum water cut was 61 percent and the maximum GOR was 708 m³/m³. Table 5 presents the results of this run.

Run No. 6

Both the upper and lower set of perforations were open in this run. The well produced for 1600 days. Initial rates were as high as 350 m³/day. The maximum GOR reached was 1031 m³/m³. The highest water cut was 64.5%. The recovery was 10528 m³ or 5.8 % of the original oil in place. Table 6 presents the results of this test.

Run No. 7

In this run only the lower set of perforations were open. The run went for 1772 days. The maximum GOR was 1,061 m³/m³. The maximum water cut was 64.8%. A total of 10,802 m³ of oil was recovered, giving a recovery of 6.0%. Table 7 presents the results of this test.

Run No. 8

In this prediction both the upper and lower set of perforations were opened. This reservoir was produced cyclically - 90 days on and then shut in for the rest of the year. The well produced for a total of 5,203 days. The maximum water cut was 66%. Maximum gas-oil ratio was $2380 \text{ m}^3/\text{m}^3$. A total 10315 m^3 of oil was recovered, giving a recovery factor of 6.0. Table 8 presents the results of this test.

Run No. 9

This run was the same as Run No. 8 except only the lower perforations were open. Some stability problems were encountered in the simulator, so it was only run for a total of 1493 days. During this time 7711 m^3 of oil was recovered. The maximum water cut was 65% and the maximum GOR was $1646 \text{ m}^3/\text{m}^3$. The run was compared to the previous run and no difference was found in recovery vs time, additional time was not spent in taking this run to completion. The results of this test are found in Table No. 9.

Run No. 10

This was the first of the horizontal well runs. The test was conducted for 575 days. The maximum GOR reached was $5386 \text{ m}^3/\text{m}^3$. The maximum water cut was 6.7%. A total of $21,661 \text{ m}^3$ of oil was recovered. This gives a recovery of 8.8% of the original oil in place. Table 10 gives the results of this run.

Run No. 11

This run had a smaller grid size, but was exactly the same run conditions as Run No. 10. The well produced for a total of 573 days. Maximum GOR reached was 6550, maximum water cut 7.81%. A total of 21440 m^3 of oil was recovered giving a recovery factor of 8.7%. The results of this test are presented in Table No. 11.

Run No. 12

This run is exactly as the same as Run No. 11, except an aquifer was attached to the reservoir. This was a strong aquifer and so the pressure has been maintained well with the water influx into the reservoir from the aquifer. The reservoir produced for 890 days. The maximum GOR was 3160. The run was terminated when the water cut reached 98%. A total of 44 492 m³ of oil was produced, giving a recovery factor of 18% of the original oil in place. Table 12 presents a tabulation of the data for this test.

Run No. 13

This run is the same as Run No. 6 except an active aquifer has been attached to the reservoir. The well produced for a total of 4896 days and recovered 31,427 m³ of oil. This is about 17% of the initial oil-in-place. Table 13 presents the results of the test.

Comparison of Runs

This section will compare similar runs and discuss the effects of the various parameters on the simulation results.

Run 1 and Run 3

The only difference between these runs is the perforated interval. Run 3 had a higher perforated interval. Both runs produced about the same amount of oil. Run 3 took longer to produce and it had a higher maximum water cut and GOR.

Run 2 and Run 4

These two runs were similar to Runs 1 and Run 3, except these runs had a higher minimum bottomhole pressure. The two runs had about the same cumulative production. The GOR's and water-cut were also similar.

Run 1 and Run 2

Increasing the minimum bottomhole pressure decreased the cumulative oil and decreased the maximum water-cut and GOR. The cumulative oil was reduced by about 26 percent.

Run 3 and Run 4

These two runs showed similar trends to the comparison between Runs 1 and 2.

Run 2 and Run 5

The only difference between these two runs was the initial producing rate. They both had similar cumulative oil recoveries. Run 2 had higher water cuts and GOR's.

Plots were made of various variables versus cumulative oil production and time. Figure 26 compares oil rate for four runs as a function of cumulative oil. Similar trends are apparent for Runs 1 and 3 and Runs 2 and 4. Runs 1 and 3 maintain higher rates for a longer period of time. Figure 27 shows the oil rate as a function of time.

Figure 28 compares GOR as a function of cumulative oil. There is some difference at early times but at later times the trend and values are similar. Figure 29 illustrates the results as a function of time. The higher minimum bottomhole pressure run shows a lower GOR at later times.

Figure 30 illustrates water-cut as a function of cumulative oil production. The trend is similar for all the wells. If more points had been obtained, the level joining the points would be more consistent. Figure 31 shows the same data as a function of time. Once again the water-cuts for runs 2 and 4 are slightly lower at longer times.

Figure 32 shows a comparison of cumulative oil for Runs 2 and 5. At early times the cumulative oil for Run 5 is higher than for Run 2, but overall the cumulatives are about the same. Run 2 takes slightly longer to produce the oil. Figure 33 is a plot of oil rate vs time for these two runs.

Figure 34 shows a plot of cumulative oil as a function of time. From this plot it can be seen that opening the upper perforations increases the time for the oil to be produced.

These runs show that perforation interval and initial rate have little effect on the ultimate recovery. High initial rates and high pressure draw-down resulted in the highest ultimate recovery. These high pressure gradients forced more oil from the matrix into the fractures. The size of the fracture system and the permeability of the system completely controlled the well performance. A review of core analysis data and well log calculations for well J37 shows zones of higher porosity and permeability than L47. Well N-28 also has zones of higher permeability, but in all wells most of the pay has low porosity and permeability.

The history match as well as the predictions indicate that the period of water free and low GOR production depends almost entirely upon the available volume of the fracture system.

In the next series of runs no rate restrictions were imposed and the use of horizontal wells was investigated.

Runs Nos. 6 and 7

The only difference between these two runs is the perforated interval. Figure 35 compares the oil rates for the two runs. Initially there is very little difference between the two rates at larger cumulative oil rates Run No. 7 with only the lower perforations shows slightly higher oil rates. Figure 36 compares the producing gas-oil ratio as a function of cumulative oil. This figure shows that at later times the GOR is slightly higher in Run No. 6 which has both sets of perforations open. Figure 37 compares the water cuts at later times in the productive life of the well. The one with the lower set of perforations open has slightly higher water cuts, but essentially there is very little difference between the water cut history for the two wells.

Run No. 6 has a slightly lower overall recovery factor than Run No. 7. For practical purposes the overall production rate and recovery is not affected by the two sets of perforations being opened. Figure 38 verifies this. It is a plot of cumulative oil production vs time for Runs 6 and 7.

Runs Nos. 8 and 9

The only difference between these two runs is that Run 8 just has the lower perforations open while Run No. 9 has both the upper and lower set of perforations open. Figure 39 compares the cumulative production from these two runs. Although Run No. 9 was not carried out for as long a time as Run No. 8, it can be seen from this graph that there is no difference between the recovery obtained from these runs. The cyclic production of the well possibly could be improved if water influx was allowed to come into the reservoir. It would build the pressure up during the shut in periods and should improve the overall recovery.

A number of cross sections have been plotted to show the gas saturations and water saturations at a number of different times for Prediction 9. Figure 40 shows the water saturation in the fractures at time 0. Figure 41 shows the water saturation in the matrix at time 0. Figure 42 shows the gas saturation profile in the fracture system at time 0. Figure 43 shows the gas

saturation in the matrix at time 0. The next set of cross sections show water saturations and gas saturation profiles at time of 90 days which is at the end of the first production cycle. Figure 44 shows the water saturation in the fractures. From this figure it can be seen that the water has coned up in the vicinity of the wellbore in the fracture system. Figure 45 shows the water saturation in the matrix and this figure shows that there has been very little change in the water saturations. Figure 46 shows the gas saturations in the fracture system. From this figure it can be seen that the gas has coned down into the perforations. Figure 47 shows the gas saturation in the matrix and this figure shows that there has been little change in the gas saturation.

The next set of figures show the profiles just at the end of the shut-in period just prior to the well being opened up again. Figure 48 shows the water saturation in the fractures. This figure shows that the water cone has decreased in height at the beginning of the production cycle. Figure 49 shows the water saturation in the matrix. Figure 50 shows the gas saturation in the fracture system. This shows that during the shut in period that the gas has migrated up through the fracture system and has collected at the top of the reservoir. It has also moved above the top of the perforations. Figure 51 shows the gas saturation in the matrix and shows the gascap area in the matrix has not grown significantly. The next series of cross sections were taken to determine if the water or gas was changing the oil saturations significantly in the matrix of the reservoir. Figure 52 shows the water saturation in the matrix at 853 days. A comparison of this figure with Figure No. 41 shows that there has been some reduction in the oil saturation in the matrix and an increase in water saturation, but it has only been a slight amount. Figure 53 shows the gas saturation in the matrix at 853 days. Comparing this with Figure 43 it can be seen that there appears to be very little difference between the two graphs. In order to better look at the gas saturation block by block, a colored cross section was made and this is shown in Figure 54. From this it can be seen that the gas saturation has increased in nearly all of the blocks in the reservoir and the gas saturation has increased as the gascap has expanded at the top of the reservoir. Figure 55 shows the gas saturation in the matrix at 1493 days.

Runs Nos. 10 and 11

These two runs were made to determine if the performance of the horizontal well was going to be affected by the grid size. In Run No. 10 a $9 \times 7 \times 8$ grid size was employed, while in Run No. 11, $11 \times 11 \times 8$ was used. Figure 56 shows a plot of cumulative oil production vs time for these two runs. It can be seen at extended time that the $11 \times 11 \times 8$ grid system gives us slightly less recovery of oil. Tables 10 and 11 show that the GOR and the water cut is only slightly affected by the smaller grid size. Therefore, it was felt for the purposes of this study that the use of $11 \times 11 \times 8$ grid system was satisfactory.

Runs Nos. 11 and 12

These two runs are exactly the same except Run 11 has no active aquifer attached to the reservoir while Run No. 12 has a very active aquifer attached to the water leg of the reservoir. Figure 57 shows the cumulative production vs time for these two runs. It can be seen that Run No. 12 produces over twice as much oil as is produced in Run No. 11. Figure 58 shows GOR history for the two runs. The Run 12 with the water input maintains the pressure in the reservoir for a much longer period of time and consequently prevents the gascap from expanding and the producing GOR from increasing. Figure 59 is a plot of the water-cut vs time for the two runs. It can be seen that the active aquifer and a horizontal well does not result in rapid increases in water production. In fact the two runs have very similar water production history up until about 600 days. After this period of time the Run No. 11 without pressure maintenance was terminated because of low reservoir pressure, while Run No. 12 is being maintained and can be produced for a longer period of time.

A number of water and gas saturation profiles were plotted for these two horizontal runs. Figure 60 shows the water saturation in the fractures at 472 days. It can be seen from this that the water is coning up towards the horizontal well. Figure 61 shows the water saturation in the matrix. Figure 62 shows the gas saturation in the fracture system and Figure 63 shows the gas saturation in the matrix. At approximately the same time for Run No. 12 with the water influx,

Figure 64 shows the water saturation in the fracture system. Comparing this with the equivalent one with no water influx, it can be seen that the water has swept a greater fraction of the fracture system. Figure 65 shows the water saturation profile for the matrix. The water does not readily imbibe into the matrix because of the oil-wet nature of this reservoir. Figure 66 shows the gas saturation in the fracture system and it can be seen that gas is coning down towards the horizontal well. Figure 67 shows the gas saturation in the matrix.

At a time of 729 days a set of profiles is presented for Run No. 11. These are the profiles at the conclusion of the run for this well. Figure 68 shows the water coning up towards the horizontal well. Figure 69 shows the water saturation in the matrix, it is little different from Figure 61. Figure 70 shows the gas saturation in the fracture system and indicates that a secondary gascap has been created in the fracture system. Figure 71 shows the gas saturation in the matrix.

The next series of graphs show the gas and water saturations at 729 days for run No. 12. Figure 72 shows the water saturation in the fracture system. Figure 73 shows the water saturation in the matrix, and once again shows little change in the water saturation in the matrix. Figure 74 shows the gas saturation in the fracture system and once again shows the gas coning down towards the horizontal well. There was no change in the gas saturation in the matrix and so a plot has not been produced.

Run 6 and Run 13

Figure No. 75 compares the oil rates between the prediction without the connected aquifer and the prediction with the aquifer. Prediction No. 6 had no connected aquifer. Prediction No. 10 has a connected aquifer. As can be seen at the aquifer maintains the oil rate at a higher rate for a much longer period of time.

Figure No. 76 compares this prediction with the horizontal well prediction that had the connected aquifer. This figure shows that much greater volumes of water must be produced to

obtain comparable recoveries, as compared to when a horizontal well is used. Initially the water cut rises very rapidly, whereas in the horizontal well case, approximately 10% of the oil is produced before any amount of water has to be lifted.

Figure No. 77 compares the oil rate between the horizontal well and the vertical well. As can be seen the horizontal well is capable of maintaining a constant $50 \text{ m}^3/\text{day}$ during the length of its prediction while the vertical well's production rate dropped quite rapidly.

PREDICTION LIMITATIONS

During the history match four basic assumptions were made:

1. Volume of the connected fracture system is small
2. The highly permeable fracture system is only weakly connected to other fracture systems in the reservoir.
3. The matrix has very low permeability.
4. The limited fracture system is connected to the gascap.

The effects of each of the above assumptions on the prediction will be briefly discussed.

Point 1

This assumption results in water and gas being coned very rapidly. It also results in a low cumulative oil recovery from the well. During the history match a number of different fracture systems were used. It was only the small weakly connected system which gave early breakthrough of oil and gas and water-cuts GOR's similar to those observed in the field test of well L47. Larger fracture systems will result in more oil production, but a poor match to observed well performance.

Point 2

A number of connections to the well fracture system and the reservoir fracture system were tried. It was only a weakly connected system that gave early breakthrough data. The weak connection still allowed oil to flow in the well fracture system, but at reduced rates. If the reservoir fracture system is better connected, then the well will produce greater volumes of oil.

Point 3

The well porosity is low, the highest being 5.4 percent. From porosity-permeability relationship this results in very low permeability. If the matrix porosity is higher in the drainage radius of well L47, the cumulative oil recovery will be higher than predicted.

Point 4

If a well is not coning gas, it may be more sensitive to the completion interval. Therefore it may be possible to increase recovery by perforating higher but we would not expect significant increases in recovery from a limited fracture system.

With limited production data it is not possible to completely define the fracture system, connectivity and aquifer strength. Nevertheless the simulation gives insight into the mechanism operating in the reservoir and suggests possible ways that the reservoir could be produced.

Once additional production history is available, the simulator model can be further tuned with more data to provide an increased degree of confidence in the prediction results.

CONCLUSIONS

From this simulation study the following is concluded:

1. The well is connected to a relatively small volume highly permeable fracture system.
2. The prediction indicated a recovery of about 10,000 m³ of oil at an economic limit of 1 m/d. Higher economic limits will result in somewhat lower recoveries. This is only a recovery factor of 5.5 percent of the original oil in place.
3. The limited fracture system resulted in rapid breakthrough of gas and water.
4. Completion interval and initial rate had little effect on the cumulative recovery.
5. High rates and low pressure drawdowns reduce the time to recover the oil, provided the aquifer is limited.
6. Producing the well at a high initial rate did not result in an increase in overall recovery.
7. The cyclic production of the reservoir did not improve recovery. This conclusion is based on the fact that there was no water influx into the reservoir. If water is allowed to influx into the reservoir the ultimate recovery should be increased.
8. A horizontal well without water influx increased the recovery by about 2 - 3%.
9. A horizontal well with a strong aquifer attached to the reservoir, when compared to a vertical well with an attached aquifer, yielded only 1% more recovery.
10. The matrix contributed very little production; most of the oil came from the fracture system.

TABLE 1
PARAMOUNT CAMERON HILLS
KEG RIVER NUMERICAL SIMULATION STUDY
PREDICTION #1 RESULTS

Lower Perfs Open, 10 m³/day Initial Rate, BHP min = 2500 kPag

Time	Oil Rate m ³ /d	GOR m ³ /m ³	Water-Cut Percent	Cumulative m ³
25	10	113	.45	248
57	10	116	1.26	567
92	10	165	45	920
524	10	543	65	5243
697	7.61	750	63	6959
1203	2.89	863	66	9311
1394	2.04	895	65	9766
1631	1.357	932	62	10154
1882	0.870	1017	59	10422

TABLE 2
PARAMOUNT CAMERON HILLS
KEG RIVER NUMERICAL SIMULATION STUDY
PREDICTION #2 RESULTS

Lower Perfs open, Initial Rate 10 m³/day, BHP min = 5000 kPa

Time	Oil Rate m ³ /d	GOR m ³ /m ³	Water-Cut Percent	Cumulative m ³
25	10	113	45	250
57	10	116	1.26	570
92	10	165	45	920
574	6.70	518	63	5414
901	3.01	637	61	6790
1162	1.67	702	58	7357
1322	1.171	744	53	7579
1477	0.80	826	47	7726

TABLE 3
PARAMOUNT CAMERON HILLS
KEG RIVER NUMERICAL SIMULATION STUDY
PREDICTION #3 RESULTS

Lower and Upper Perfs Open, 10 m³/day Initial Rate, BHP min = 2500 kPa

Time	Oil Rate m ³ /d	GOR m ³ /m ³	Water-Cut Percent	Cumulative m ³
9	10	56	.34	90
23	10	56	.4	230
40	10	65	.6	400
68	10	119	1.86	680
424	10	453	64	4240
706	8.2	696	70	7012
1445	1.92	883	64	9828
1720	1.214	927	62	10241
2120	0.601	1092	53	10577

TABLE 4
PARAMOUNT CAMERON HILLS
KEG RIVER NUMERICAL SIMULATION STUDY
PREDICTION #4 RESULTS

Lower and Upper Perfs Open, 10 m³/day Initial Rate, BHP min = 2500 kPa

Time	Oil Rate m ³ /d	GOR m ³ /m ³	Water-Cut Percent	Cumulative m ³
9	10	56	.34	90
23	10	56	.4	230
40	10	65	.6	400
68	10	119	1.86	680
424	10	453	64	4240
975	2.65	651	61	7010
1250	1.65	619	54	7555
1526	0.81	765	49	7871

TABLE 5
PARAMOUNT CAMERON HILLS
KEG RIVER NUMERICAL SIMULATION STUDY
PREDICTION #5 RESULTS

Lower and Upper Perfs Open, 10 m³/day Initial Rate, BHP min = 2500 kPa

Time	Oil Rate m ³ /d	GOR m ³ /m ³	Water-Cut Percent	Cumulative m ³
4.0	20	56	.3	80
15	20	60	.5	300
30	20	155	15	600
103	20	323	60	2060
672	3.75	579	61	6641
947	2.07	638	58	7386
1128	1.56	605	53	7701
1327	0.93	708	49	7937

TABLE 6
PARAMOUNT CAMERON HILLS
KEG RIVER NUMERICAL SIMULATION STUDY
PREDICTION #6 RESULTS

Upper and Lower Perfs Open, BHP = 2500 kPag

Time	Oil Rate m ³ /d	GOR m ³ /m ³	Water-Cut Percent	Cumulative m ³
0.5	342	414	34.6	488
40.3	28.4	344	64.1	2202
689.24	4.45	730	64.5	8673
864.24	3.1	796	64.4	9310
1101.7	2	852	63.2	9892
1268.6	1.49	897	61.9	10172
1412.1	1.15	943	60.4	10347
1599.6	0.817	1031	57.2	10528

TABLE 7
PARAMOUNT CAMERON HILLS
KEG RIVER NUMERICAL SIMULATION STUDY
PREDICTION #7 RESULTS

Lower Perfs Open, BHP = 2500 kPag

Time	Oil Rate m ³ /d	GOR m ³ /m ³	Water-Cut Percent	Cumulative m ³
0.875	244.45	363	37.7	540
53.285	24.4	353	64.8	2551
784.71	3.8	754	64.4	9106
1222.2	1.763	852	62.7	10189
1497.2	1.11	921	59.9	10568
1772.2	0.672	1061	54.8	10802

TABLE 8
PARAMOUNT CAMERON HILLS
KEG RIVER NUMERICAL SIMULATION STUDY
PREDICTION #8 RESULTS

Upper and Lower Perfs Open, Cyclic Production BHP = 2500 kPag

Time	Oil Rate m ³ /d	GOR m ³ /m ³	Water-Cut Percent	Cumulative m ³
0.525	344	414	34.6	488
40.25	28.44	344	64.1	2202
90	20.821	374	65.1	3301
91	0	0	0	3301
365	0	0	0	3301
422.46	16.57	460	63.7	4626
455	13.84	496	64.7	5110
456	0	0	0	5110
730	0	0	0	5110
745.78	17.48	512	66	5507
820	10.318	581	63.6	6420
821	0	0	0	6420
1095	0	0	0	6420
1186	7.59	668	64.2	7355
1187	0	0	0	7355
1461	0	0	0	7355
1501.7	7.26	707	65.9	7747
1551	5.78	730	64.9	8032
1552	0	0	0	8032
1826	0	0	0	8032
1830.6	10.257	766	60.9	8104
1916	4.506	761	64.8	8555
1917	0	0	0	8555
2191	0	0	0	8555
2199	5.57	926	66	8625
2281	3.73	737	63.4	8965
2282	0	0	0	8965
2556	0	0	0	8965
2560.9	5.57	916	35.1	9000
2647	2.9	780	64.4	9284
2648	0	0	0	9284
2922	0	0	0	9284
2928.9	3.49	1094	28.4	9314
2941.3	3.05	856	65.2	9355
3012	2.39	777	63.5	9533
3013	0	0	0	9533
3287	0	0	0	9533
3288.1	3.15	2379	3.22	9535
3298.1	2.06	1278	43.5	9561
3377	1.9856	762	61.4	9732
5203	0.96	637	30.3	10315

TABLE 9
PARAMOUNT CAMERON HILLS
KEG RIVER NUMERICAL SIMULATION STUDY
PREDICTION #9 RESULTS

Lower Perfs Open, Cyclic Production BHP = 2500 kPag

Time	Oil Rate m ³ /d	GOR m ³ /m ³	Water-Cut Percent	Cumulative m ³
0.875	244.45	363	37.7	540
53.3	25.404	353	64.8	2551
90	20.904	374	65.1	3319
91	0	0	0	3319
365	0	0	0	3319
365.02	446	551	46.8	3335
365.61	87.1	431	67.9	3413
455	14.2	489	64.5	5114
456	0	0	0	5114
730	0	0	0	5114
730.51	75.4	552	63	5181
820	10.6	580	63.6	6399
821	0	0	0	6399
1095	0	0	0	6399
1095.5	67.8	721	48.9	6452
1173.7	8	650	63.8	7285
1186	7.6	660	63.9	7378
1186	0	0	0	7378
1461	0	0	0	7378
1461.1	119.58	1646	5	7387
1463.6	17.2	755	59.8	7457
1492	7.9	702	66.5	7711
1493	0	0	0	7711

TABLE 10
PARAMOUNT CAMERON HILLS
KEG RIVER NUMERICAL SIMULATION STUDY
HOR 1 RESULTS

9 x 7 x 8 Grid 50 m³/m³/day Initial Rate, BHP = 2500 kPag, No Water Influx

Time	Oil Rate m ³ /d	GOR m ³ /m ³	Water-Cut Percent	Cumulative m ³
3.9	50	56	0	195
15	50	56	0	750
29.2	50	56	0	1461
57.2	50	56	0	2862
77.5	50	55	0	3876
97.1	50	55	0	3857
116.8	50	55	0	5838
142.8	50	54	0	7141
168	50	54	0	8399
190.2	50	53	0	9508
220.7	50	53	0.5	11034
254.15	50	767	0.8	12706
312.9	50	1057	1.12	15647
359.8	50	1045	1.34	17992
412	50	898	1.62	20600
475	16.816	875	1.76	21659
575	0.02	5386	6.7	21661

TABLE 11
PARAMOUNT CAMERON HILLS
KEG RIVER NUMERICAL SIMULATION STUDY
HOR 2 RESULTS

11 x 11 x 8 Grid HOR2 50 m³/m³/Day Initial Rate, BHP = 2500 kPag, no water influx

Time	Oil Rate m ³ /d	GOR m ³ /m ³	Water-Cut Percent	Cumulative m ³
3.9	50	56	0	195
11.5	50	56	0	576
23	50	56	0	1149
67.9	50	56	0	3398
101.5	50	55	0	5074
127	50	54	0	6350
148.2	50	54	0	7408
177.6	50	53	0	8882
225.9	50	471	0.6	11296
308.1	50	1040	1.1	15408
354.88	50	1020	1.33	17745
408.1	50	878	1.6	20404
472.5	16.1	850	1.72	21438
572.5	0.02	6550	7.81	21440

TABLE 12
PARAMOUNT CAMERON HILLS
KEG RIVER NUMERICAL SIMULATION STUDY
HOR 3 RESULTS

11 x 11 x 8 Grid 50 m³/day Initial Rate, BHP = 2500 kPag, water influx

Time	Oil Rate m ³ /d	GOR m ³ /m ³	Water-Cut Percent	Cumulative m ³
0.78	50	56	0	39
3.9	50	56	0	195
22	50	56	0	1099
47.5	50	56	0	2375
68.6	50	56	0	3928
104.6	50	56	0	5229
130.58	50	56	0.4	6529
182.6	50	56	0.6	9128
234.6	50	56	0.6	11728
284.6	50	56	0.7	14228
334.6	50	56	0.7	16728
365.6	50	56	0.8	18276
409.2	50	56	0.9	20456
443	50	56	1.17	22172
477.8	50	56	1.72	23888
508.2	50	56	2.04	25407
538.5	50	56	2.67	26926
575.2	50	56	3.8	28759
611.9	50	56	6.71	30592
641.2	50	56	20.5	32056
676.7	50	56	64.3	33834
696.21	50	56	75.5	34809
729	50	56	83.5	36448
774	50	55	87.9	38699
816.4	50	55	91.3	40820
857.8	50	1600	95.9	42886
889.9	50	3160	98	44492

TABLE 13
PARAMOUNT CAMERON HILLS
KEG RIVER NUMERICAL SIMULATION STUDY
VERTICAL WELL WITH CONNECTED AQUIFER

Time Days	Oil Rate m ³	Gas-oil Ratio m ³ /m ³	Water Cut Percent	Cum Oil m ³	Recovery Percent
0.50	345.00	414	35	488	0.27
32.00	30.90	328	64	1991	1.10
245.00	21.70	139	67	6724	3.71
701.00	12.30	66	82	14433	7.97
840.00	11.60	52	84	16058	8.86
1021.00	11.00	51	85	18113	10.00
1167.00	10.20	53	86	19658	10.85
1317.00	9.10	54	88	21103	11.65
1507.00	7.70	54	90	22698	12.53
1741.00	5.90	55	93	24274	13.40
1936.00	4.80	58	94	25308	13.97
2144.00	4.00	62	95	26215	14.47
2365.00	3.30	65	96	27003	14.90
2574.00	2.80	68	97	27633	15.25
2796.00	2.50	71	97	28216	15.57
3030.00	2.20	74	98	28751	15.87
3280.00	1.90	77	98	29251	16.14
4224.00	1.20	90	99	30681	16.93
4896.00	1.00	94	99	31427	17.35

FIGURE 1

POROSITY WELL L47

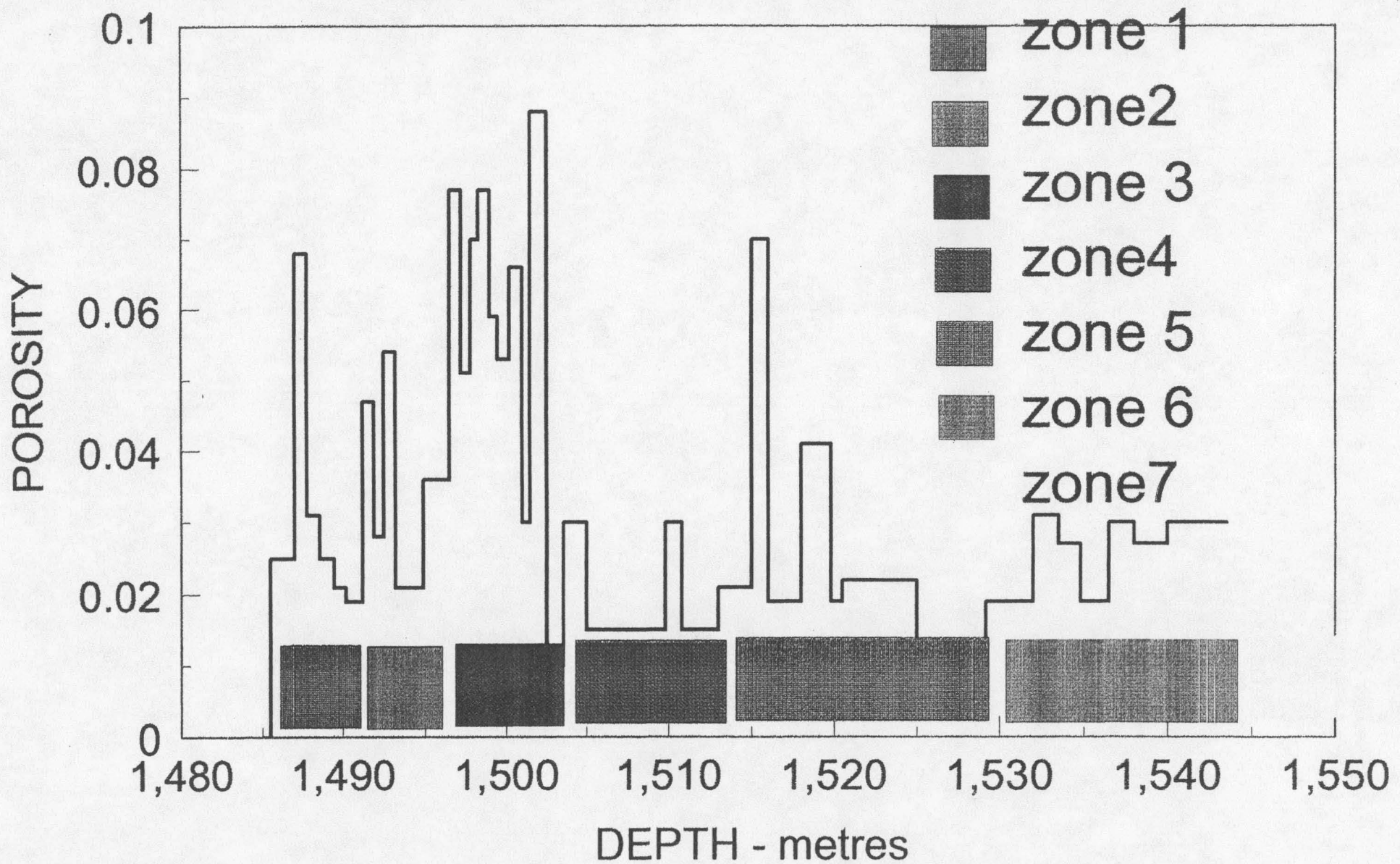


FIGURE 2

PVT PROPERTIES

OIL FORMATION VOLUME FACTOR

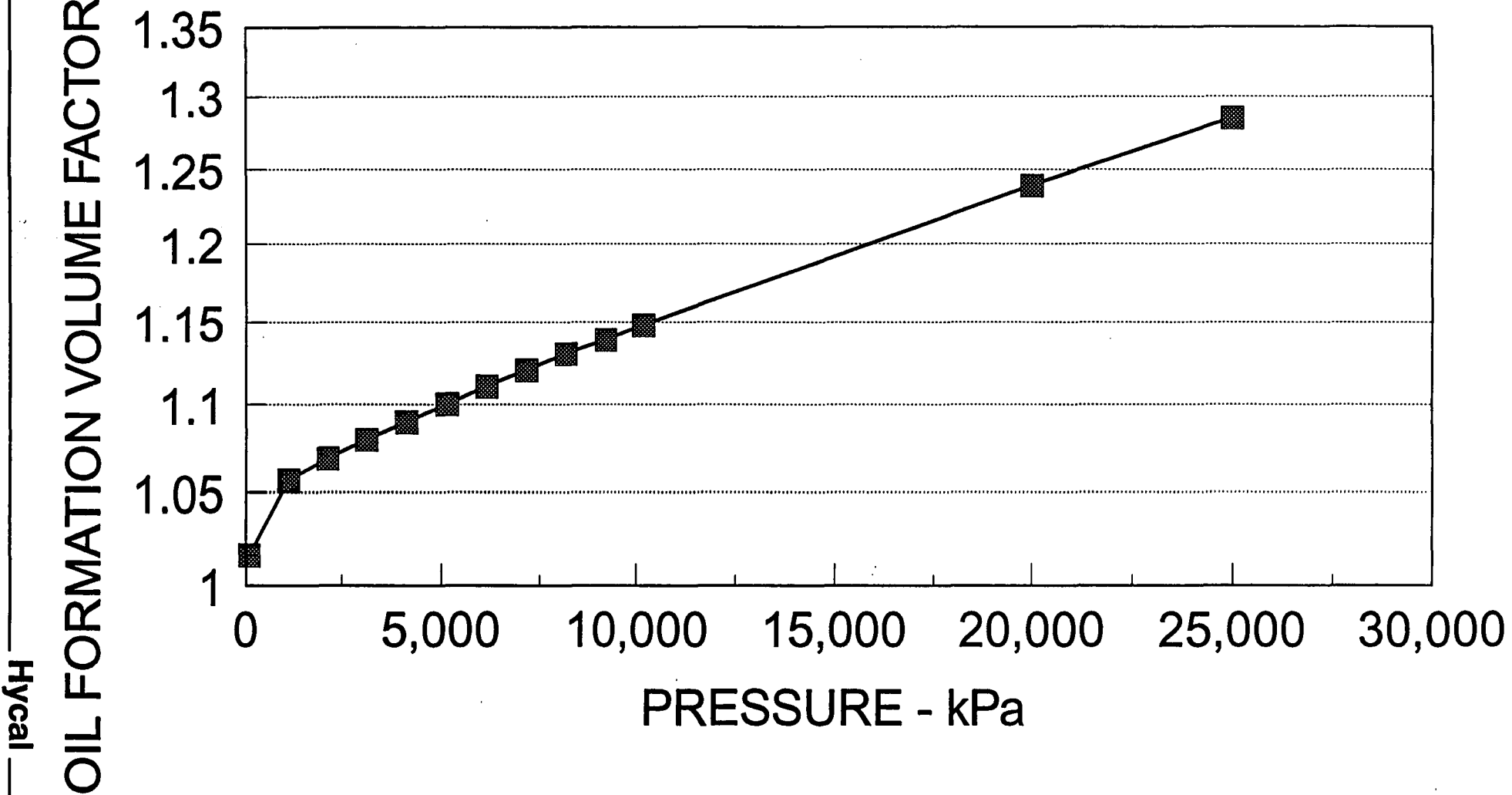


FIGURE 3

PVT PROPERTIES

SOLUTION GAS-OIL RATIO

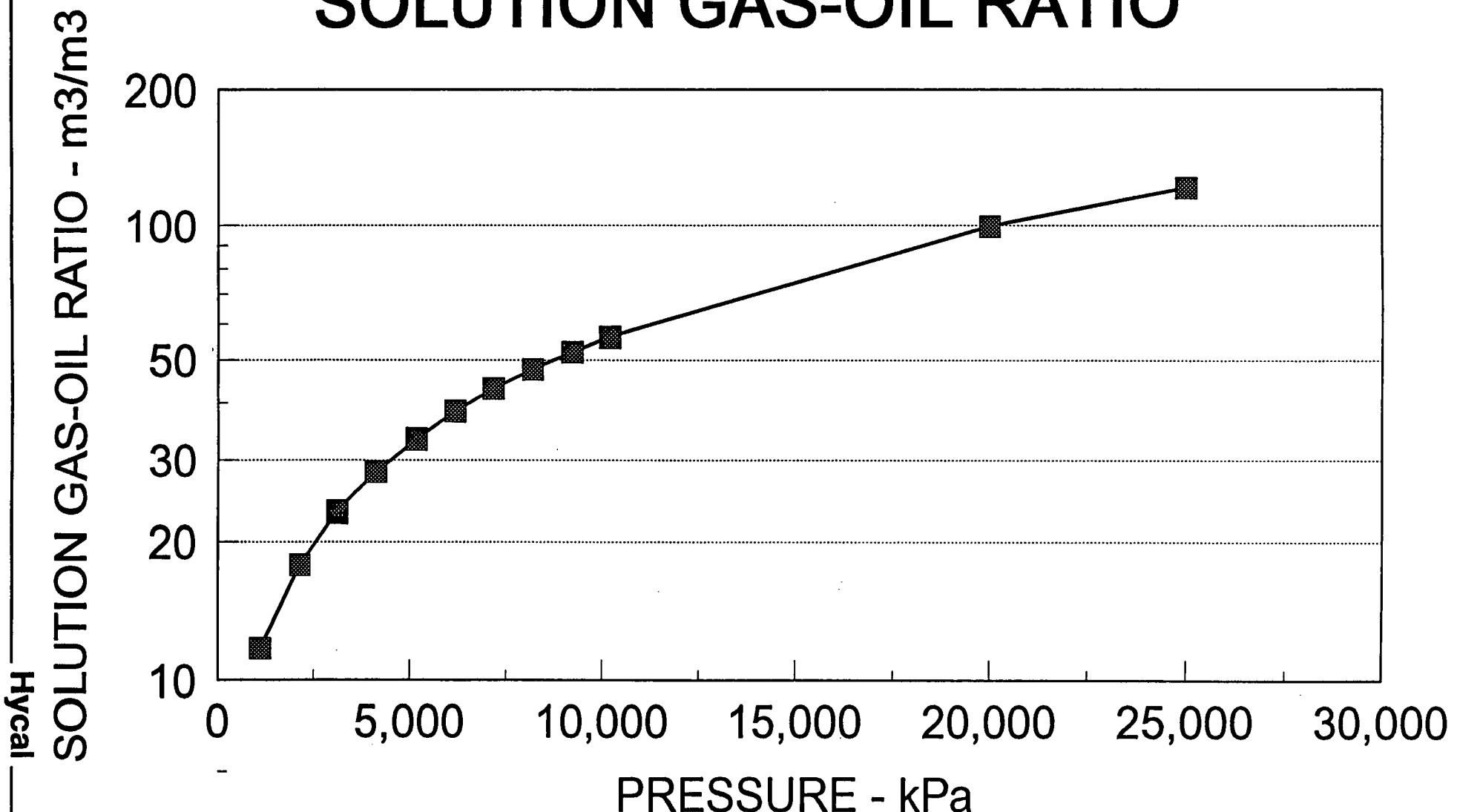


FIGURE 4

PVT PROPERTIES

GAS COMPRESSIBILITY FACTOR

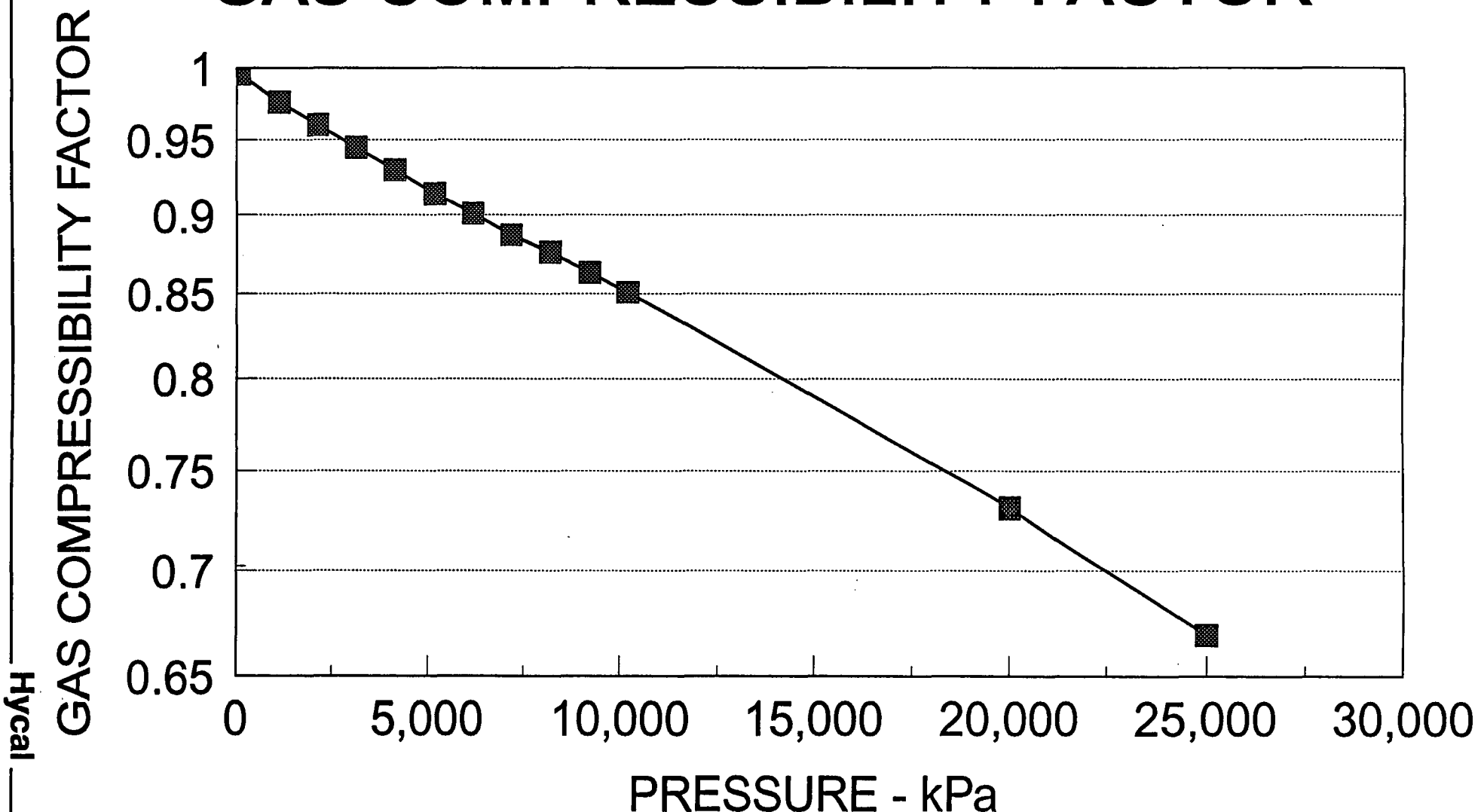


FIGURE 5

PVT PROPERTIES

OIL VISCOSITY

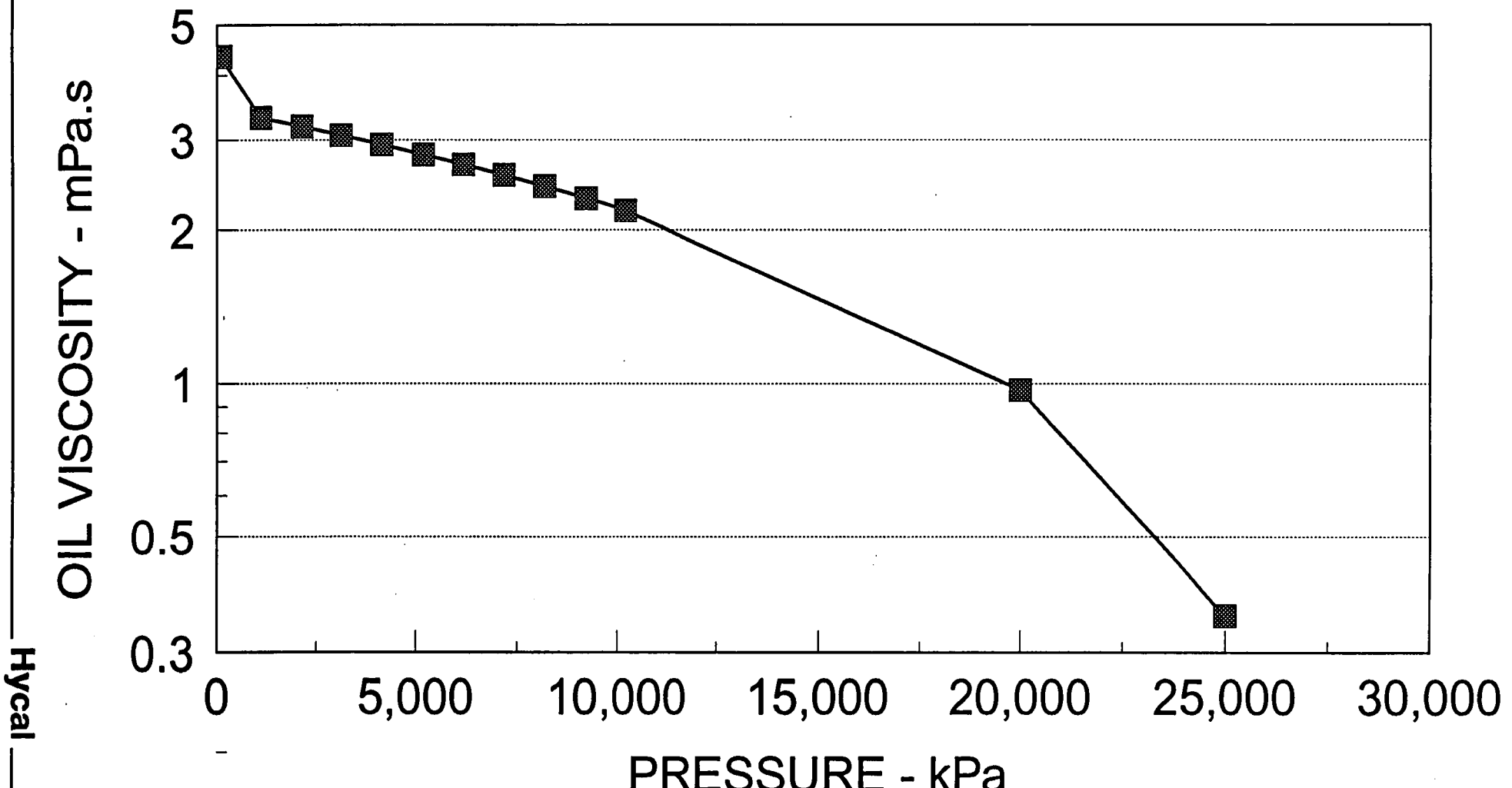


FIGURE 6

PVT PROPERTIES

GAS VISCOSITY

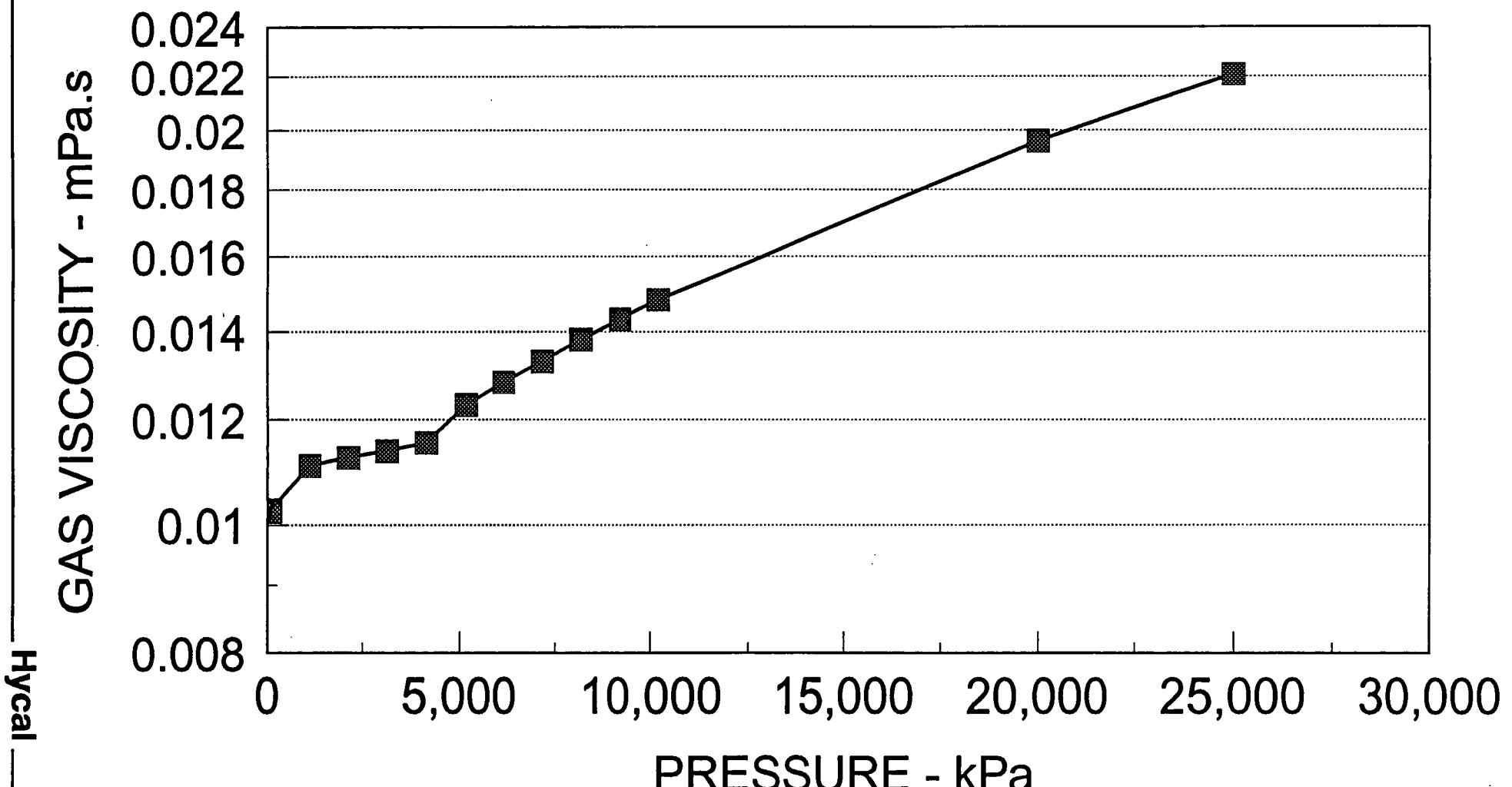


FIGURE 7

MATRIX RELATIVE PERMEABILITY

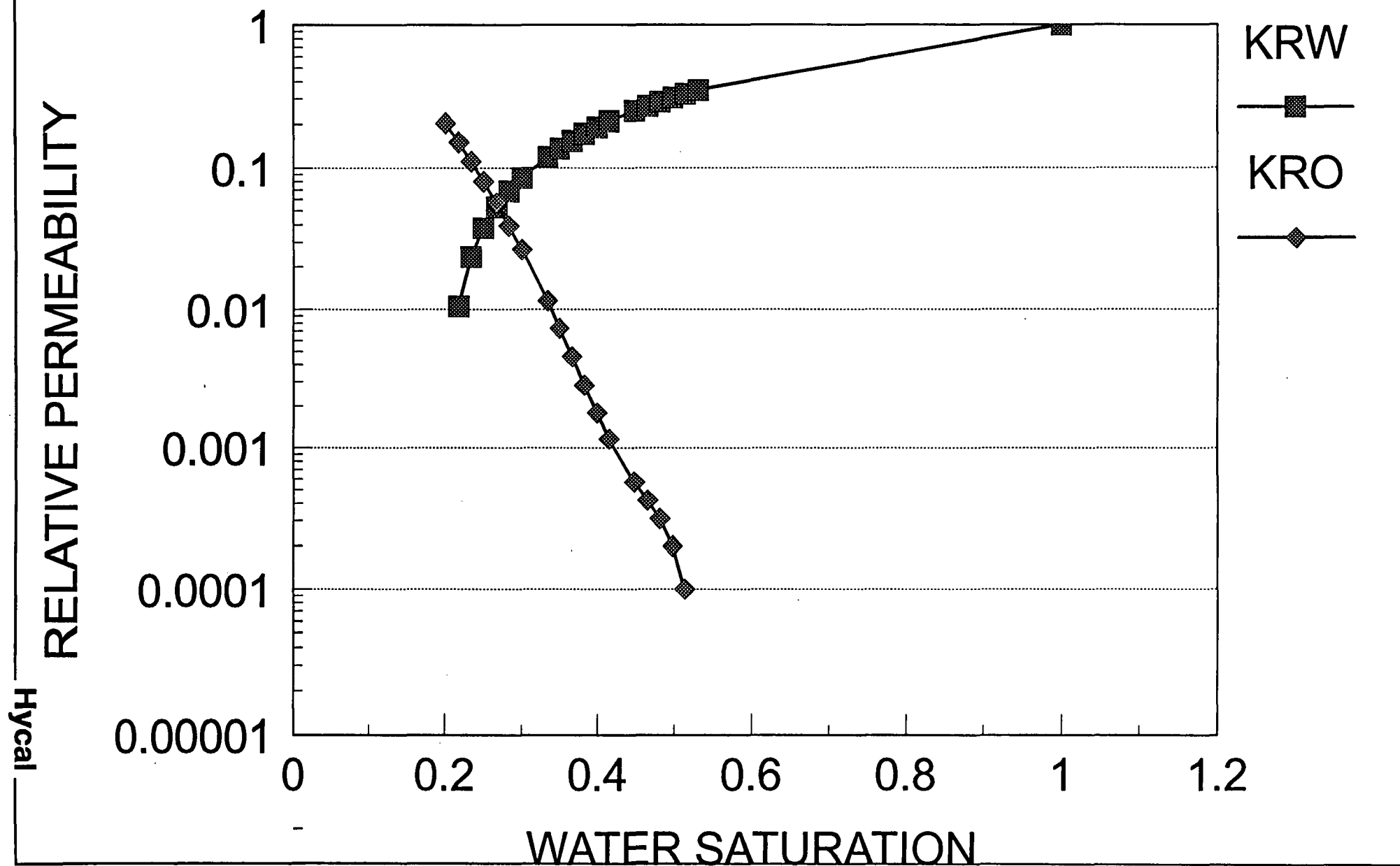


FIGURE 8

MATRIX RELATIVE CAPILLARY PRESSURE

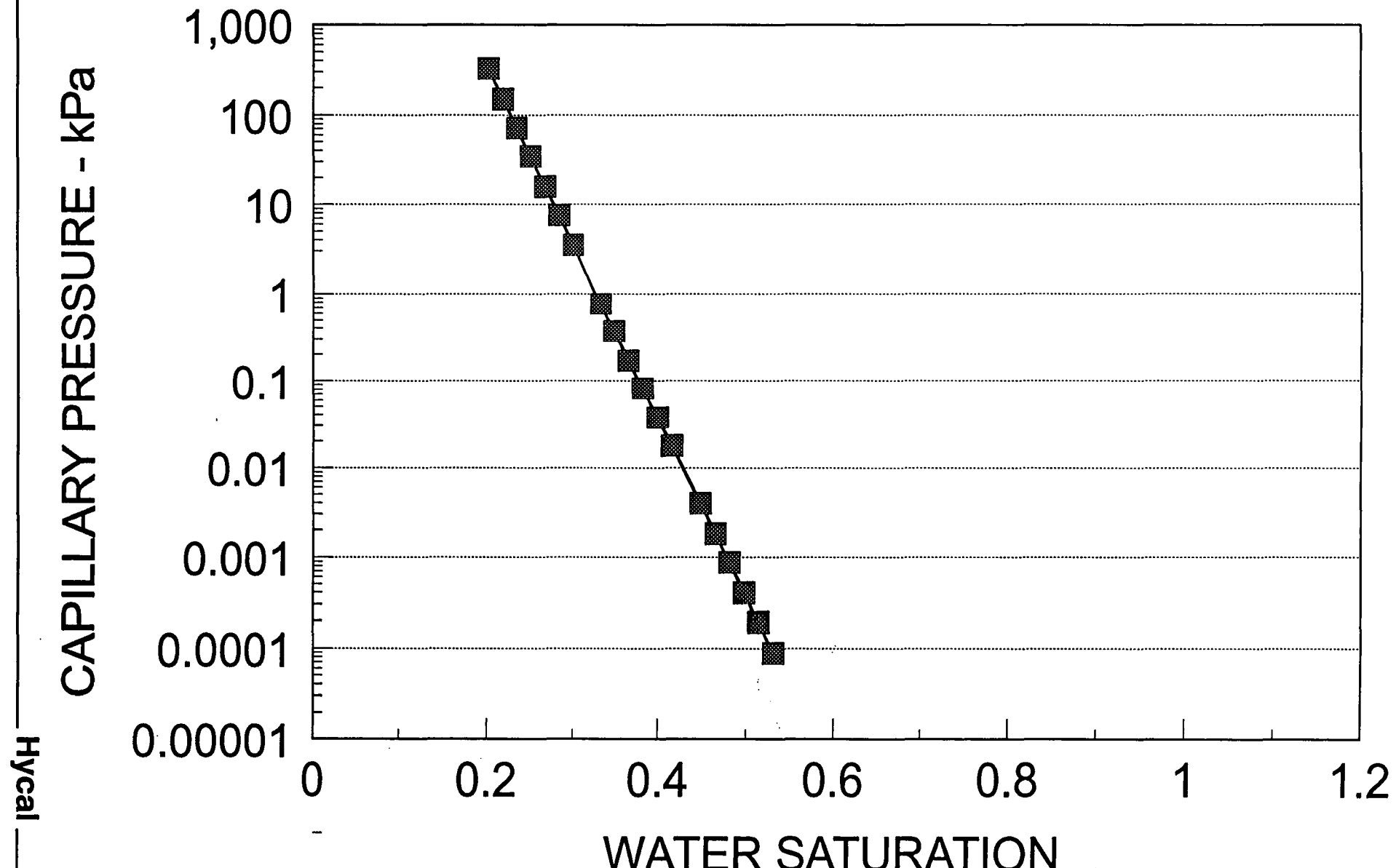


FIGURE 9

MATRIX RELATIVE PERMEABILITY

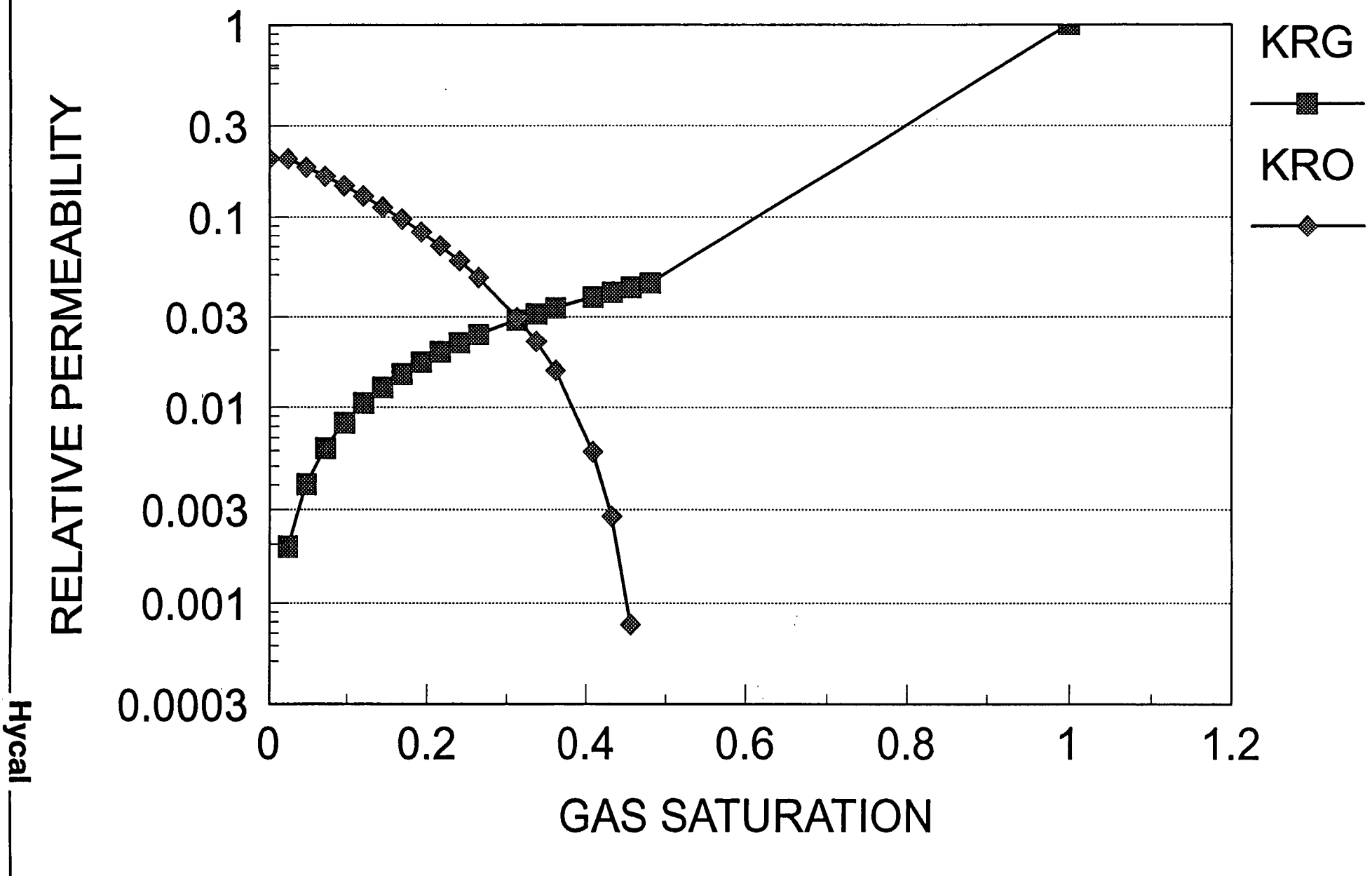


FIGURE 10

FRACTURE RELATIVE PERMEABILITY

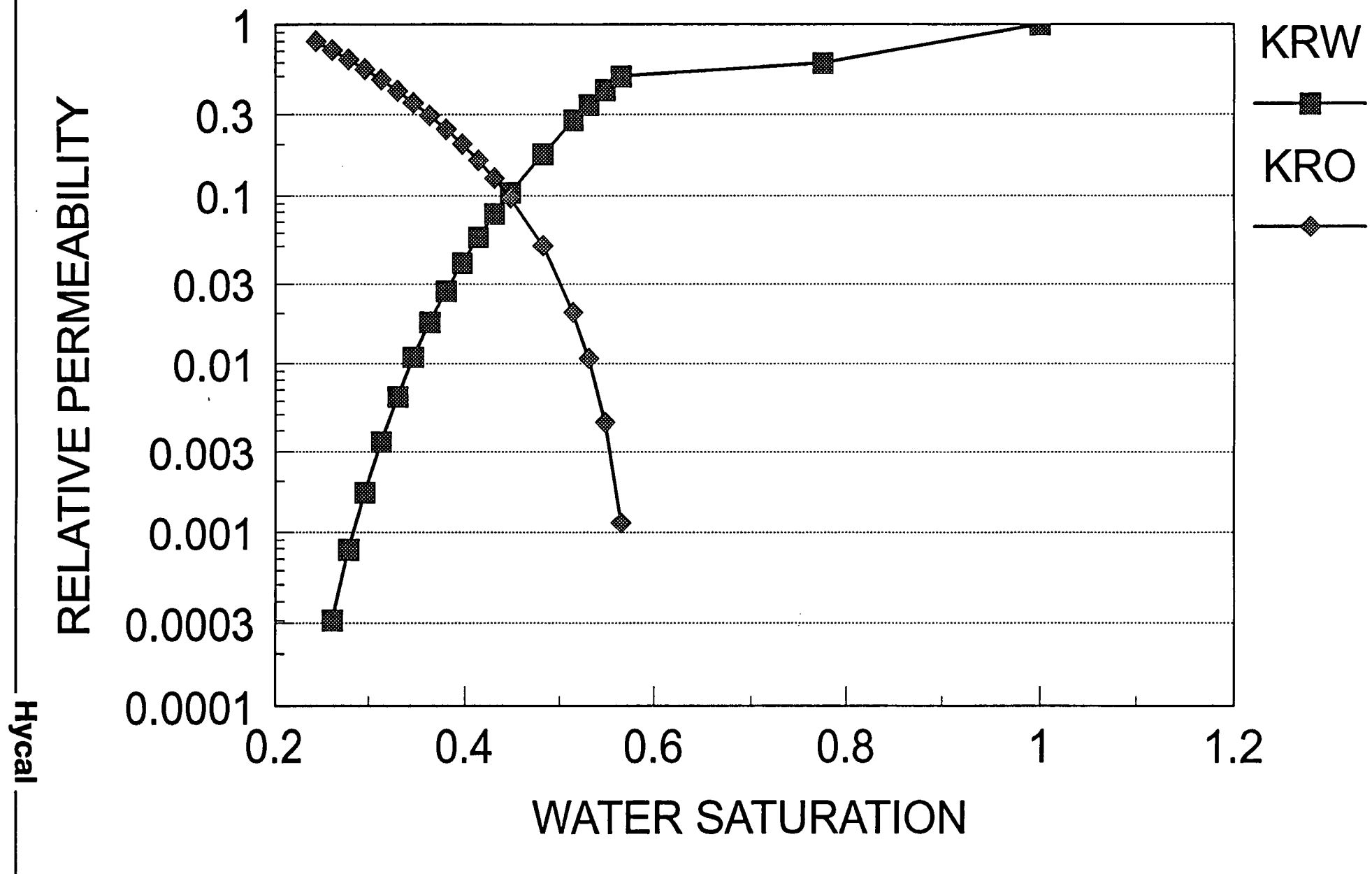


FIGURE 11

FRACTURE RELATIVE CAPILLARY PRESSURE

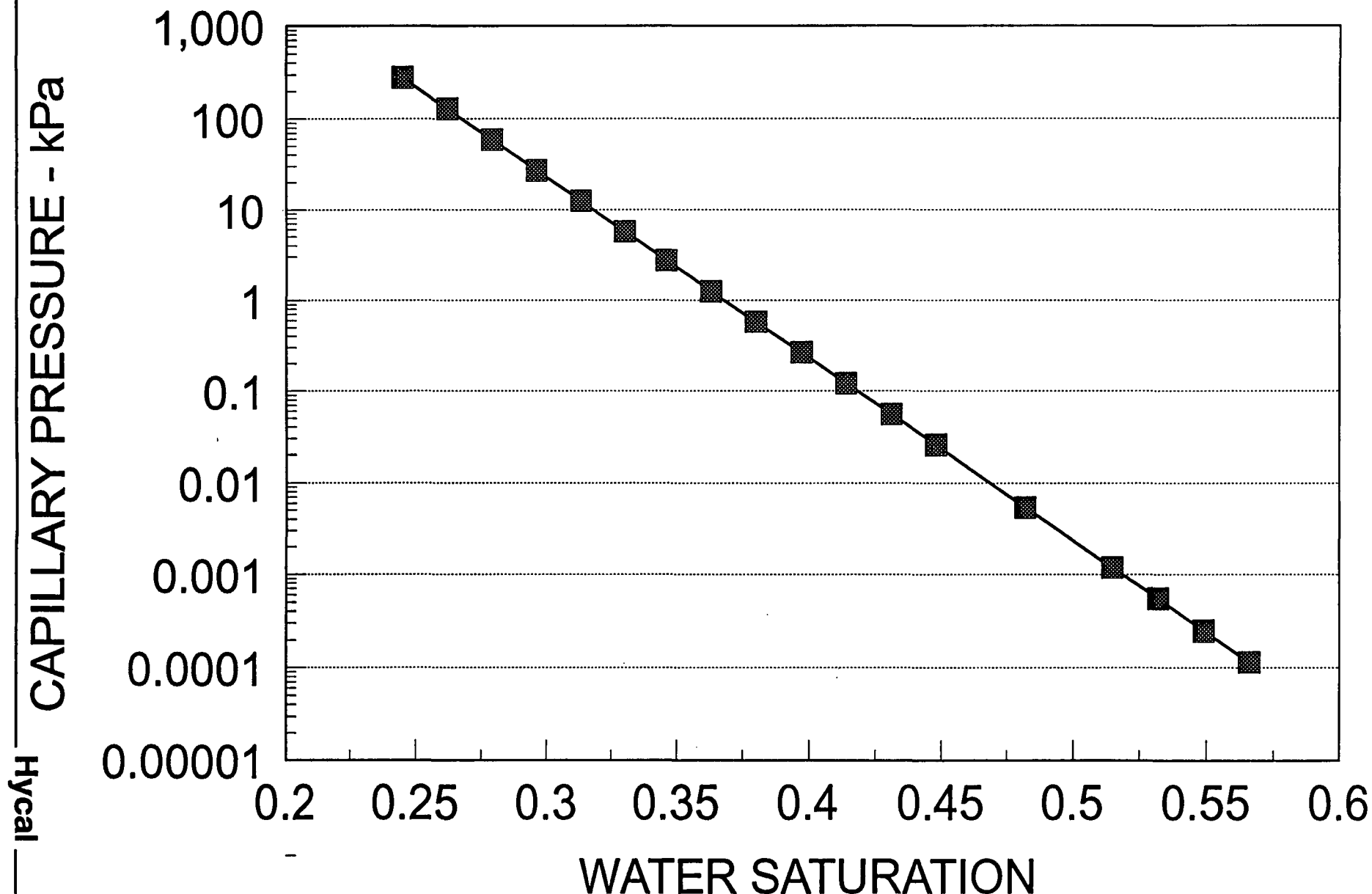


FIGURE 12

MATRIX RELATIVE PERMEABILITY

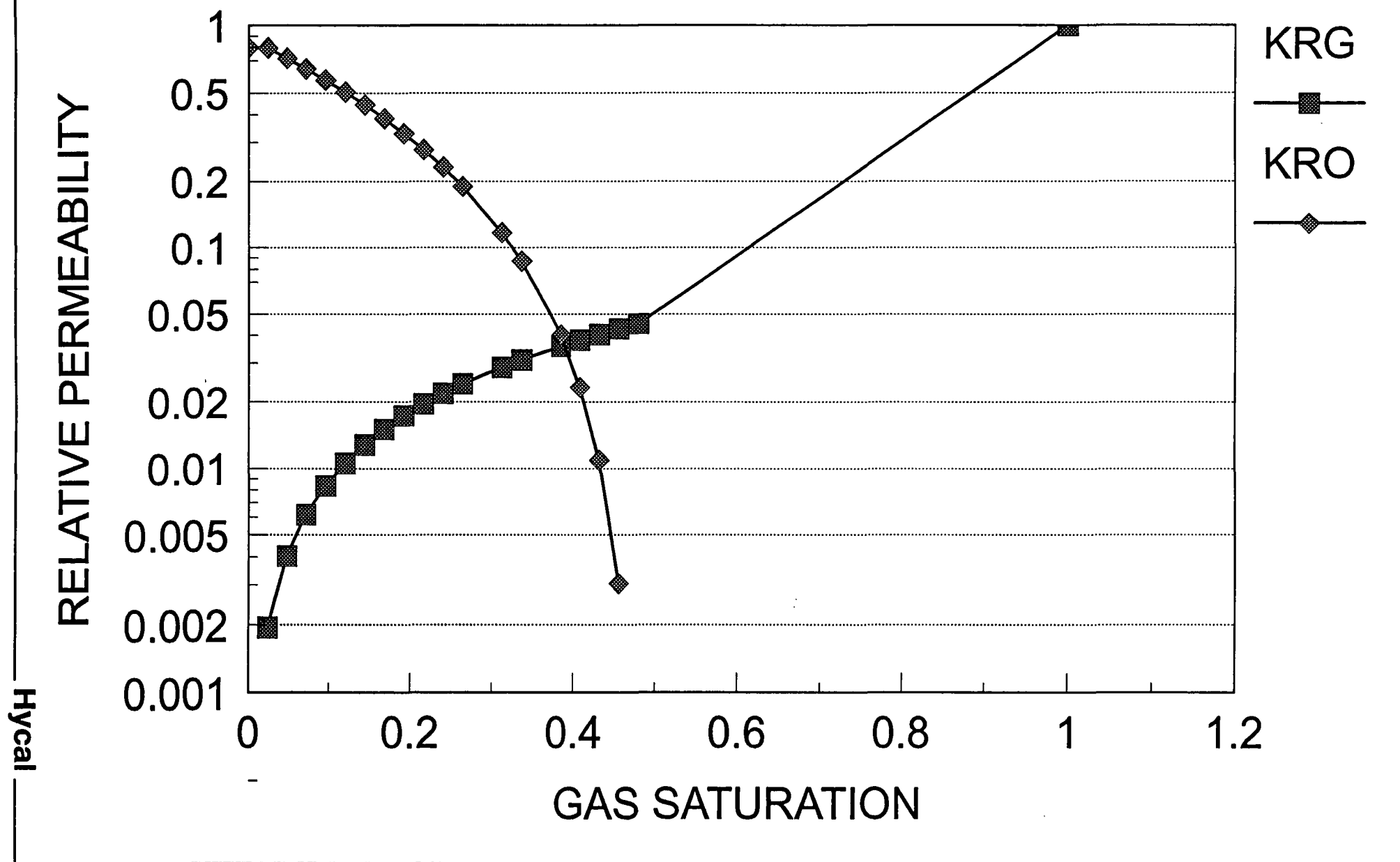


FIGURE 13

HISTORY MATCH GOR

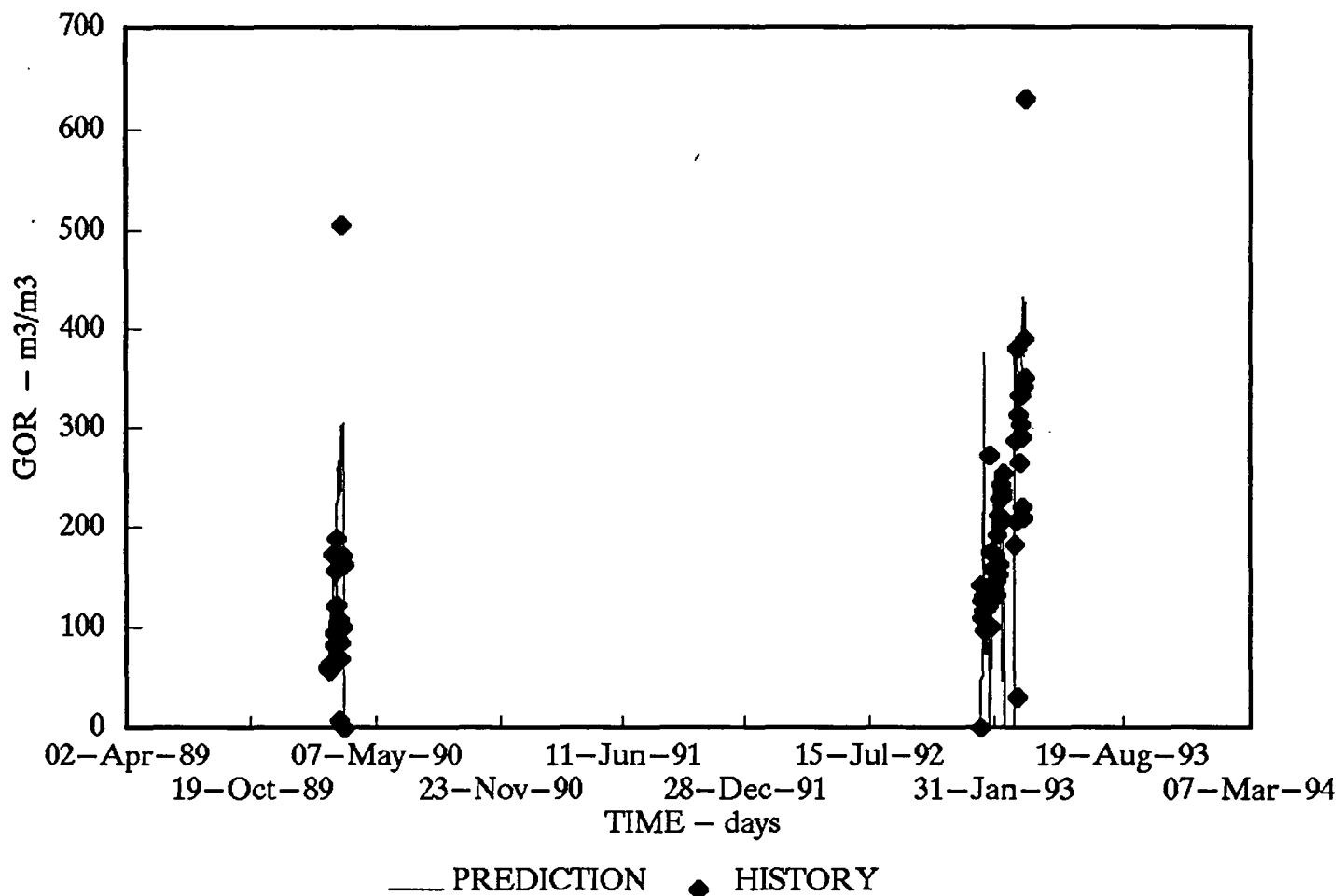
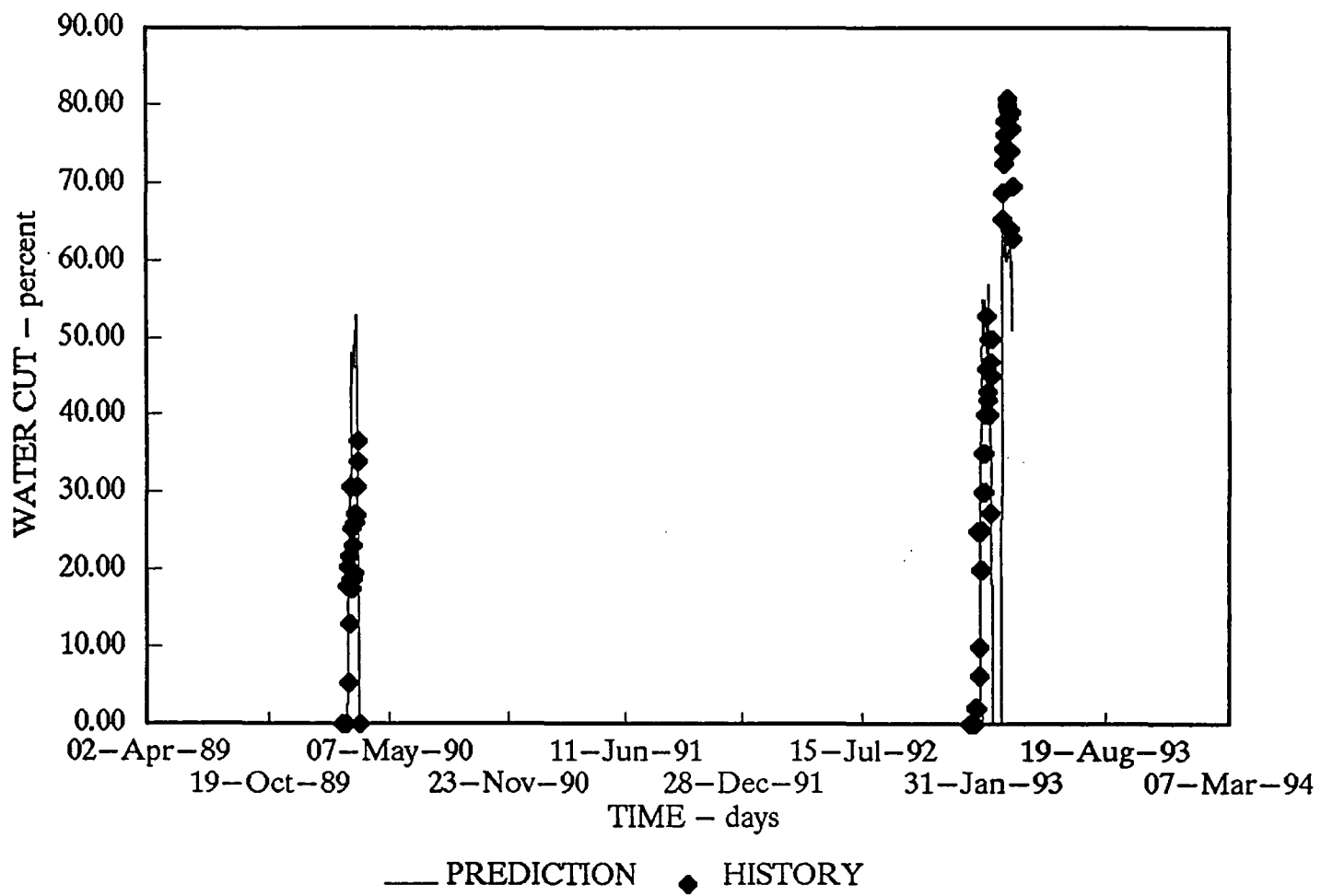


FIGURE 14

HISTORY MATCH WATER CUT



PARAMOUNT CAMERON L47

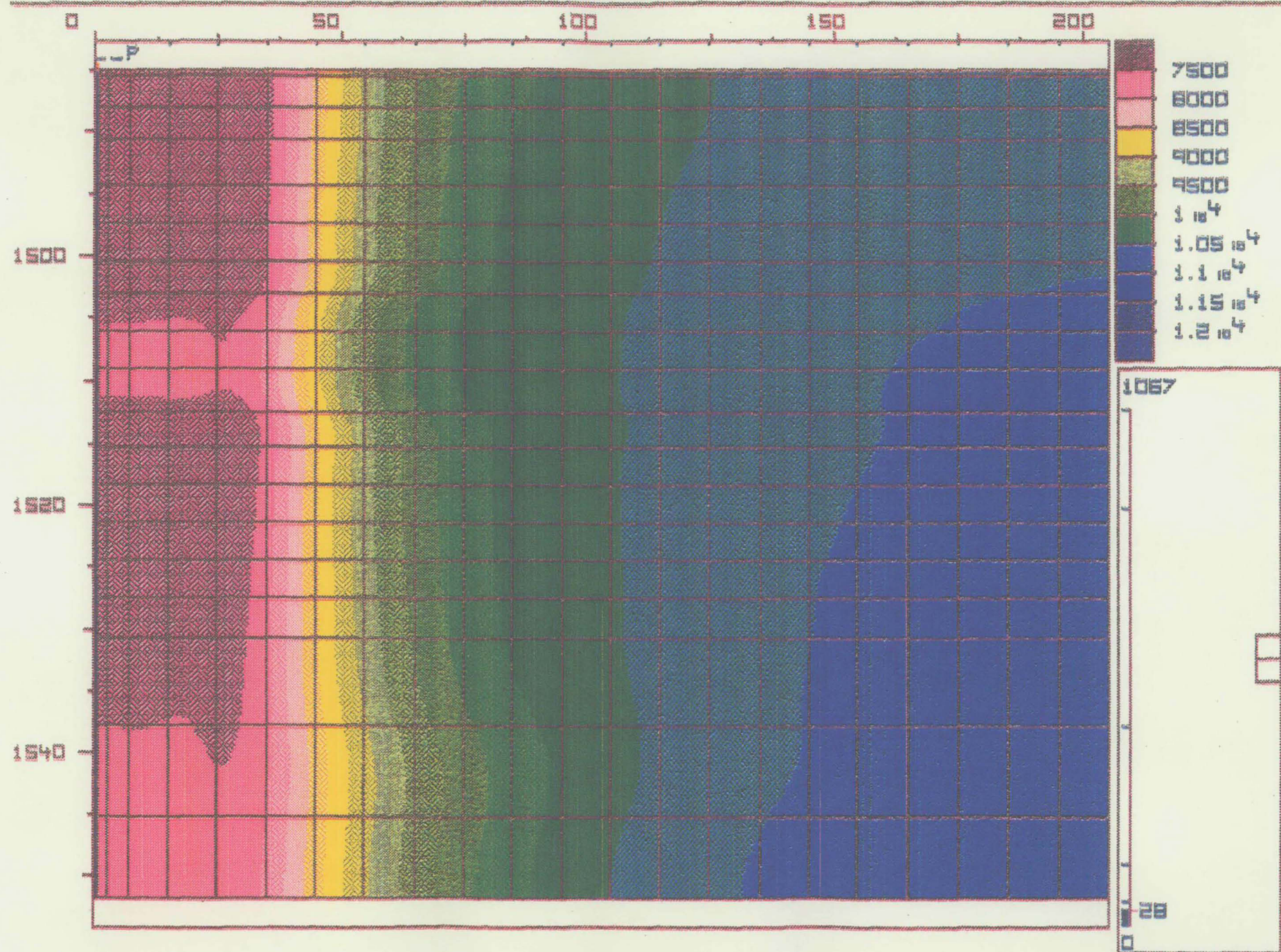


FIGURE 15 MATRIX PRESSURE 28 DAYS

PARAMOUNT CAMERON L47

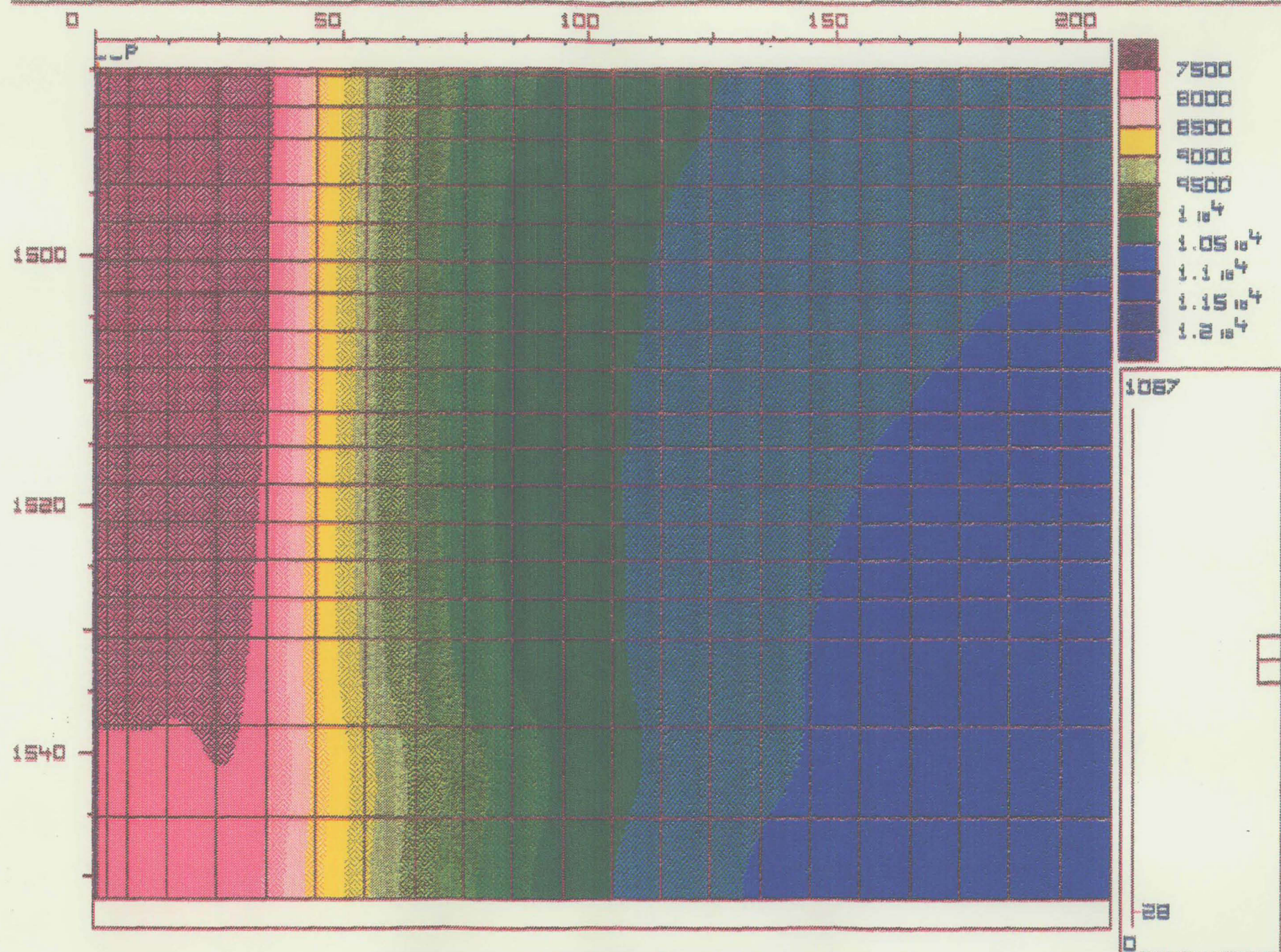


FIGURE 16 FRACTURE PRESSURE 28 DAYS

SimStation

PARAMOUNT CAMERON L47

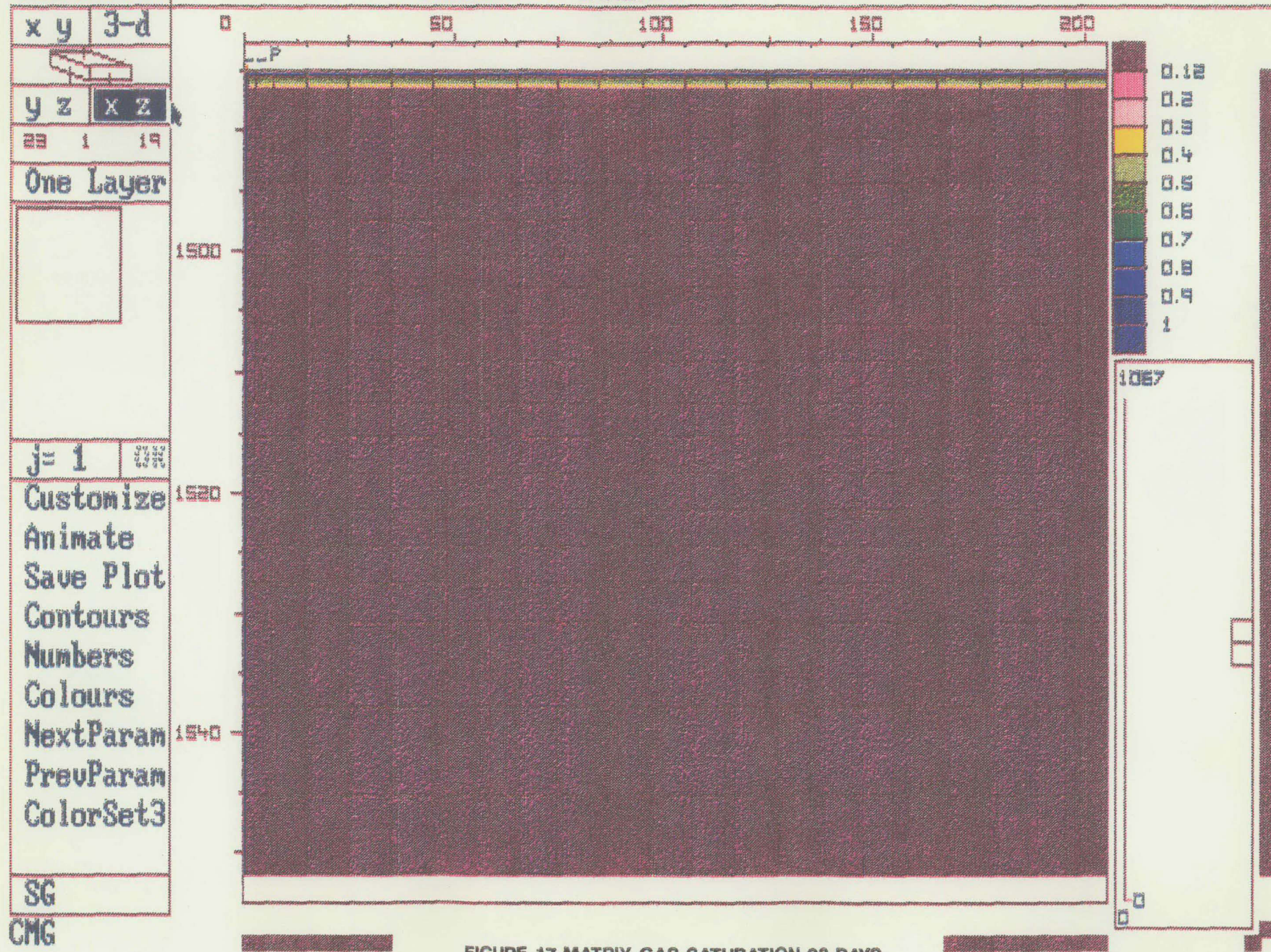


FIGURE 17 MATRIX GAS SATURATION 28 DAYS

SimStation

PARAMOUNT CAMERON L47

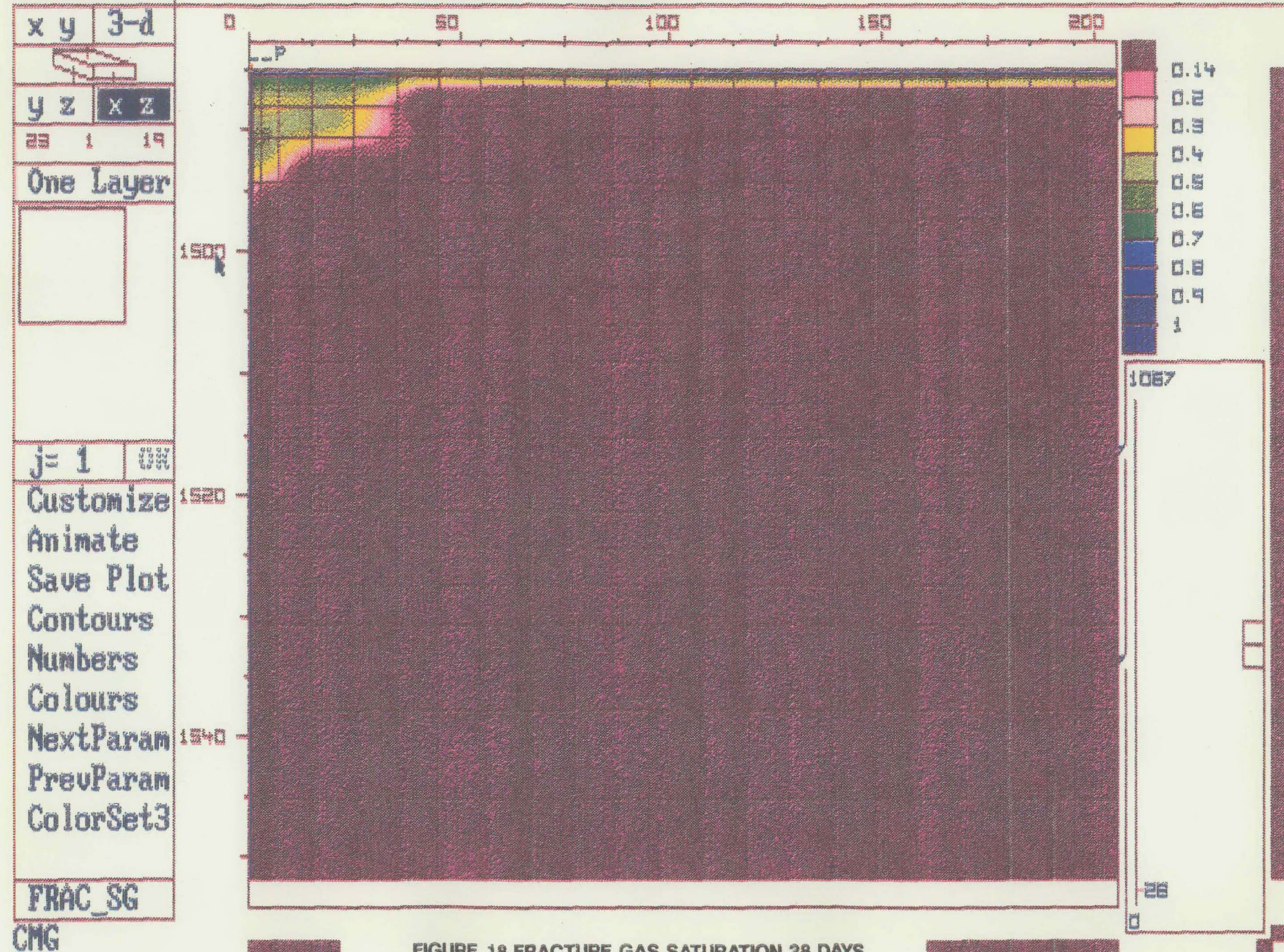


FIGURE 18 FRACTURE GAS SATURATION 28 DAYS

PARAMOUNT CAMERON L47

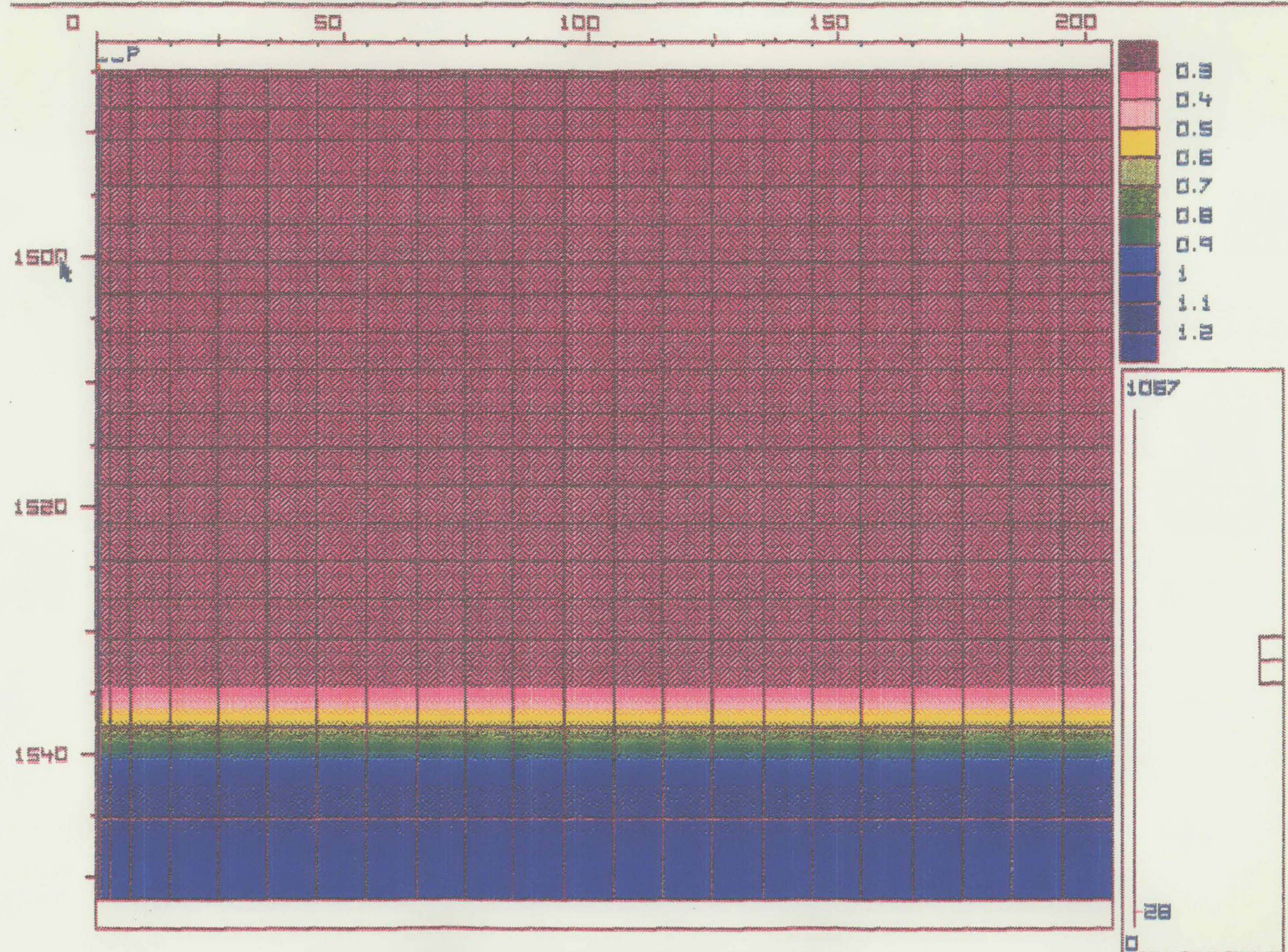


FIGURE 19 MATRIX WATER SATURATION 28 DAYS

PARAMOUNT CAMERON L47

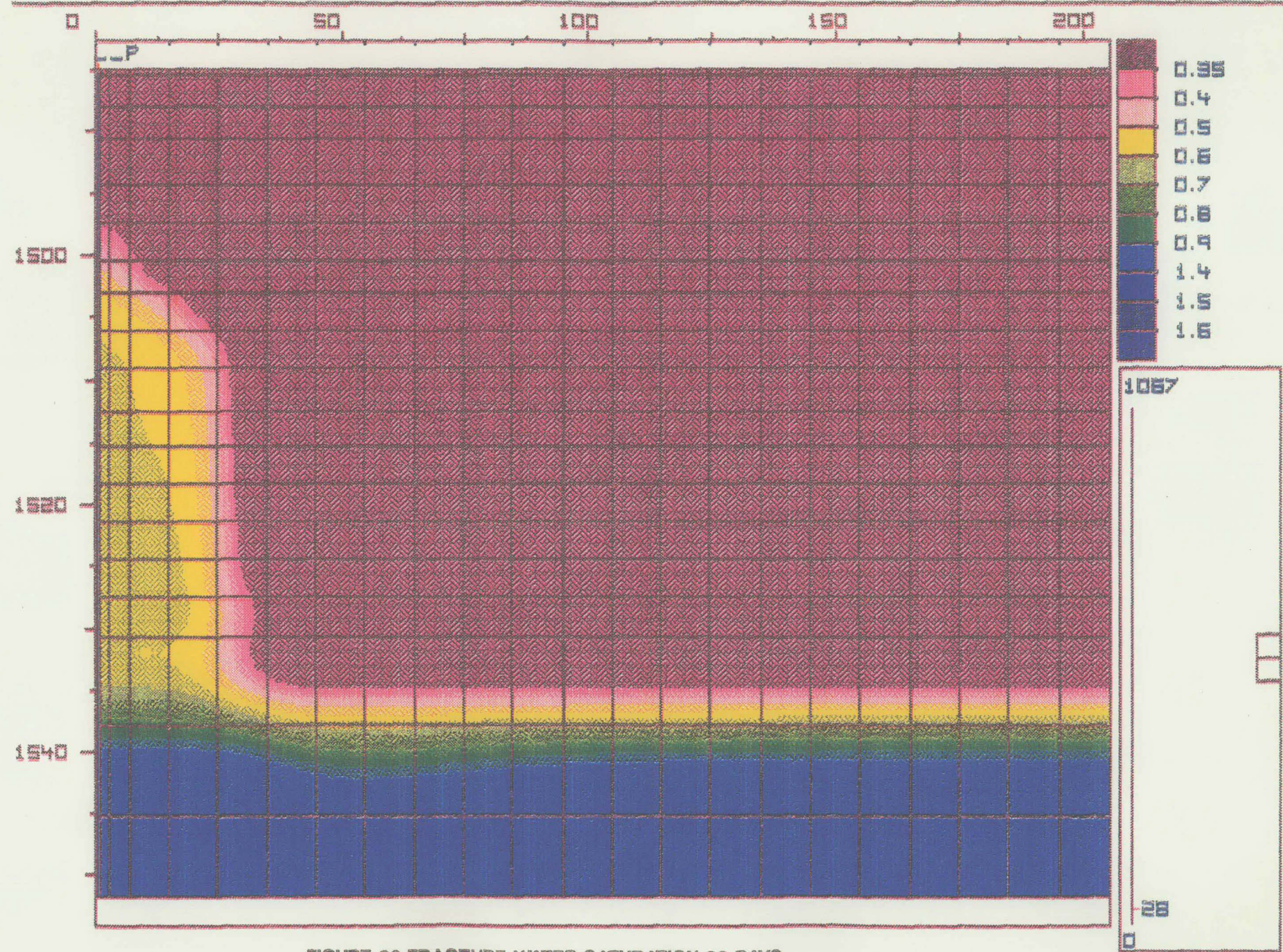


FIGURE 20 FRACTURE WATER SATURATION 28 DAYS

PARAMOUNT CAMERON L47

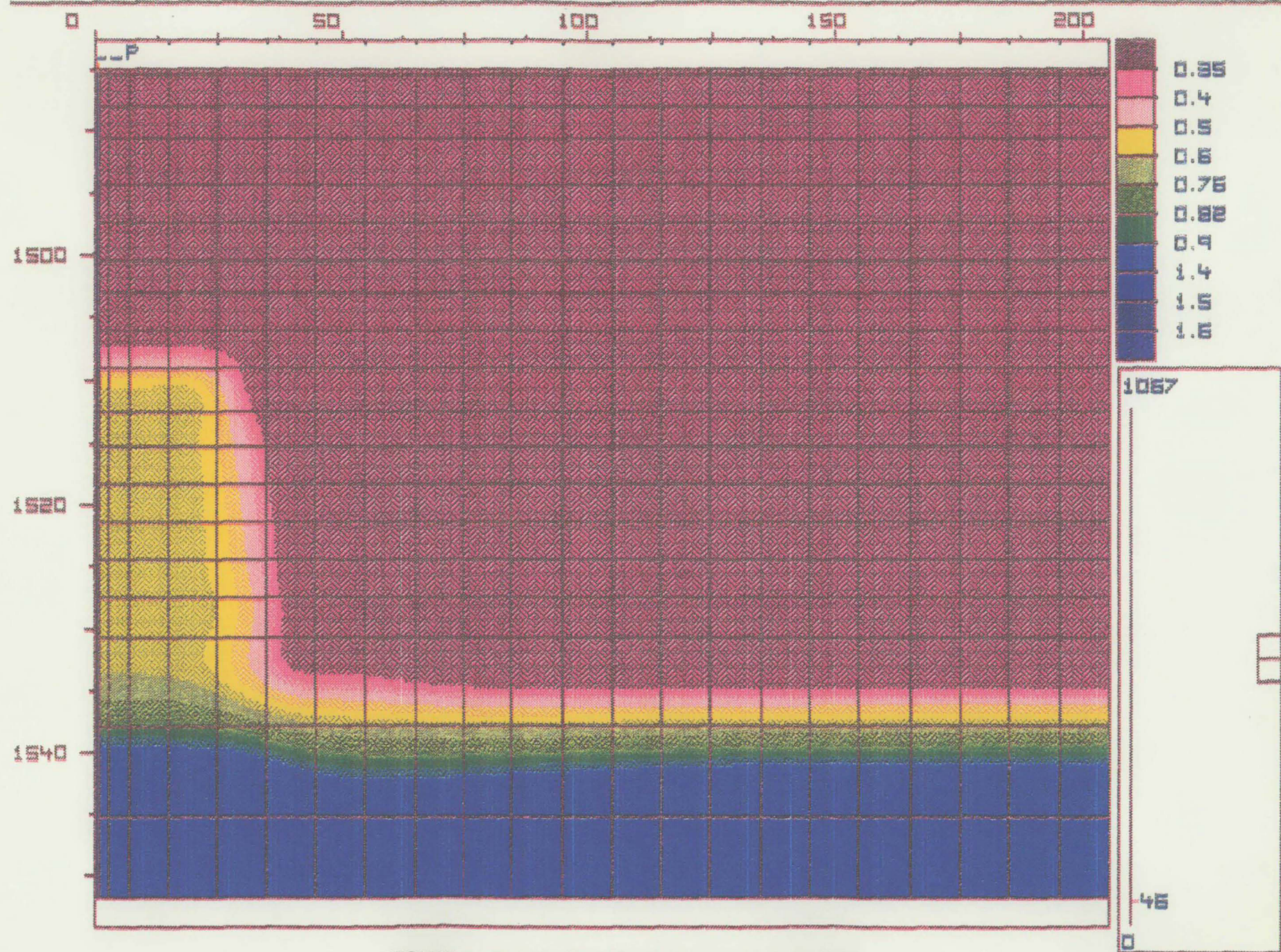


FIGURE 21 FRACTURE WATER SATURATION 46 DAYS

PARAMOUNT CAMERON L47

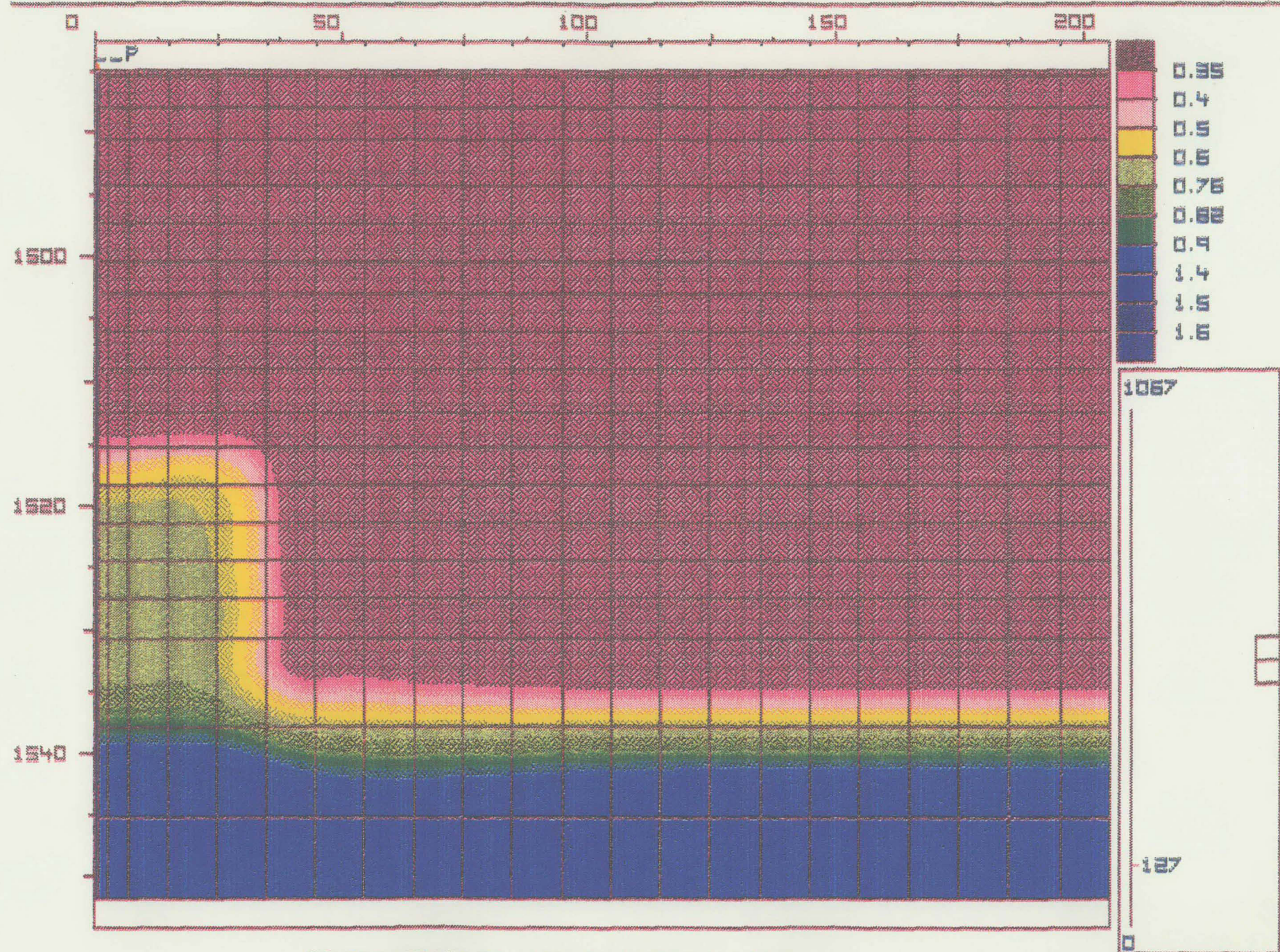


FIGURE 22 FRACTURE WATER SATURATION 127 DAYS

PARAMOUNT CAMERON L47

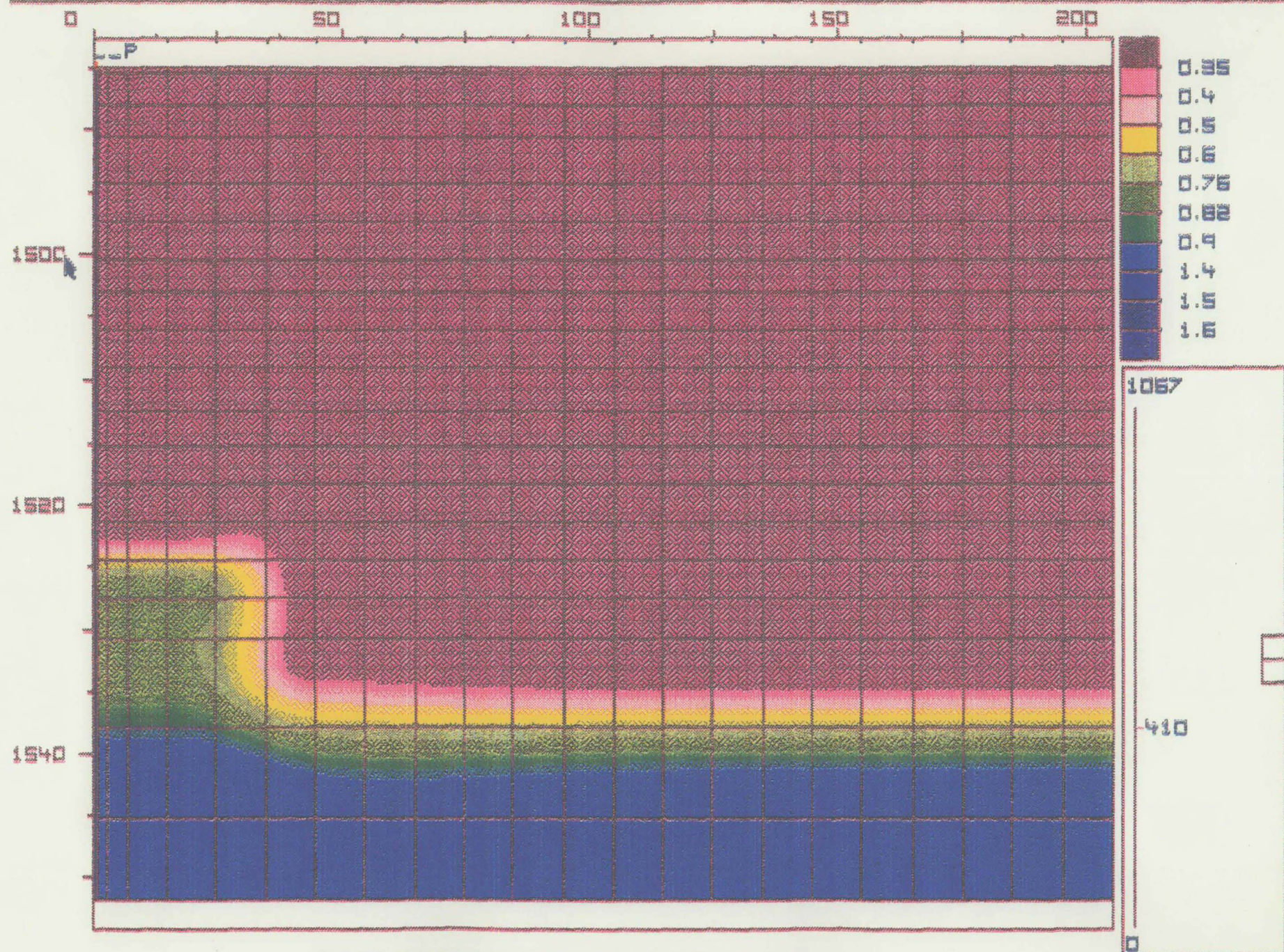
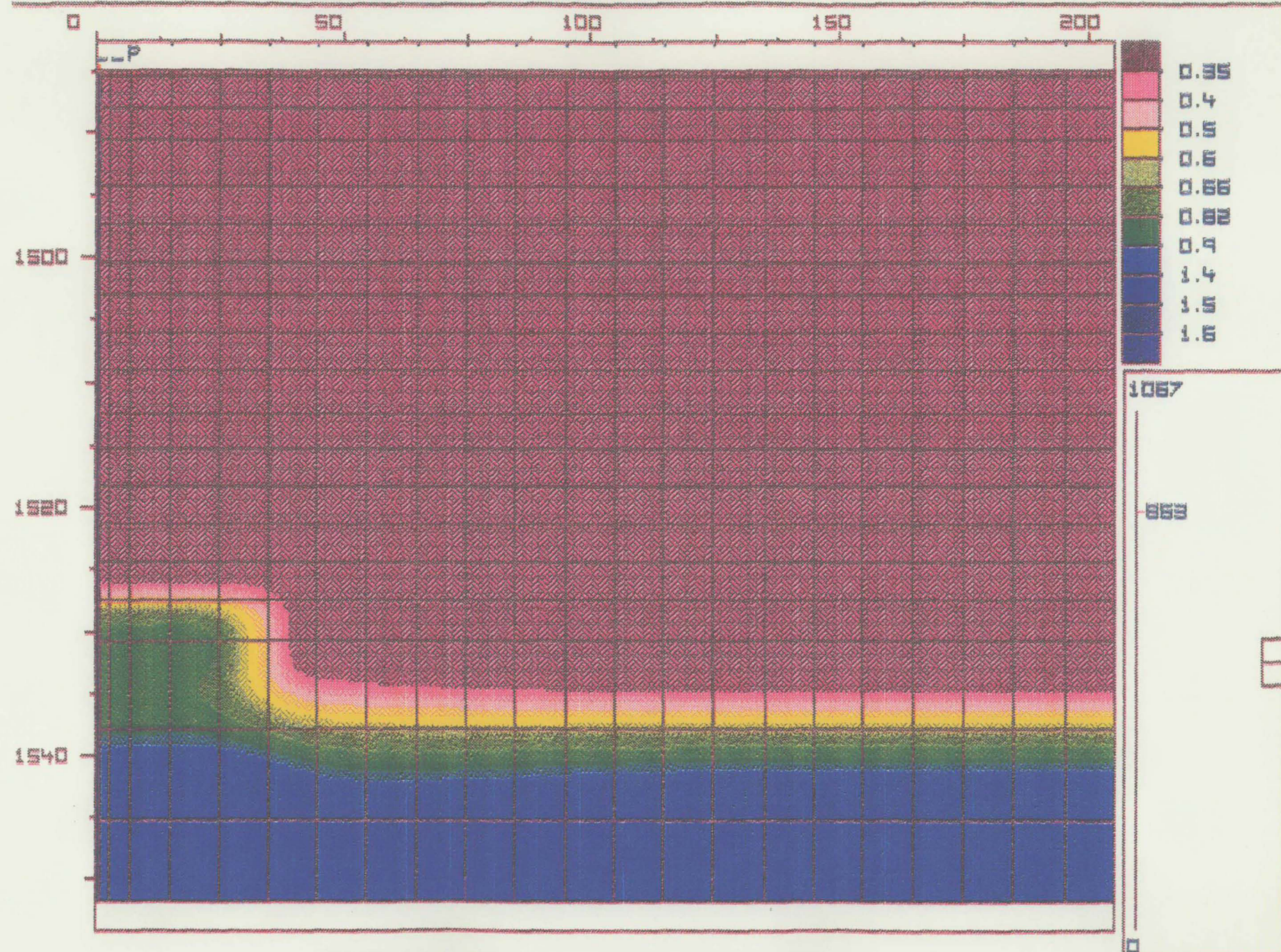


FIGURE 23 FRACTURE WATER SATURATION 410 DAYS

PARAMOUNT CAMERON L47



PARAMOUNT CAMERON L47

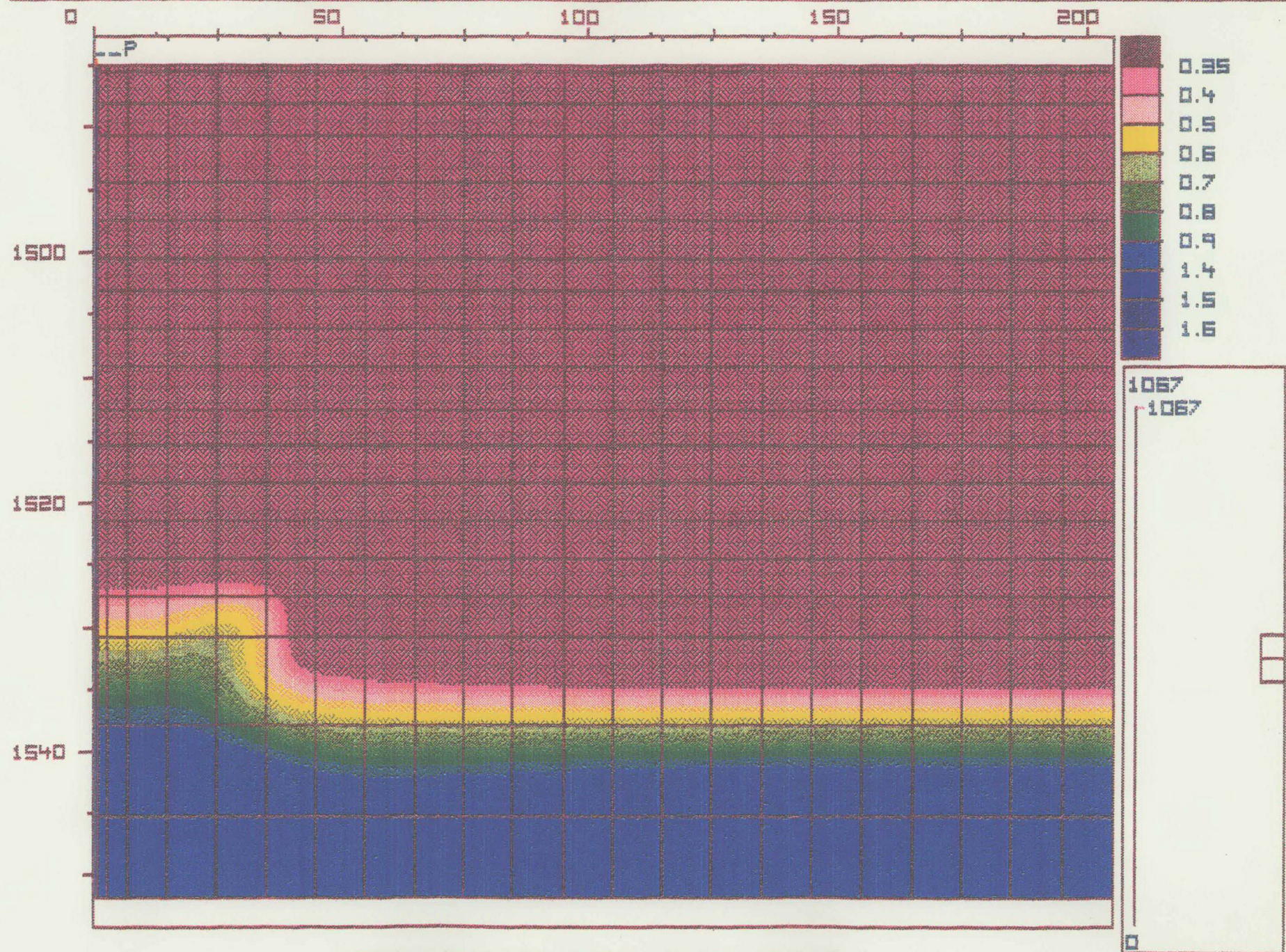


FIGURE 26

COMPARISON OF OIL RATES

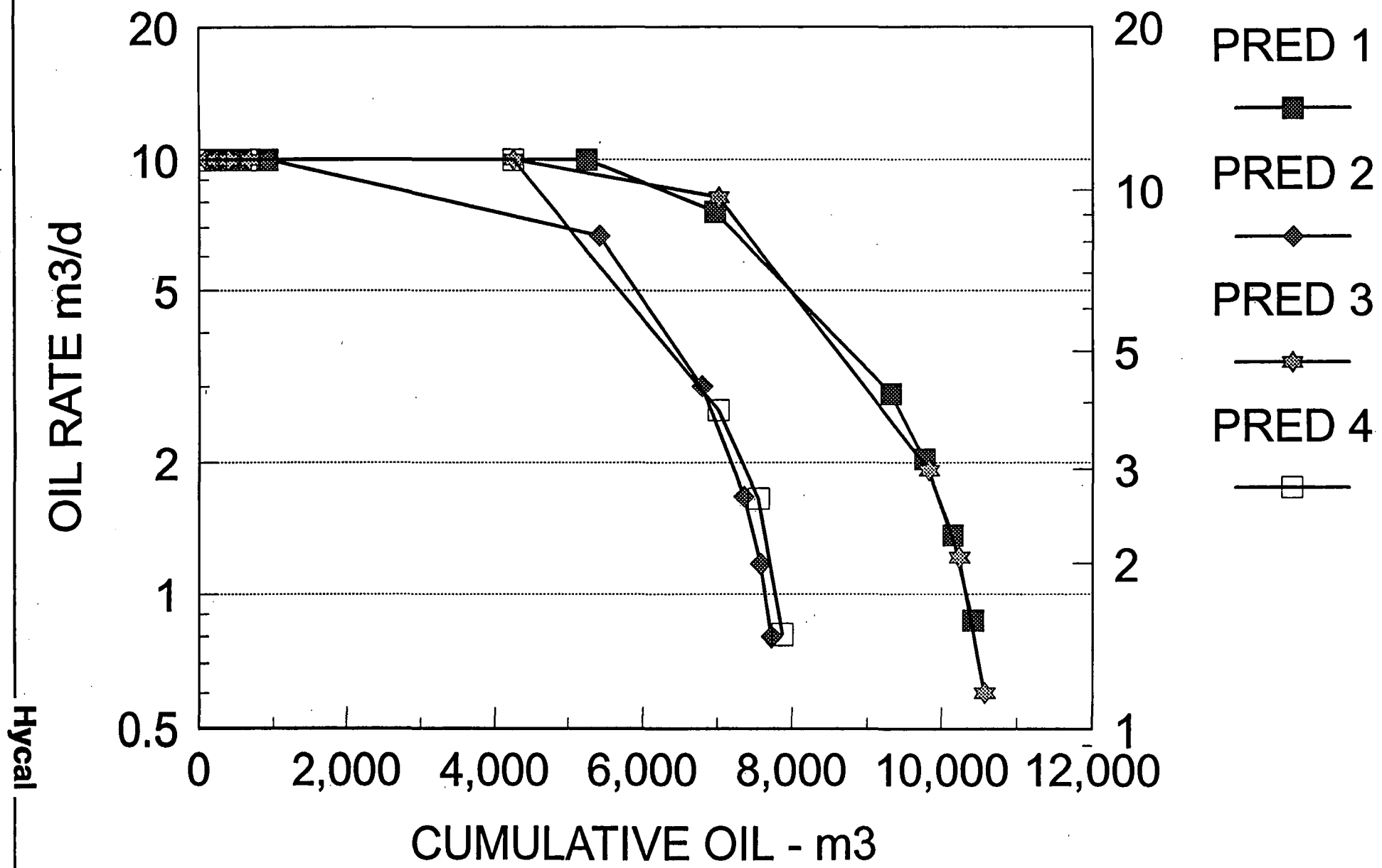


FIGURE 27

COMPARISON OF OIL RATES

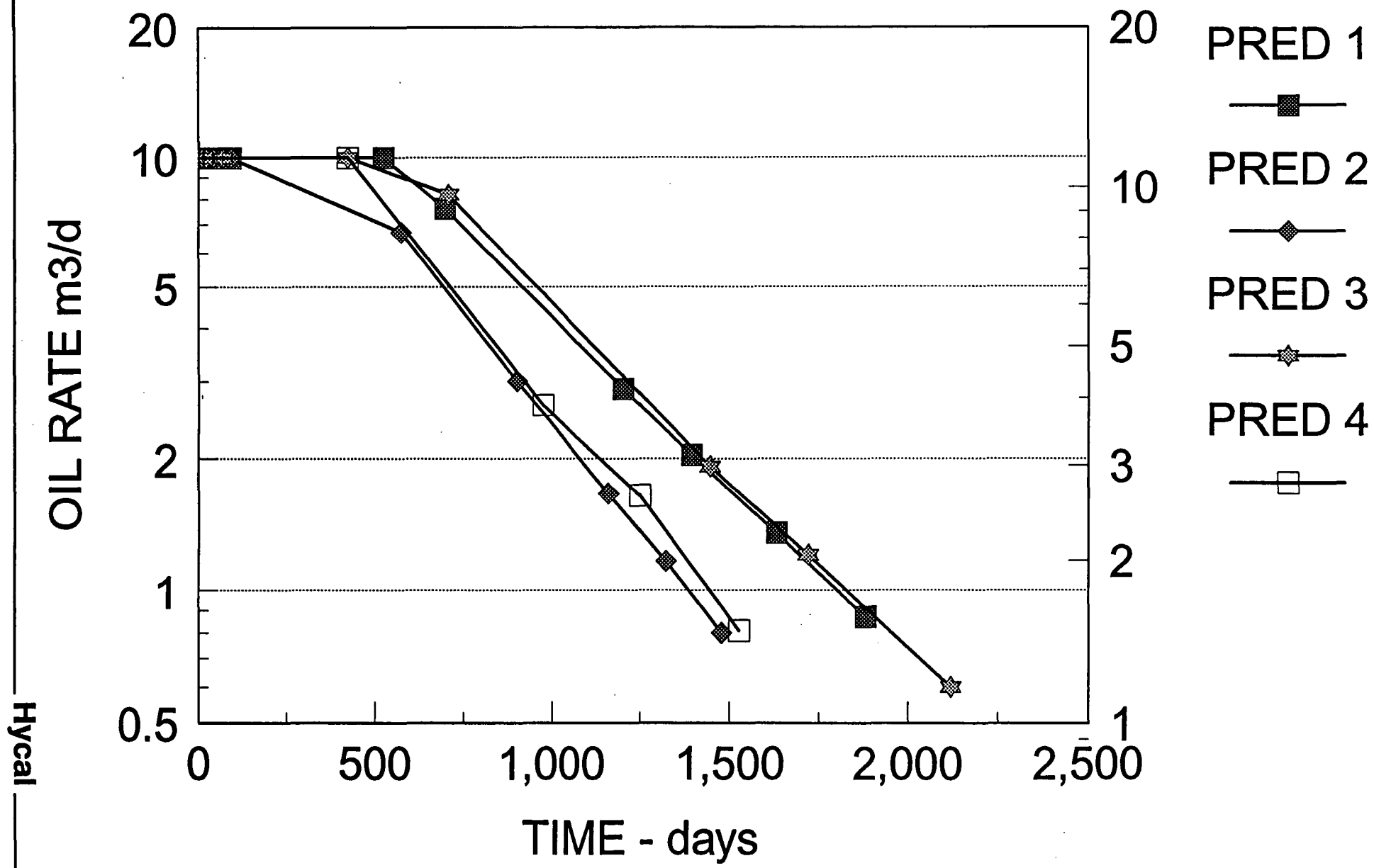


FIGURE 28

COMPARISON OF PRODUCING GAS OIL RATIOS

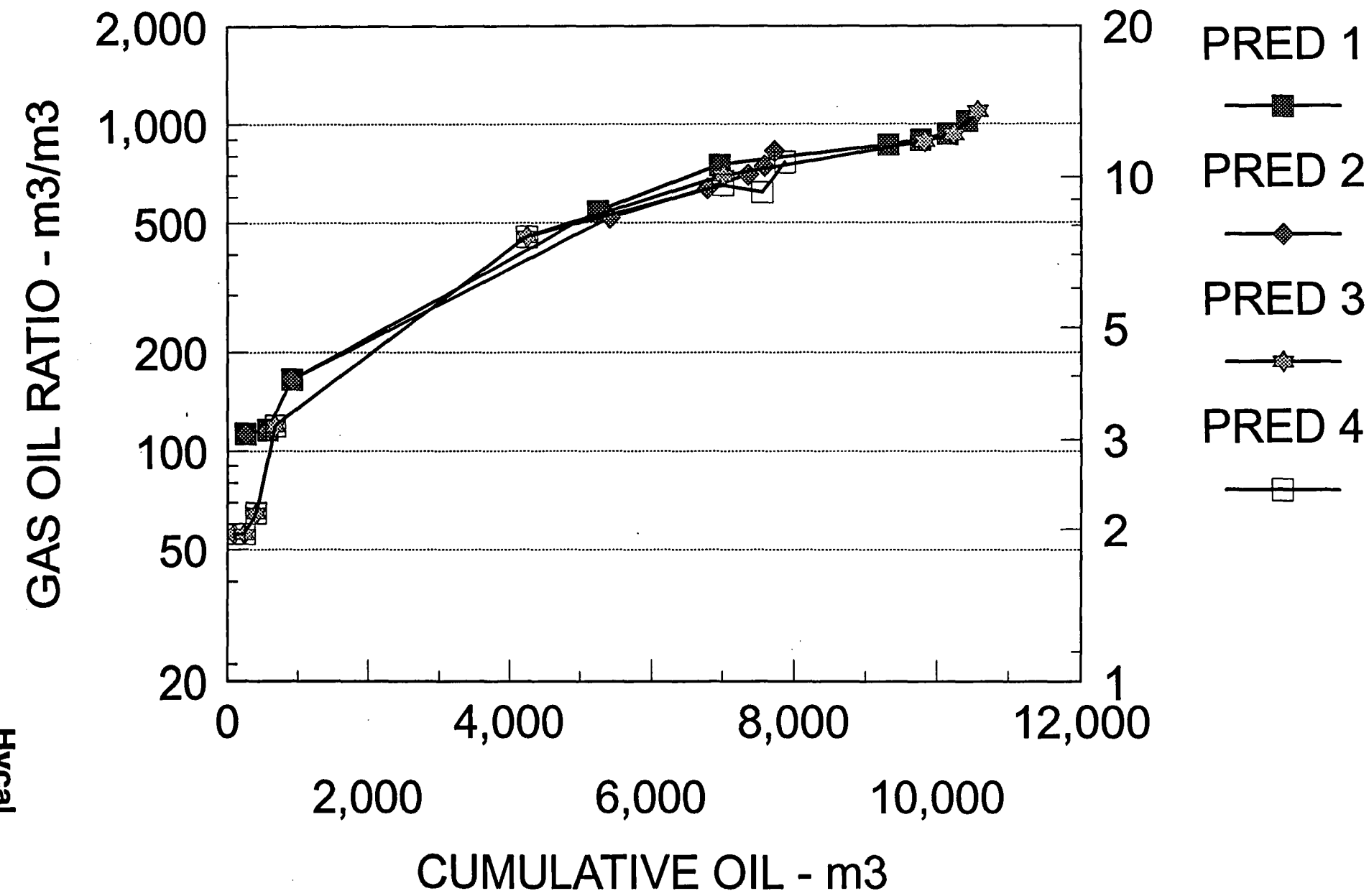


FIGURE 29

COMPARISON OF PRODUCING GAS OIL RATIOS

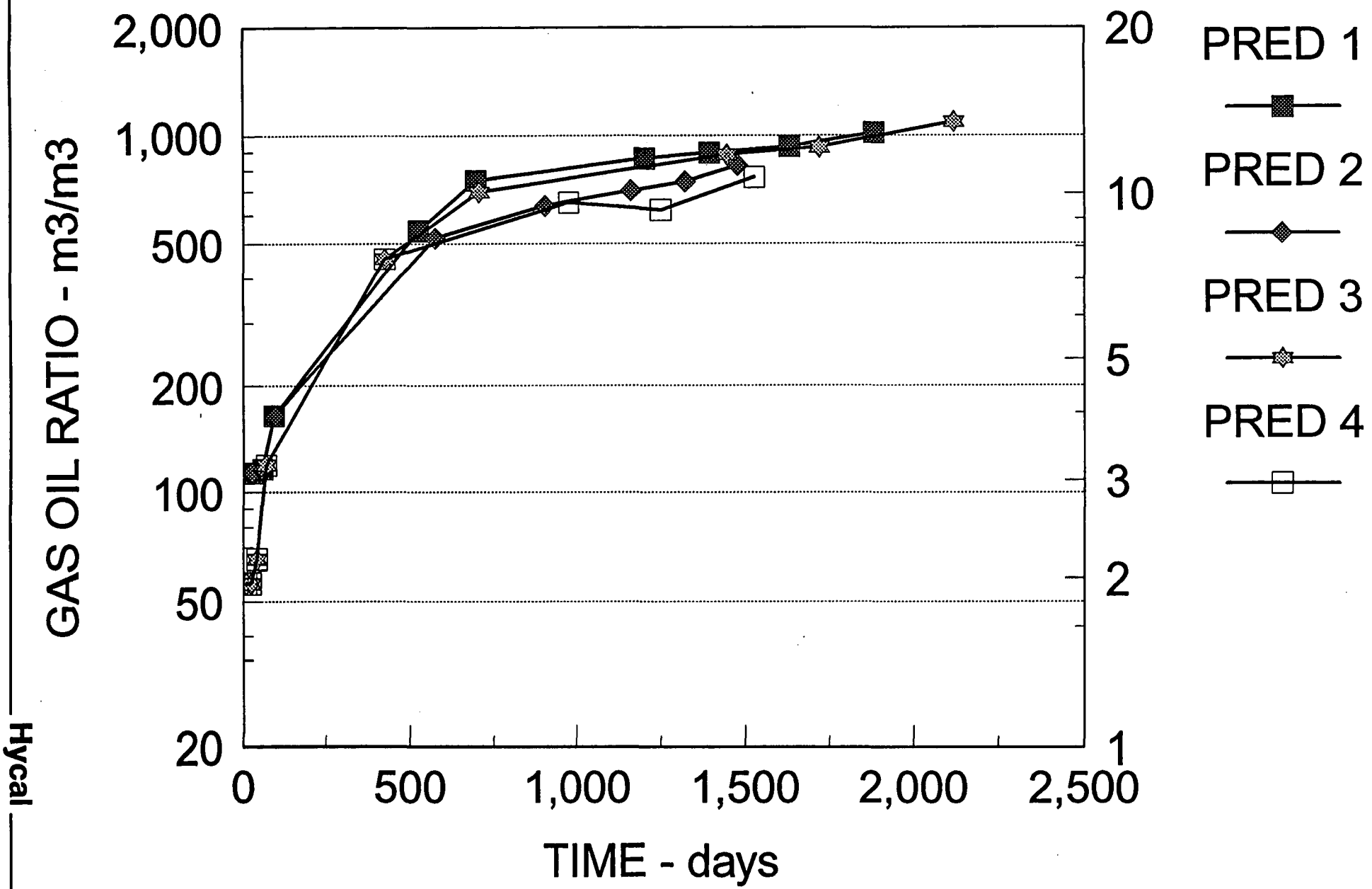


FIGURE 30

COMPARISON OF WATER CUT

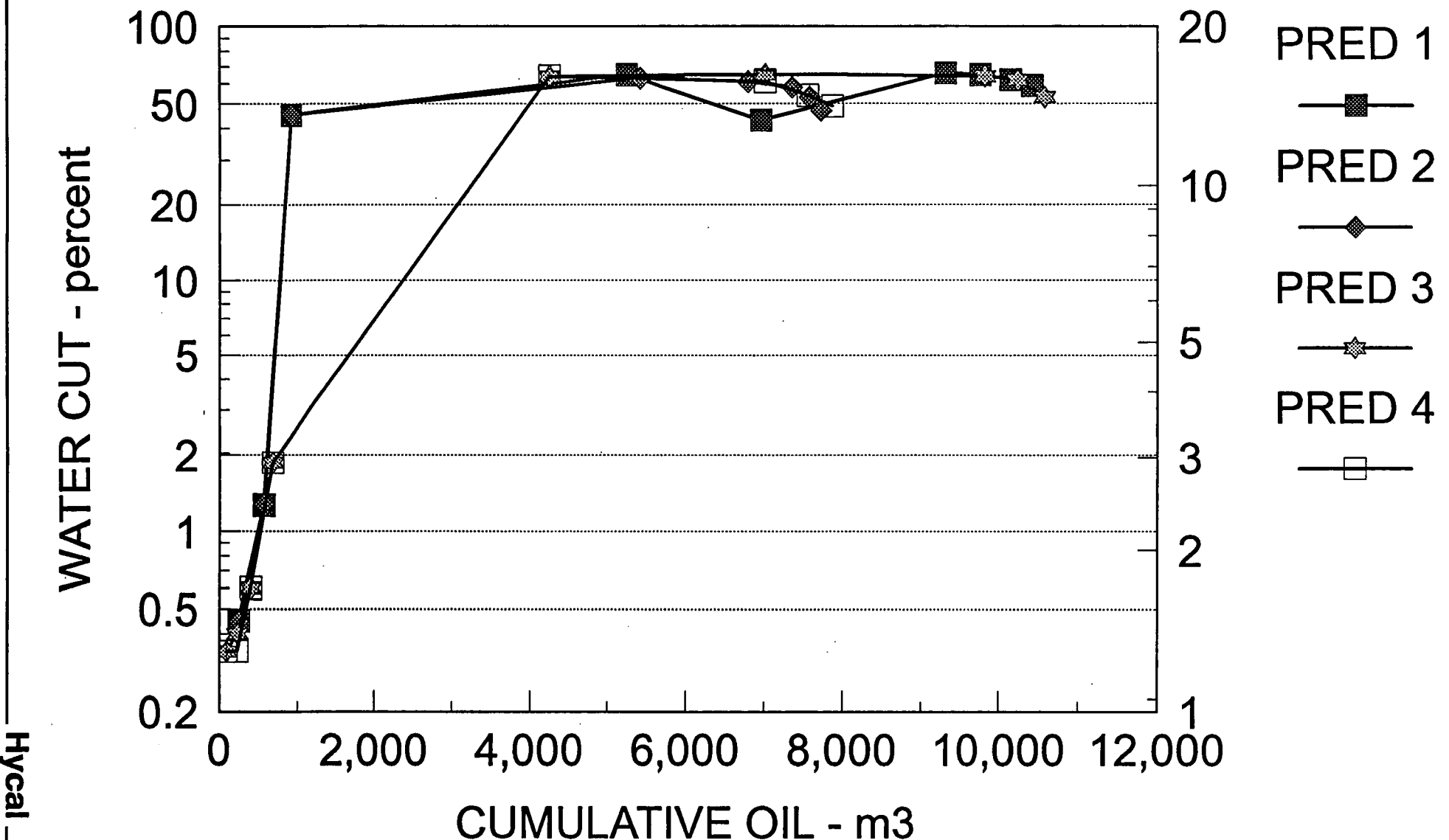


FIGURE 31

COMPARISON OF WATER CUT

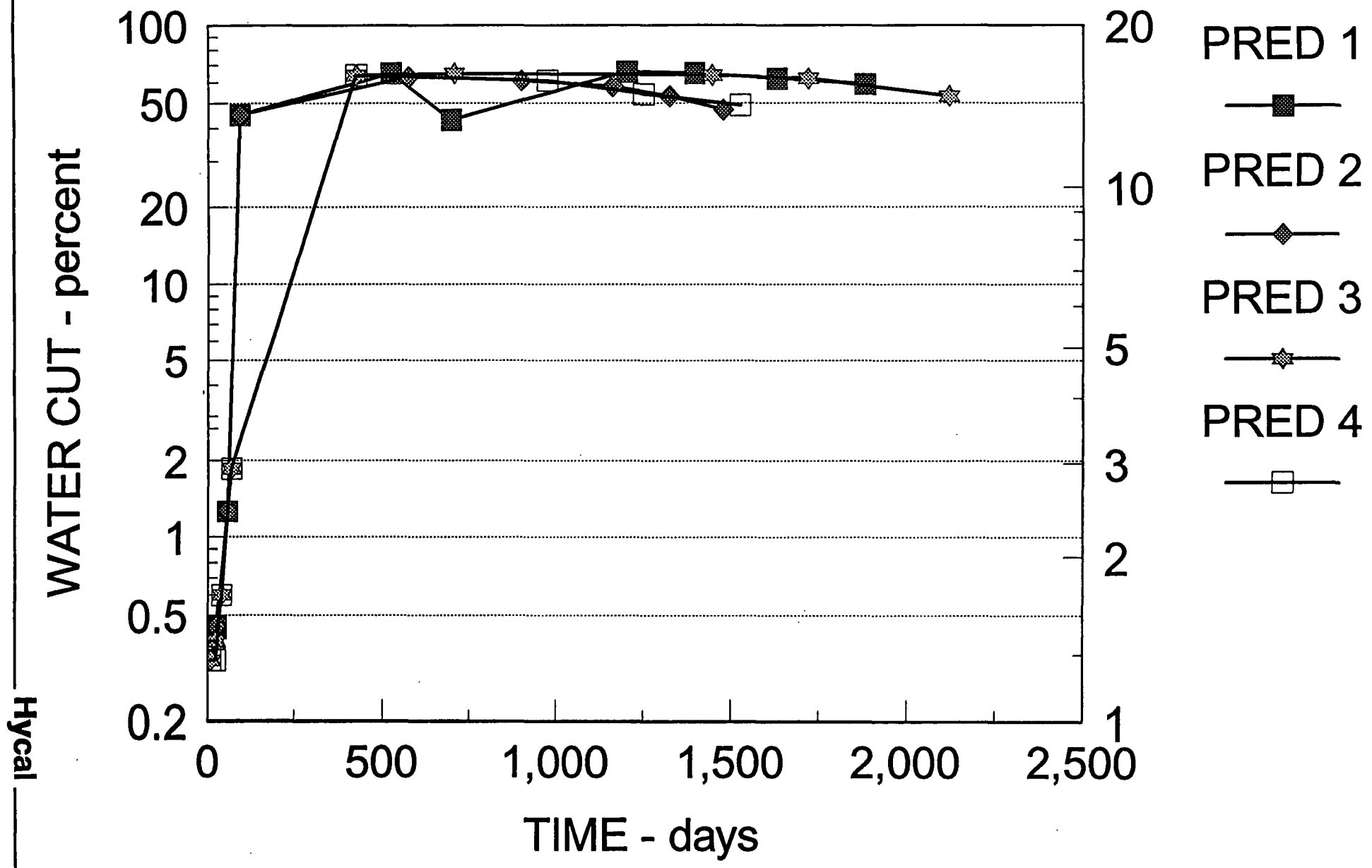


FIGURE 32

COMPARISON OF CUMULATIVE OIL

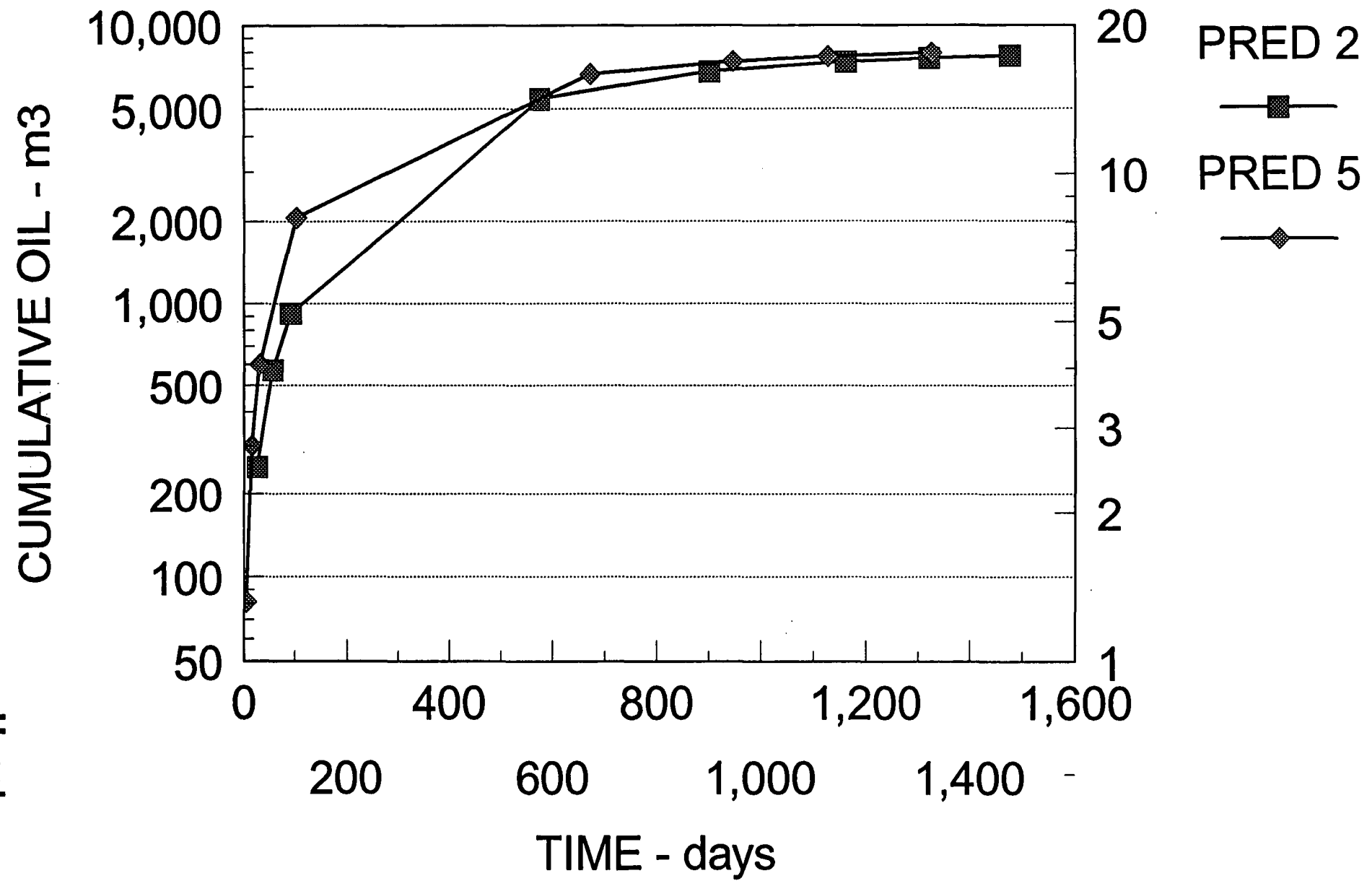


FIGURE 33

COMPARISON OF OIL RATES

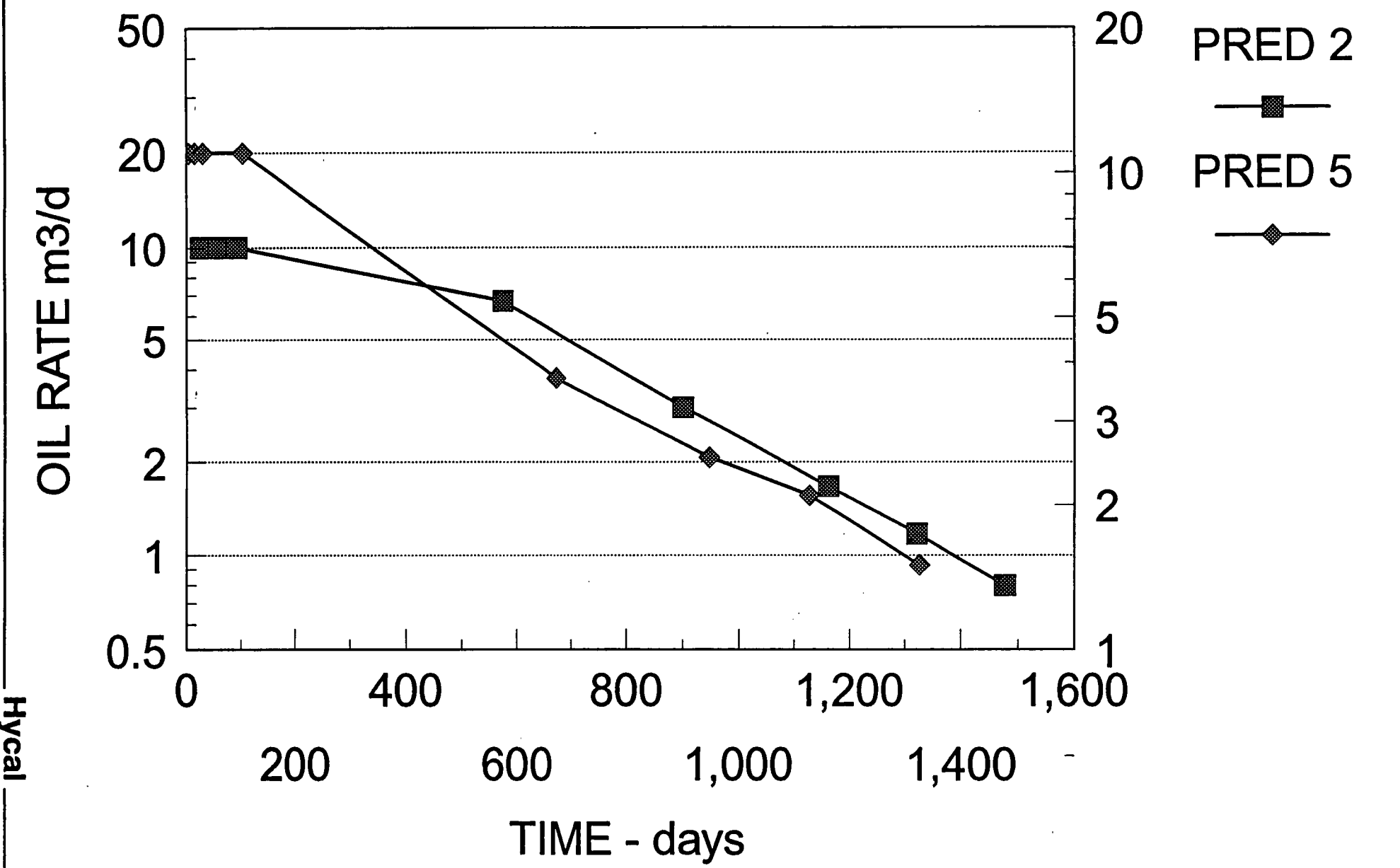


FIGURE 34

COMPARISON OF OIL RATES

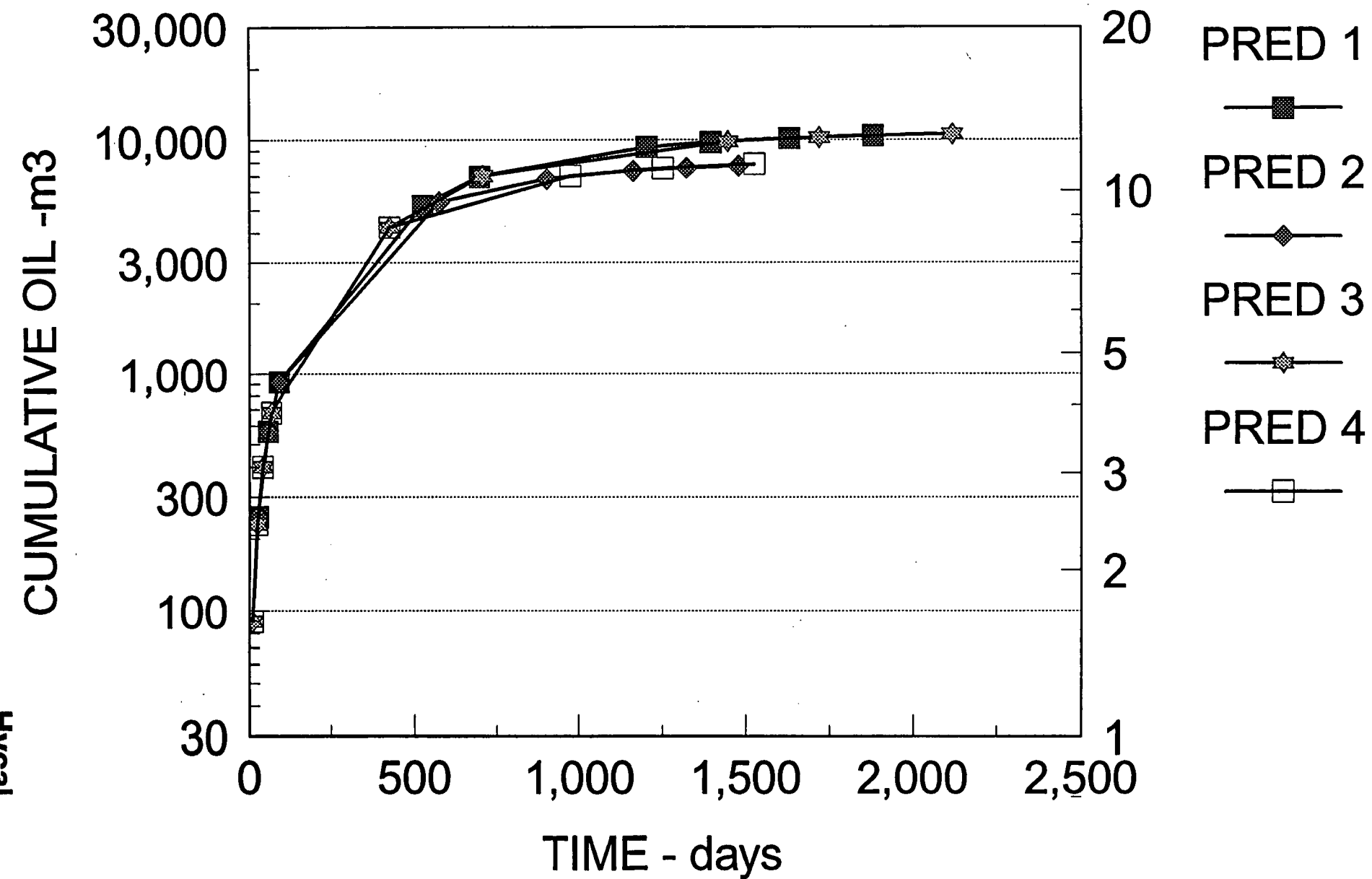


FIGURE 35

COMPARISON OF OIL RATES

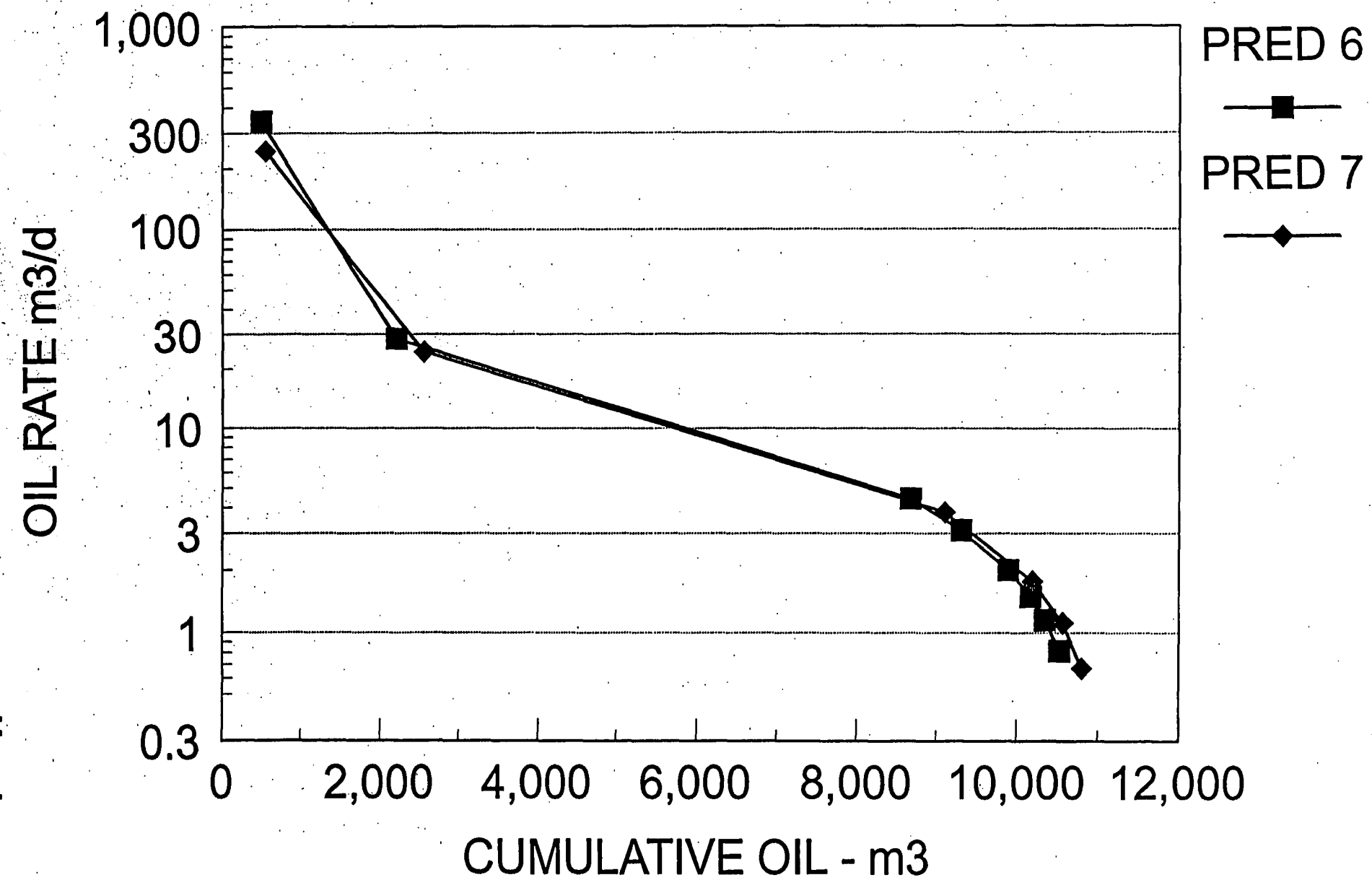


FIGURE 36

COMPARISON OF PRODUCING GAS OIL RATIOS

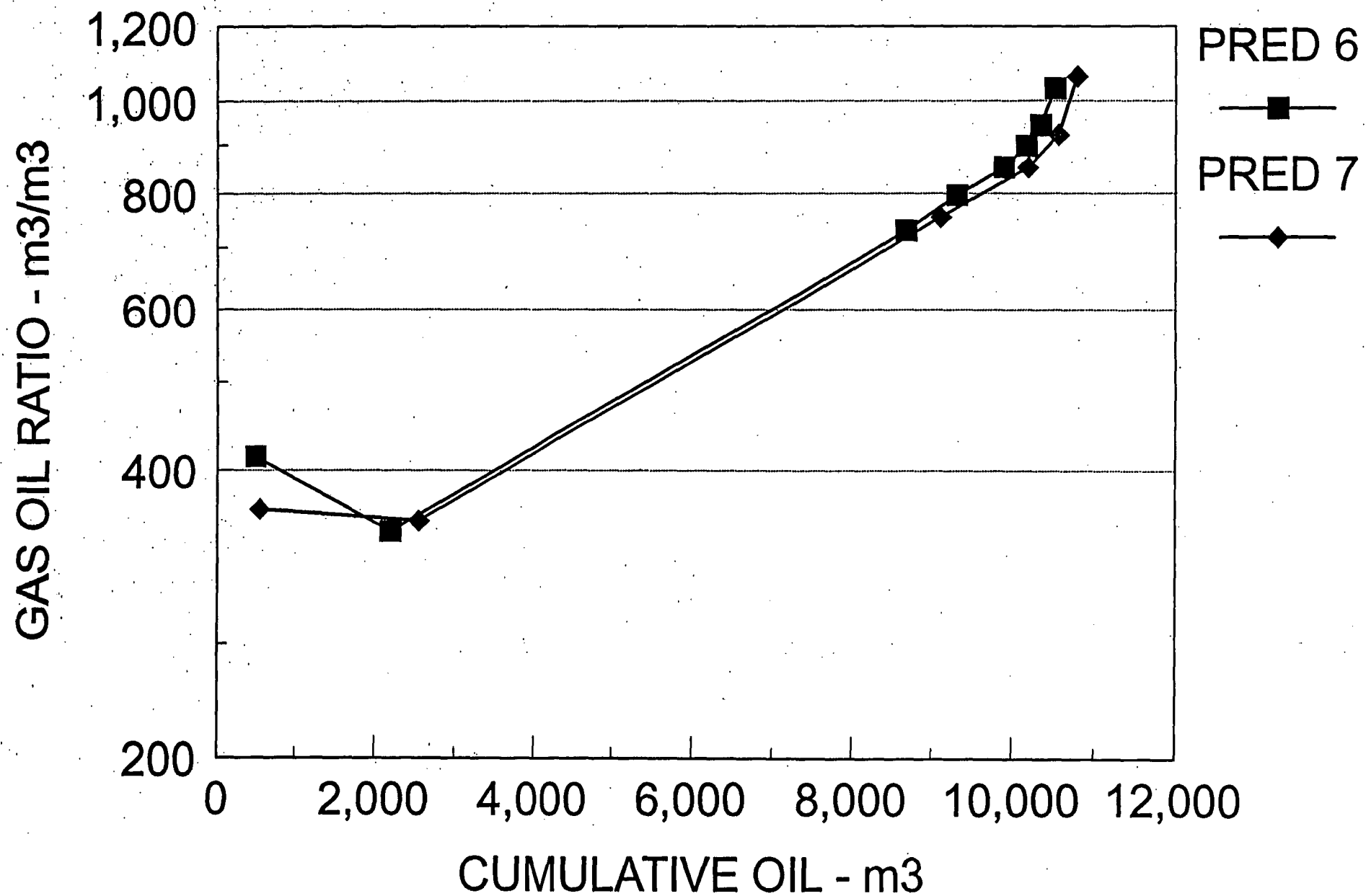


FIGURE 37

COMPARISON OF WATER CUT

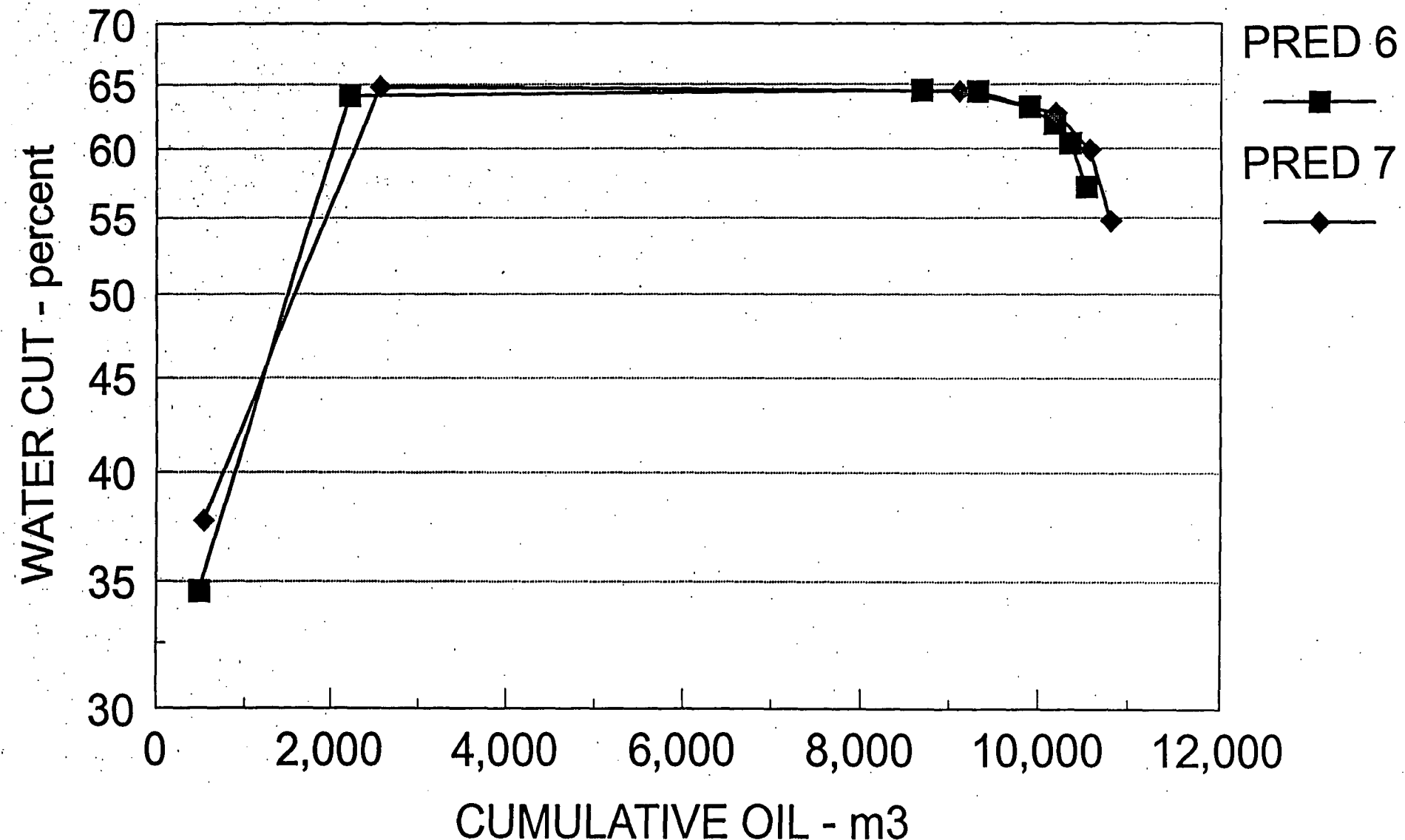


FIGURE 38

COMPARISON OF CUMULATIVE OIL

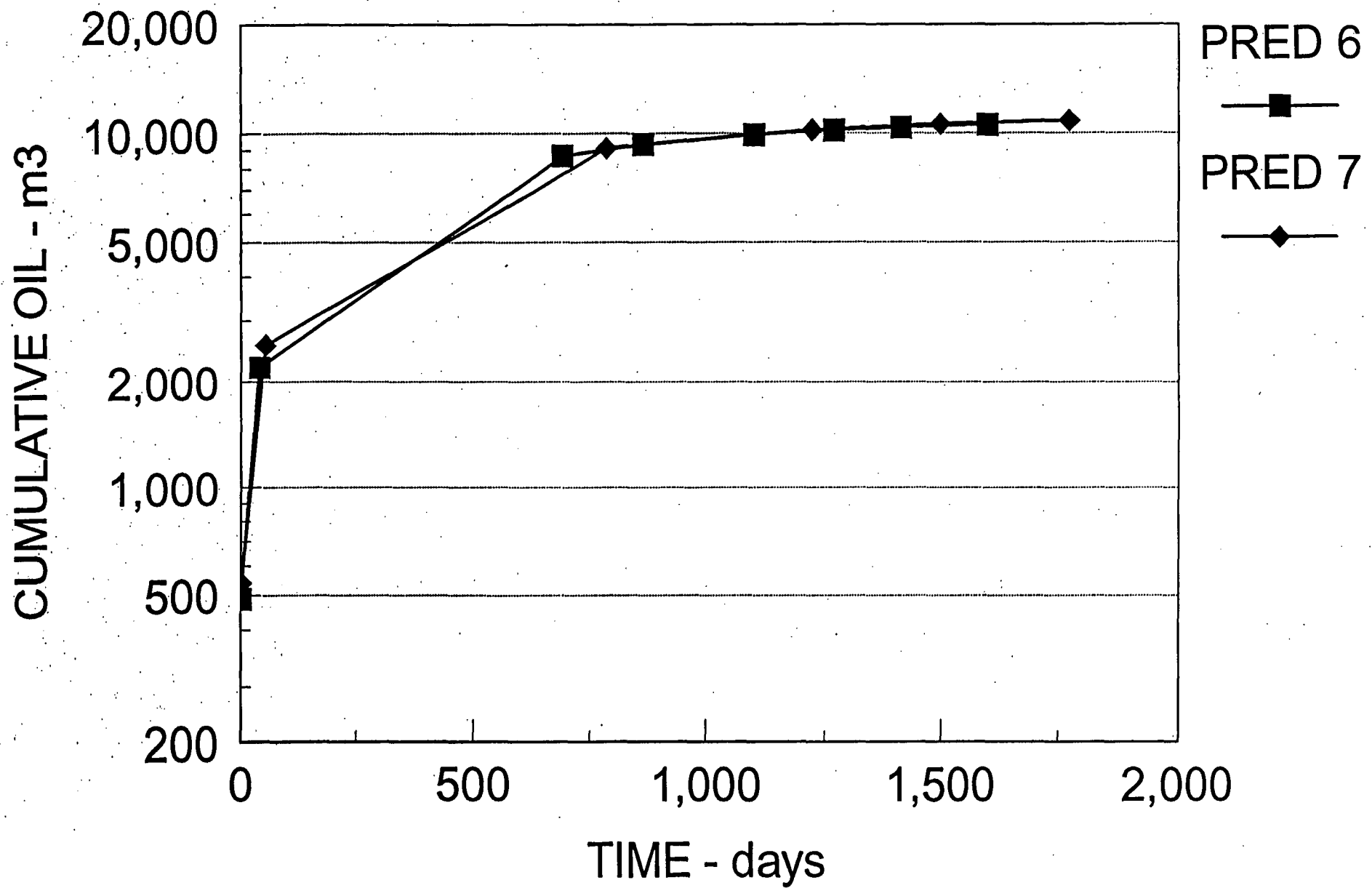
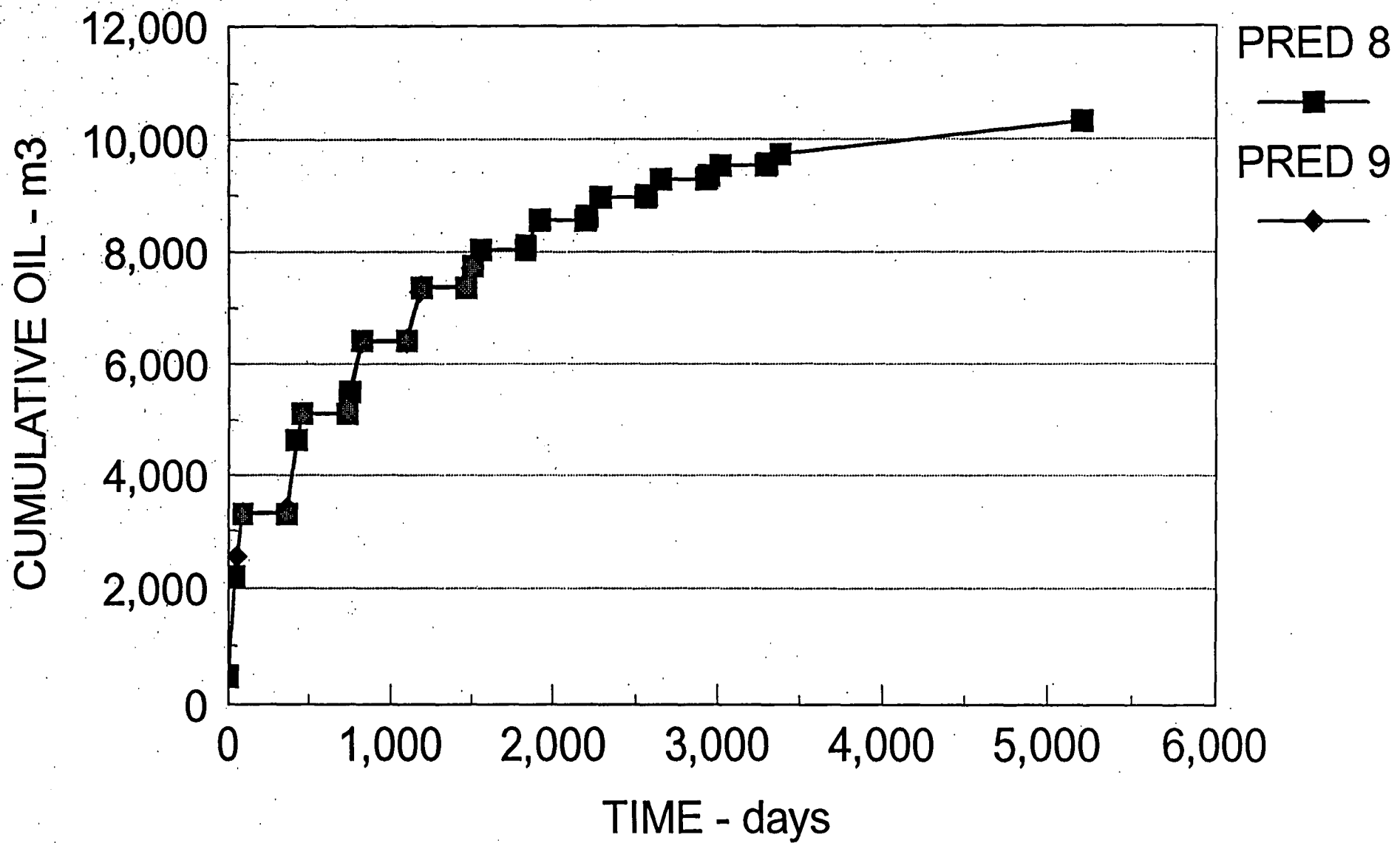


FIGURE 39

COMPARISON OF CUMULATIVE OIL



PARAMOUNT CAMERON L47

PRED9

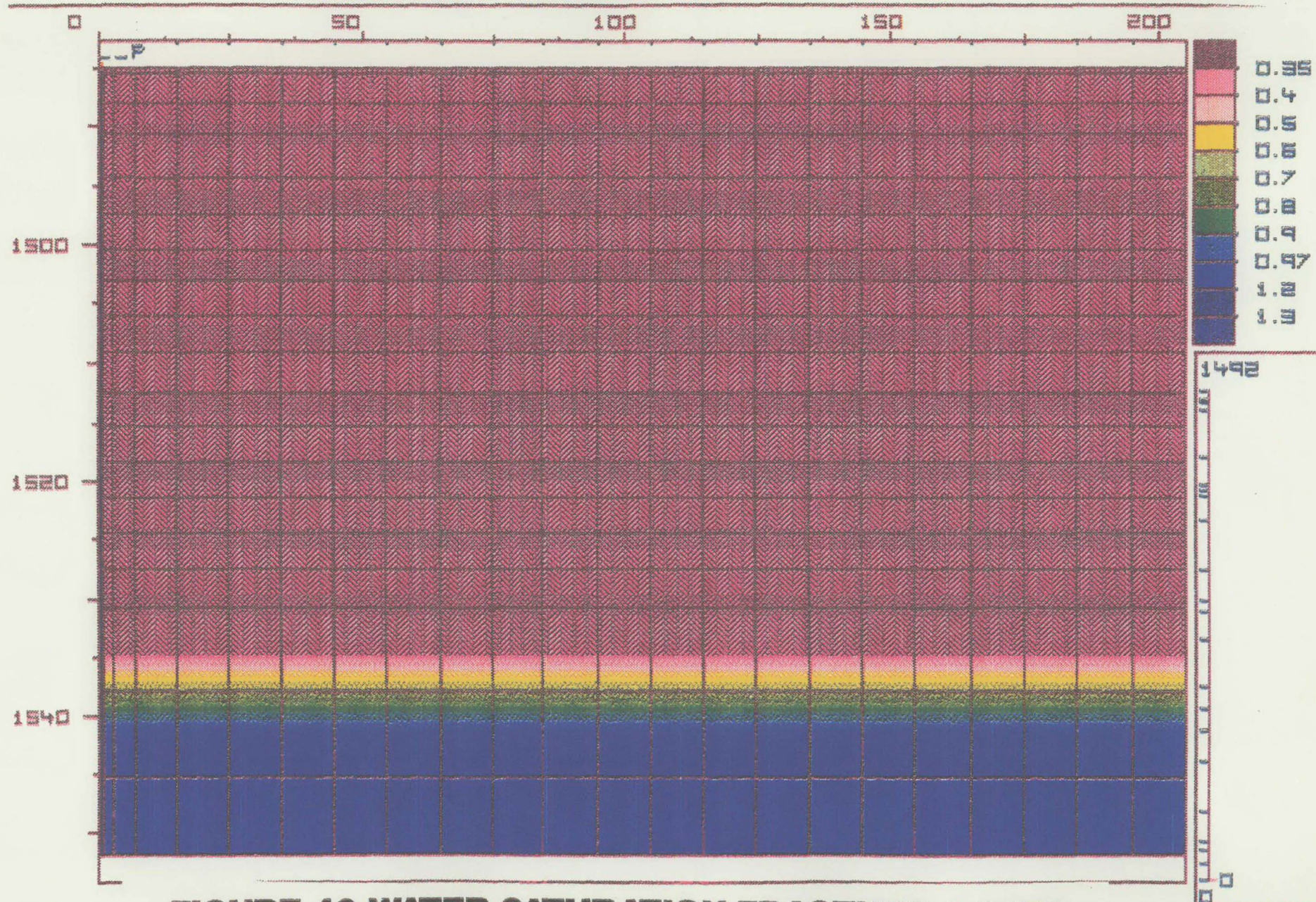


FIGURE 40 WATER SATURATION FRACTURE-0 DAYS

PARAMOUNT CAMERON L47

PRED9

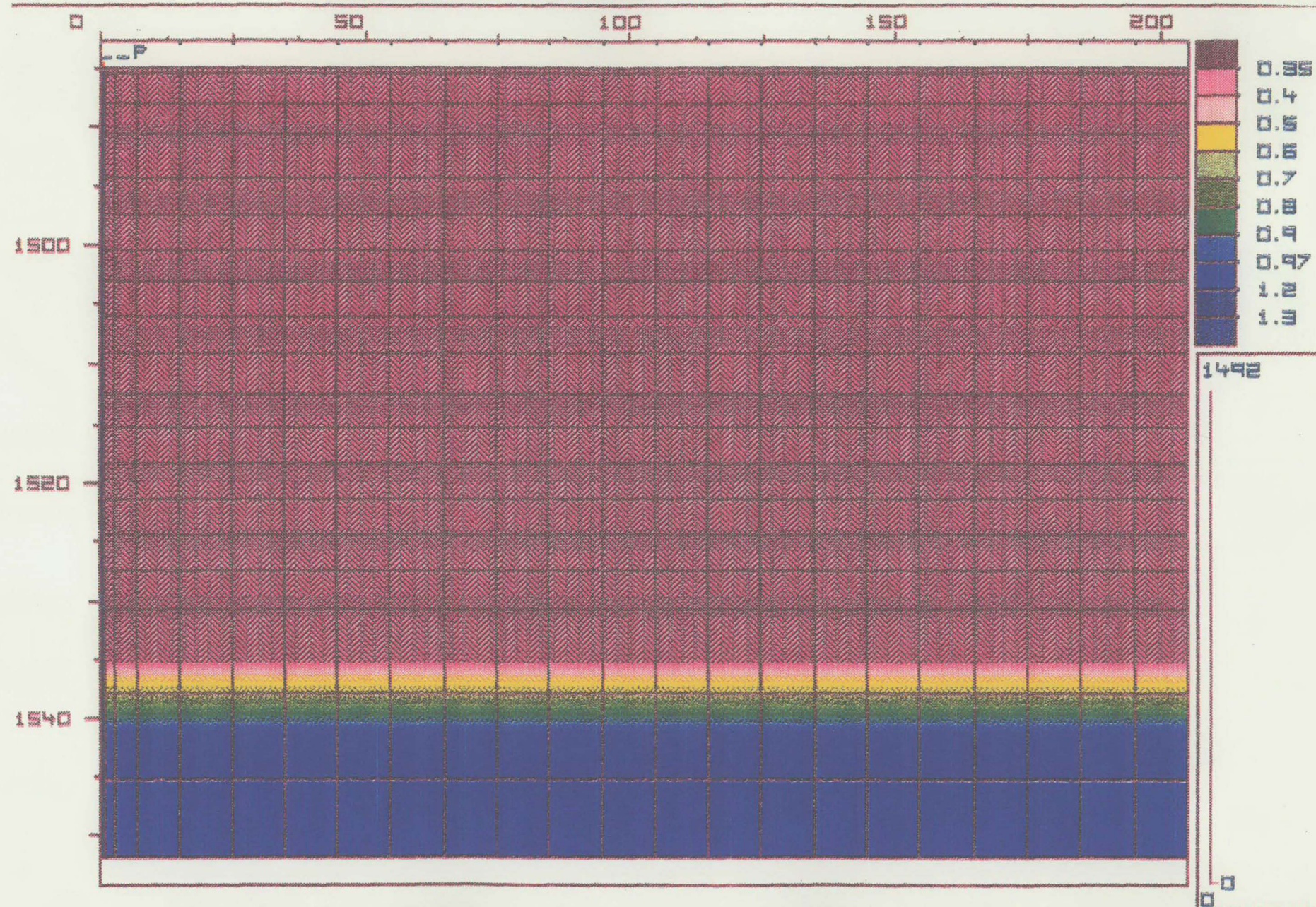


FIGURE 41 WATER SATURATION MATRIX-0 DAYS

PARAMOUNT CAMERON L47

PRED9

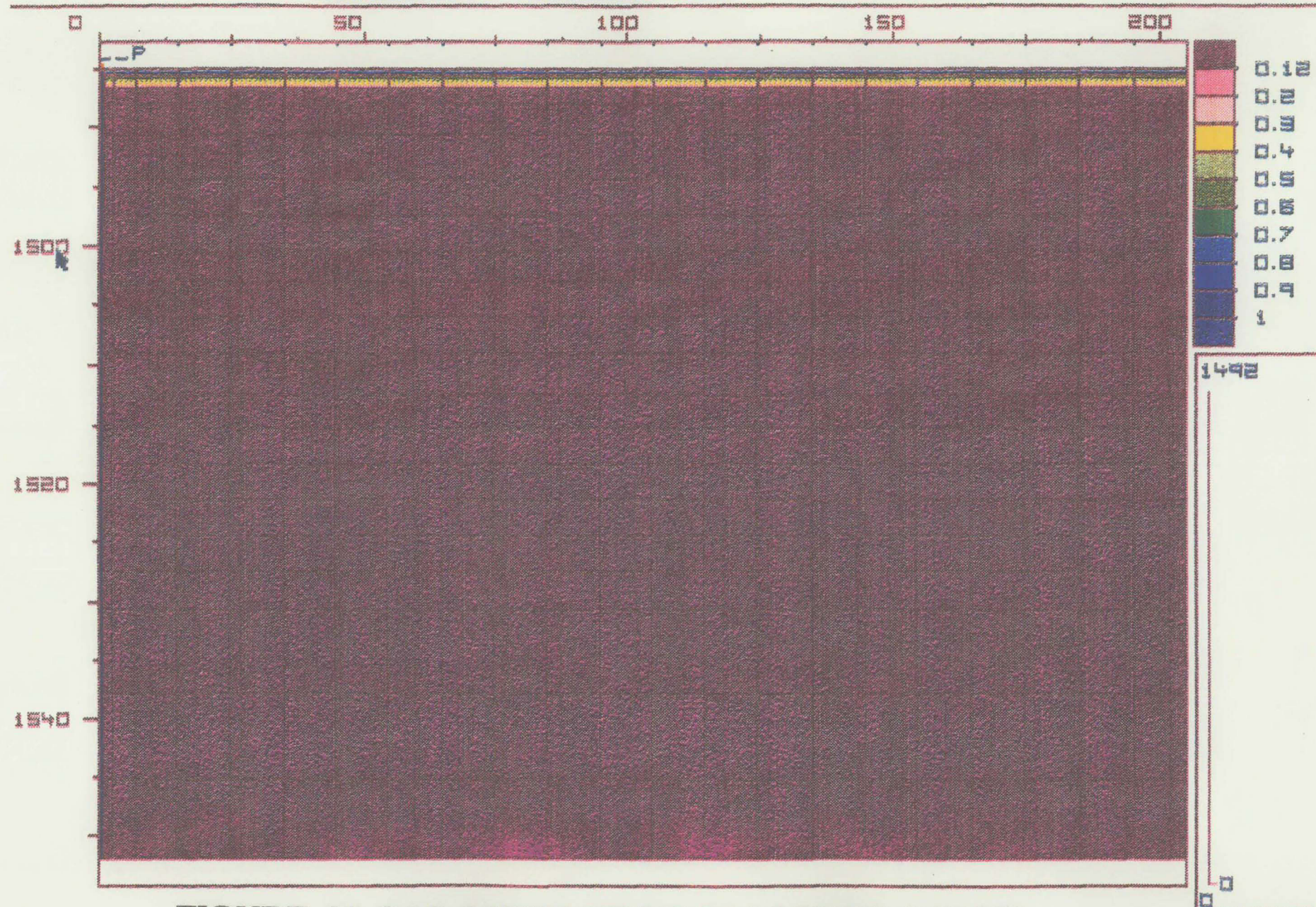


FIGURE 42 GAS SATURATION FRACTURE-0 DAYS

PARAMOUNT CAMERON L47

PRED9

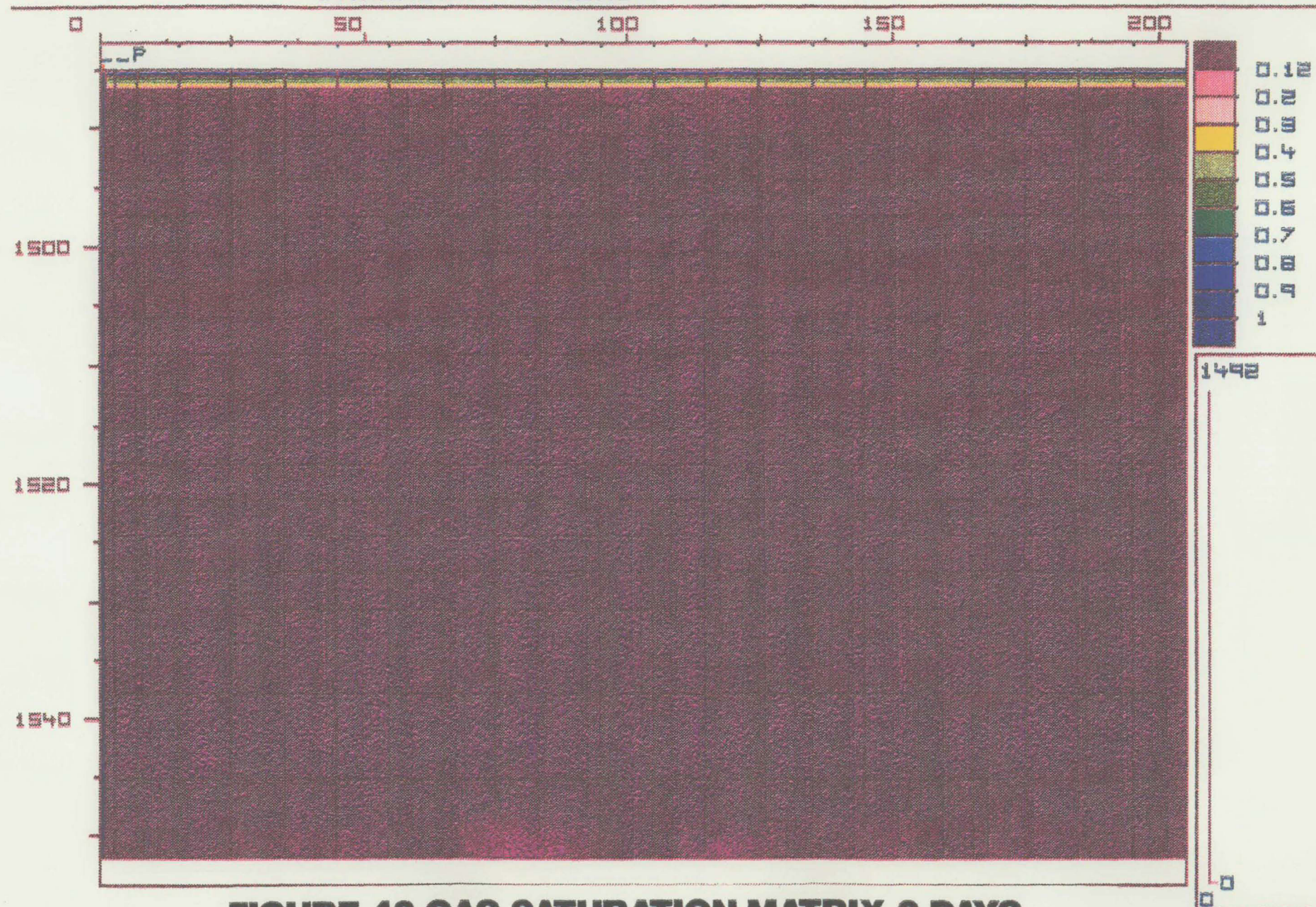


FIGURE 43 GAS SATURATION MATRIX-0 DAYS

PARAMOUNT CAMERON L47

PRED9

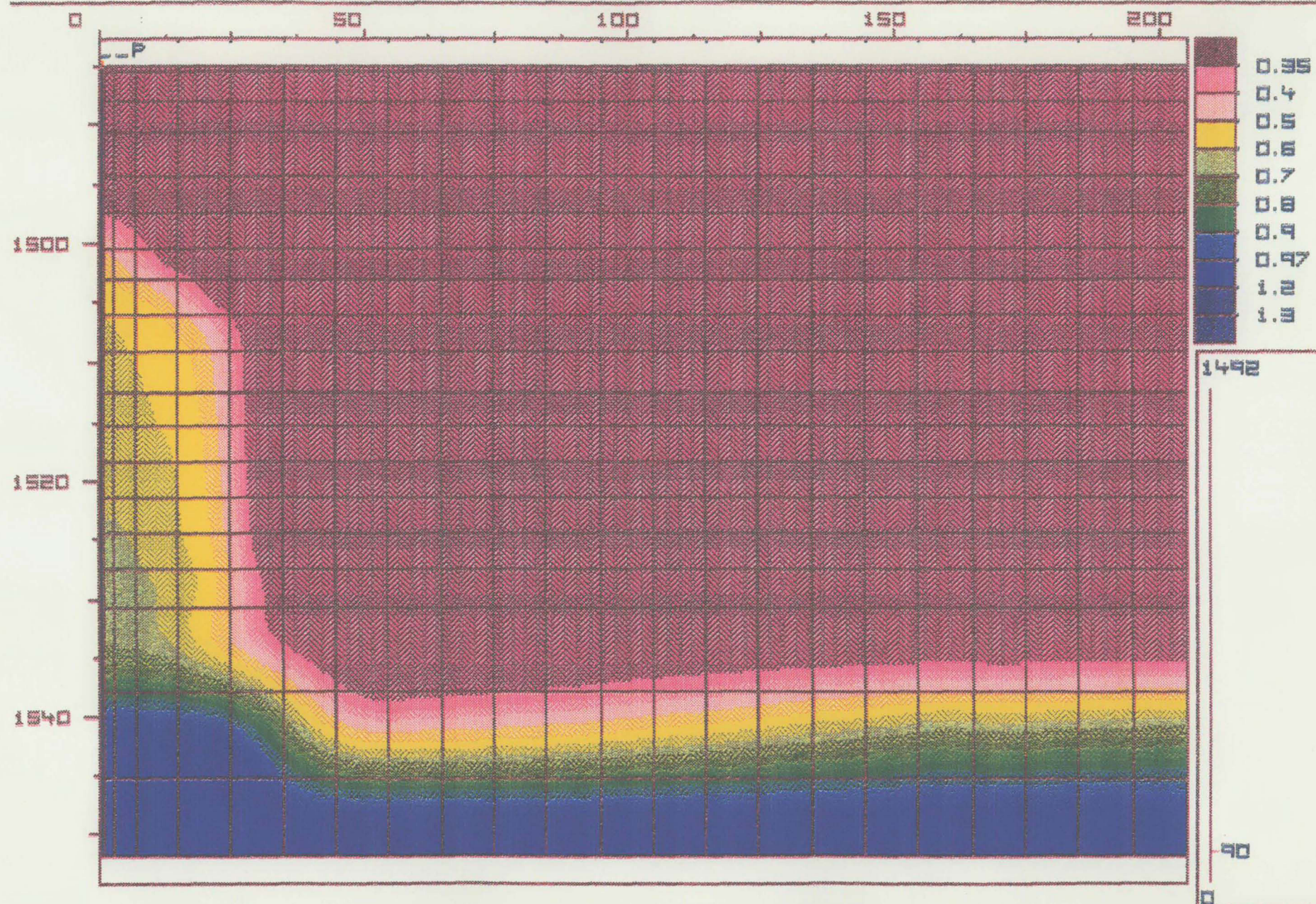


FIGURE 44 WATER SATURATION FRACTURE-90 DAYS

PARAMOUNT CAMERON L47

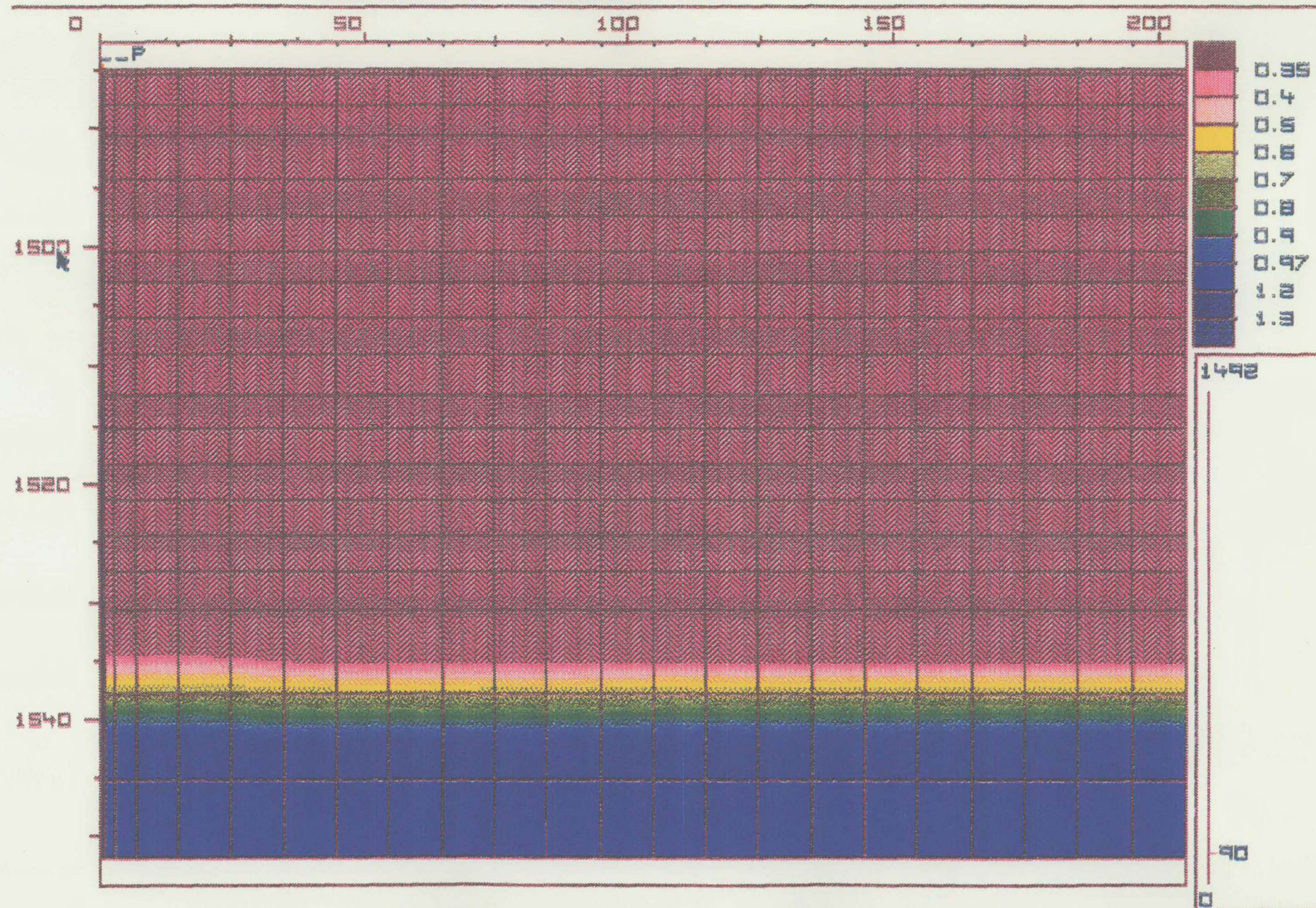


FIGURE 45 WATER SATURATION MATRIX-90 DAYS

PARAMOUNT CAMERON L47

PRED9

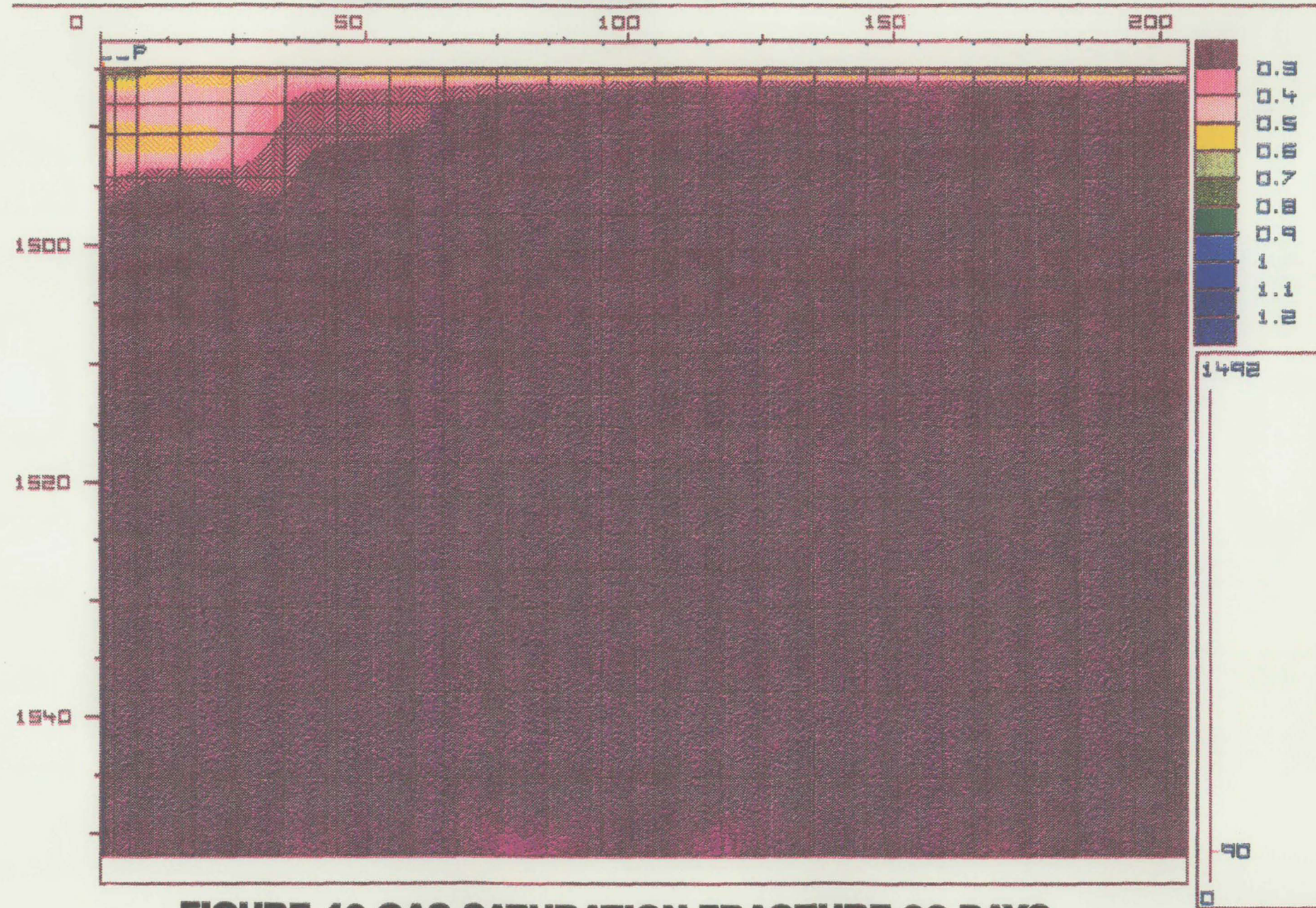


FIGURE 46 GAS SATURATION FRACTURE-90 DAYS

PARAMOUNT CAMERON L47

PRED9

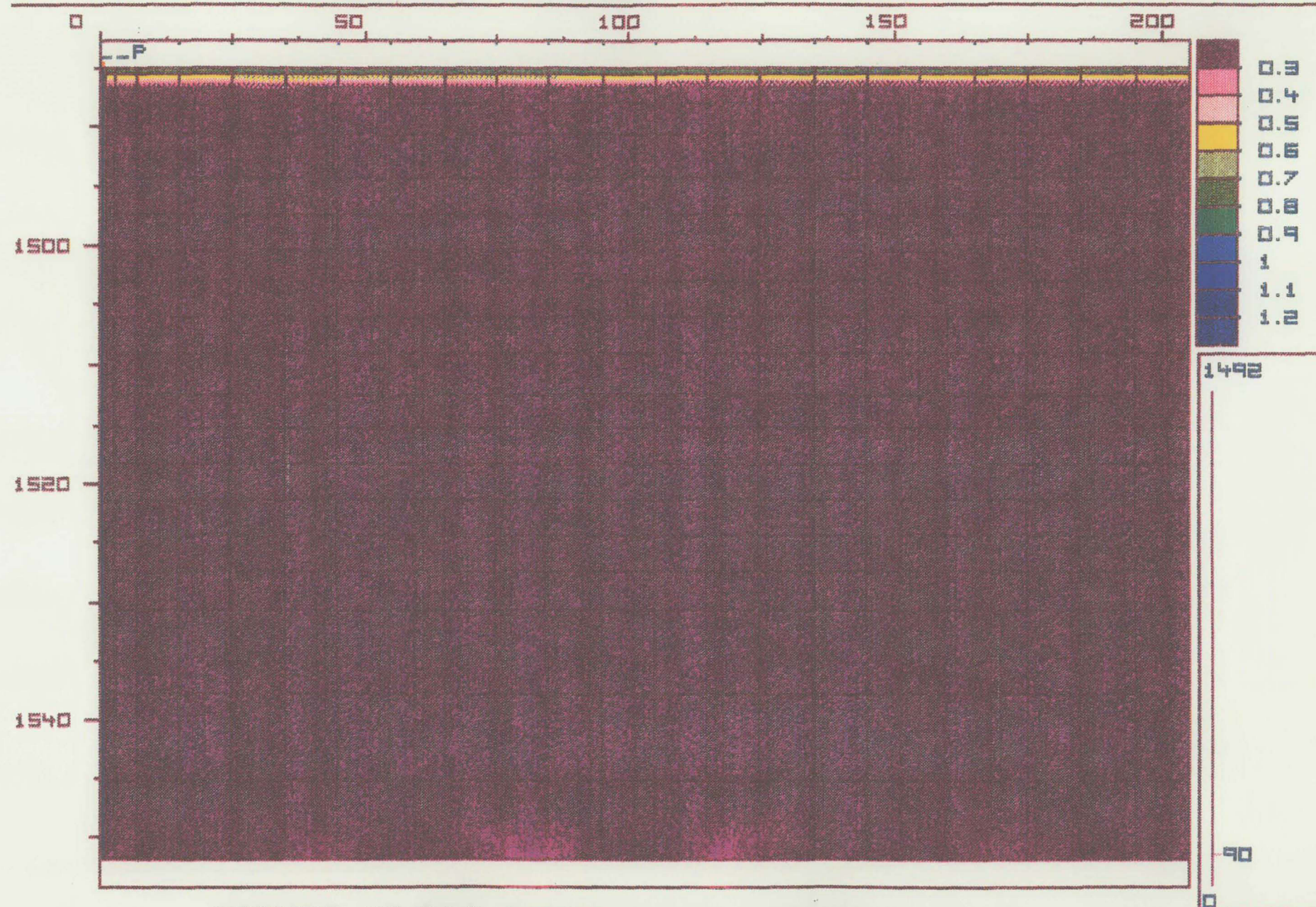


FIGURE 47 GAS SATURATION MATRIX-90 DAYS

PARAMOUNT CAMERON L47

PRED9

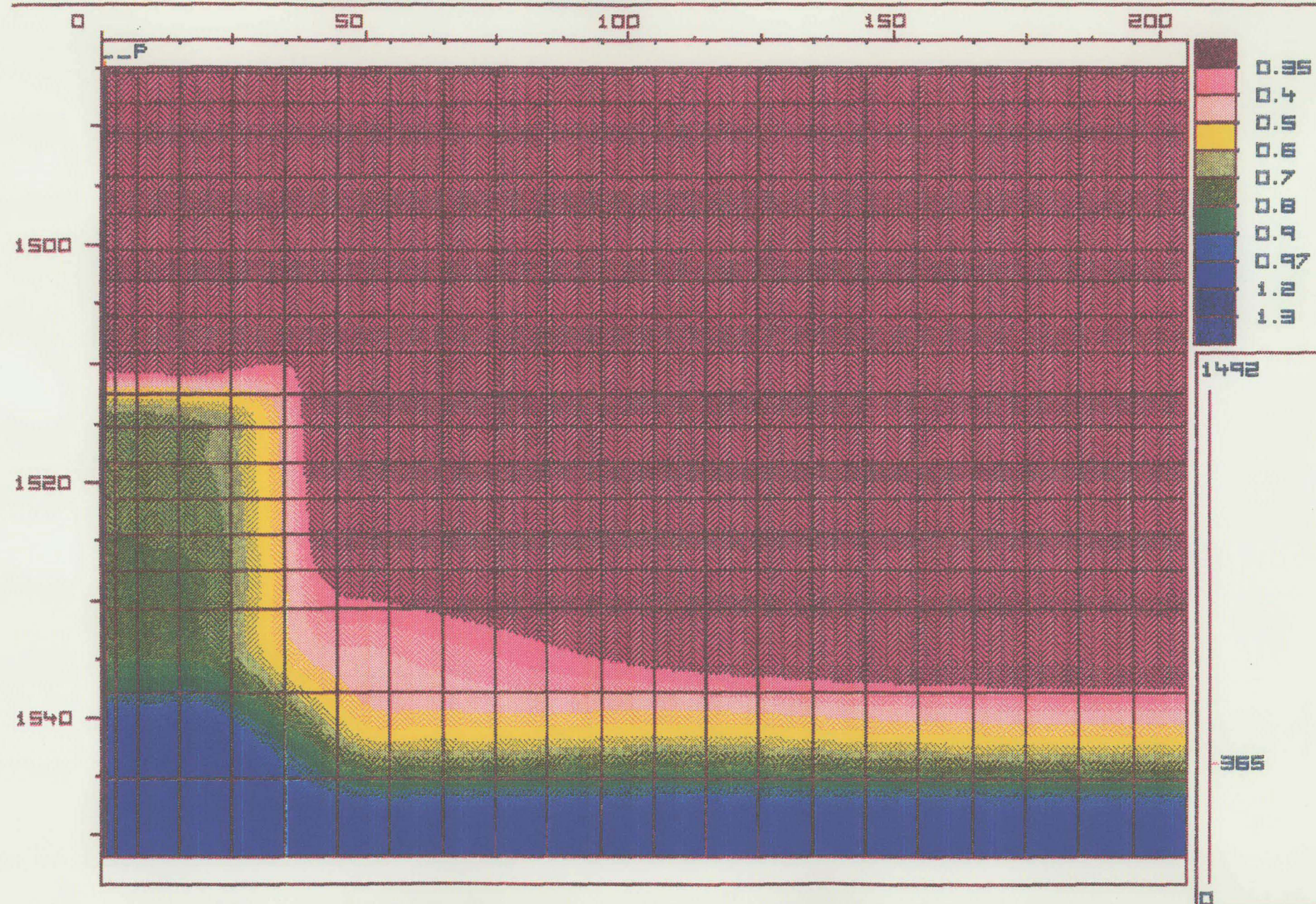


FIGURE 48 WATER SATURATION FRACTURE-365 DAYS

PRED9

PARAMOUNT CAMERON L47

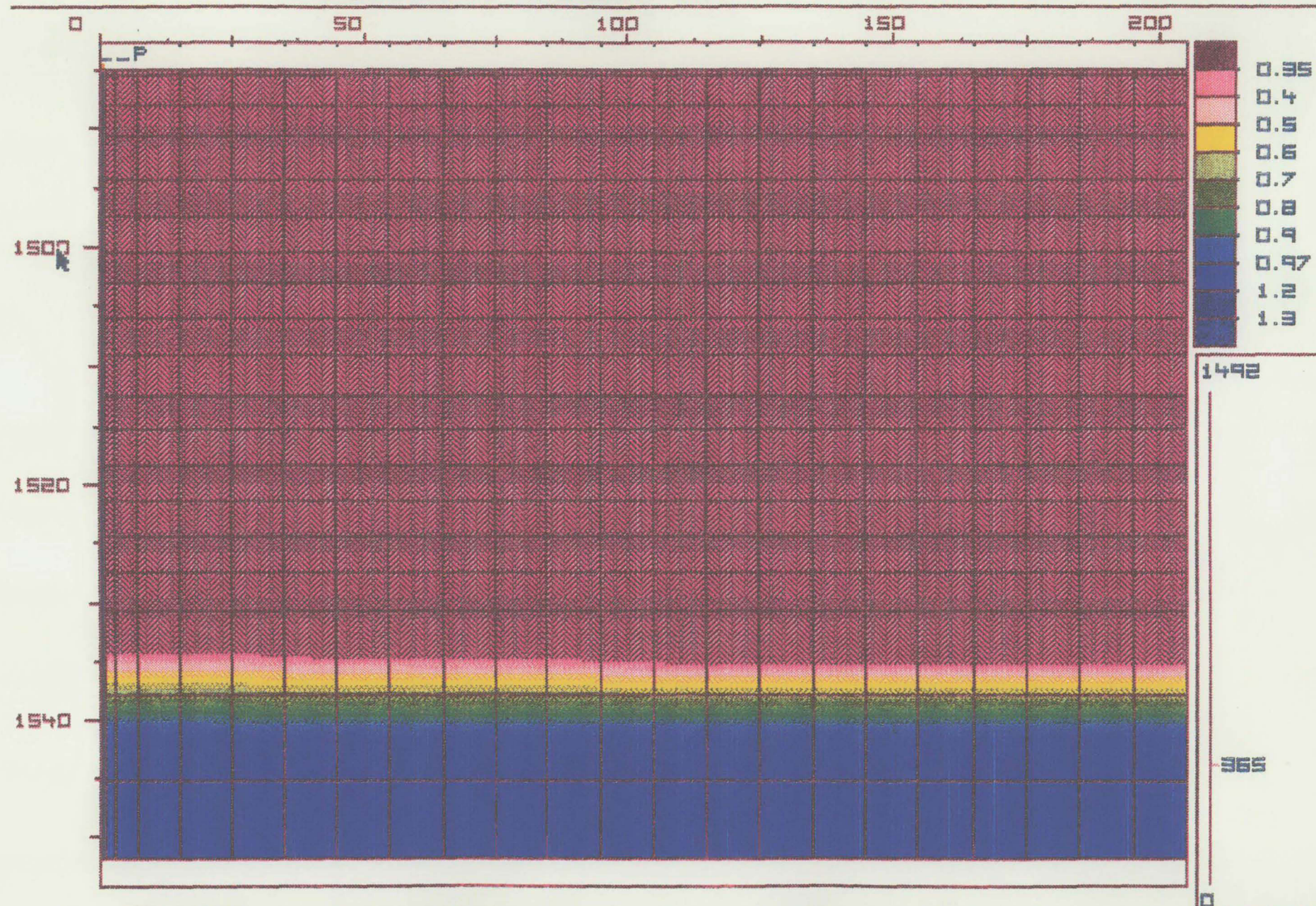


FIGURE 49 WATER SATURATION MATRIX-365 DAYS

PARAMOUNT CAMERON L47

PRED9

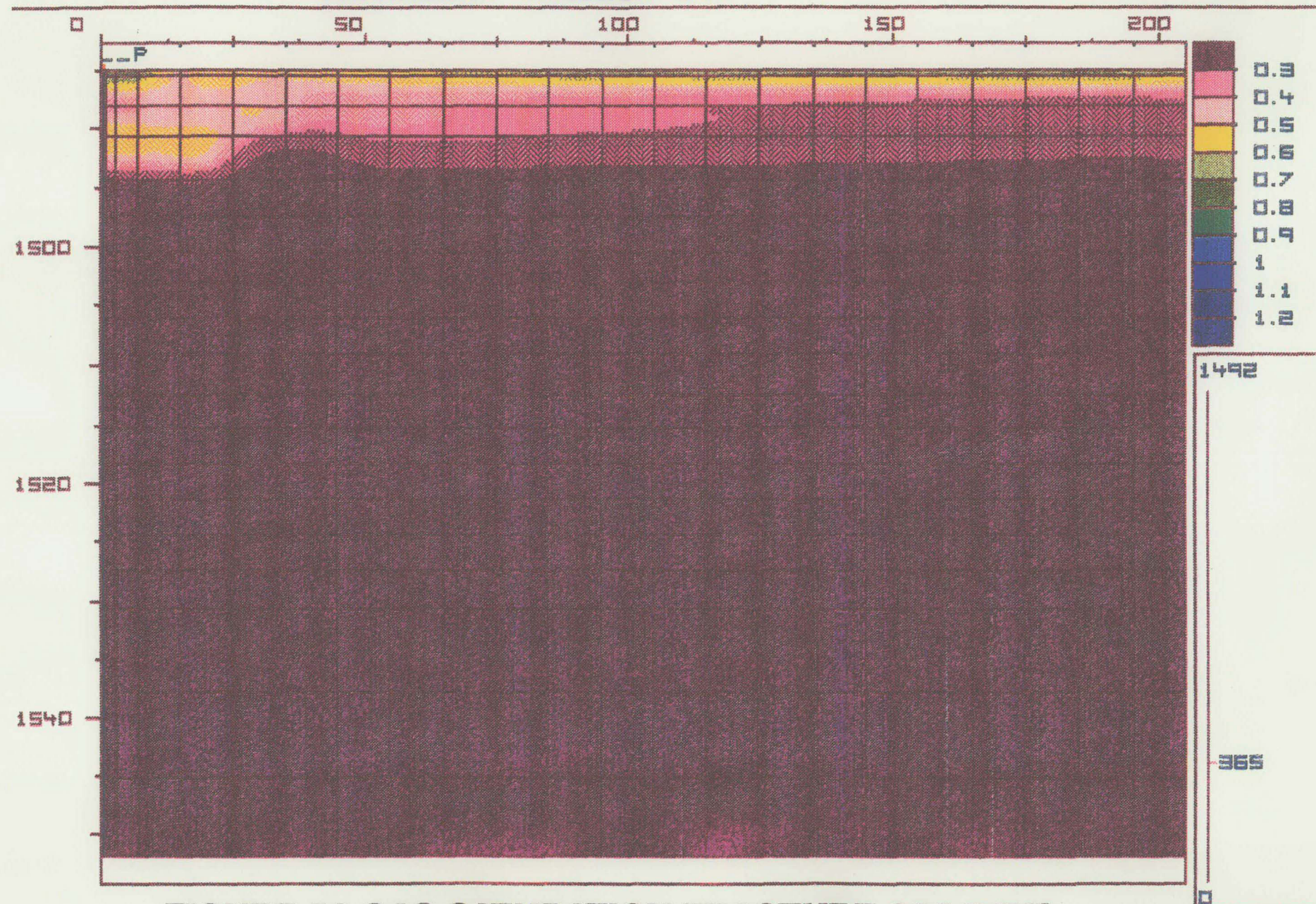


FIGURE 50 GAS SATURATION FRACTURE-365 DAYS

PARAMOUNT CAMERON L47

PRED9

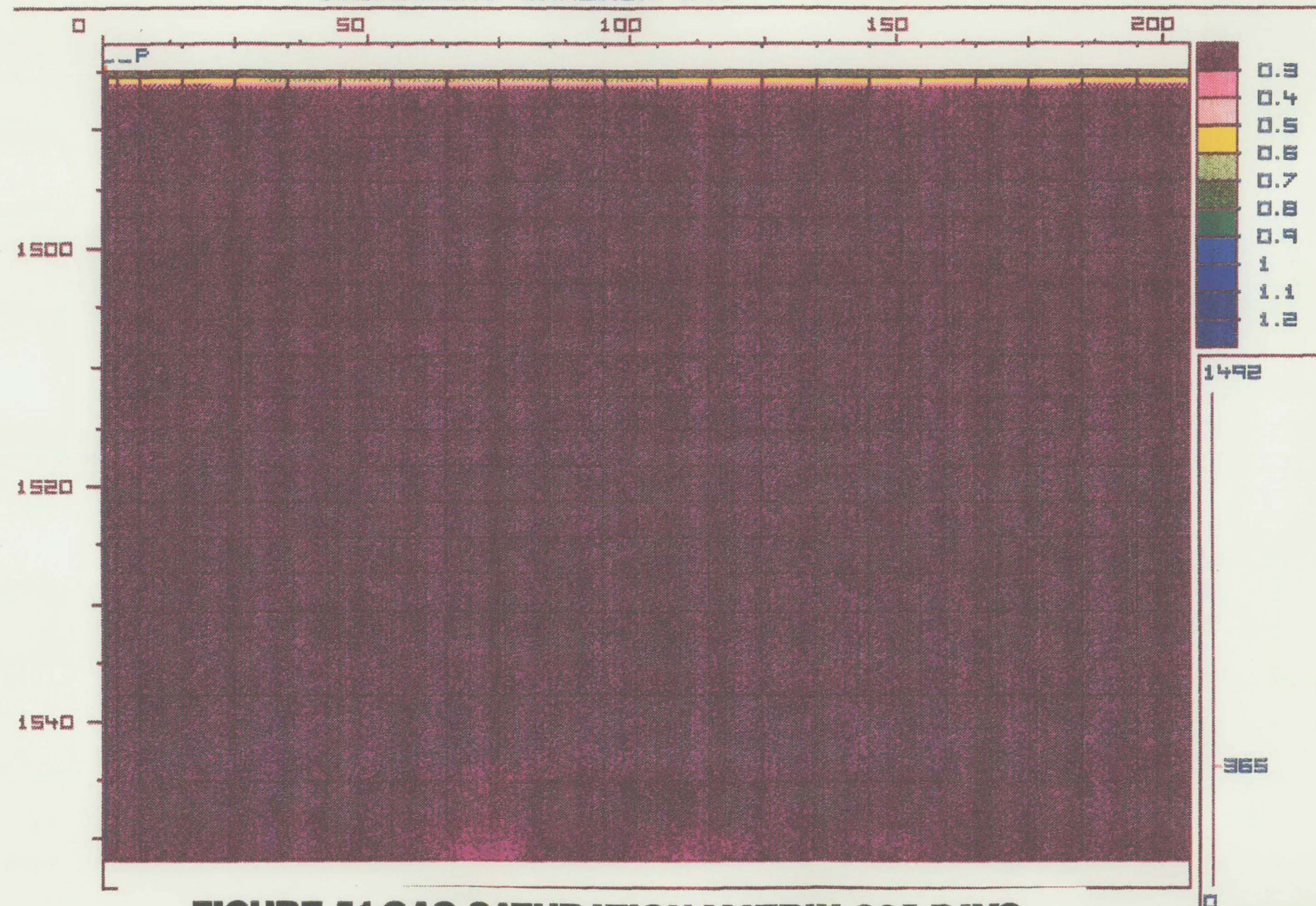


FIGURE 51 GAS SATURATION MATRIX-365 DAYS

PRED9

PARAMOUNT CAMERON L47

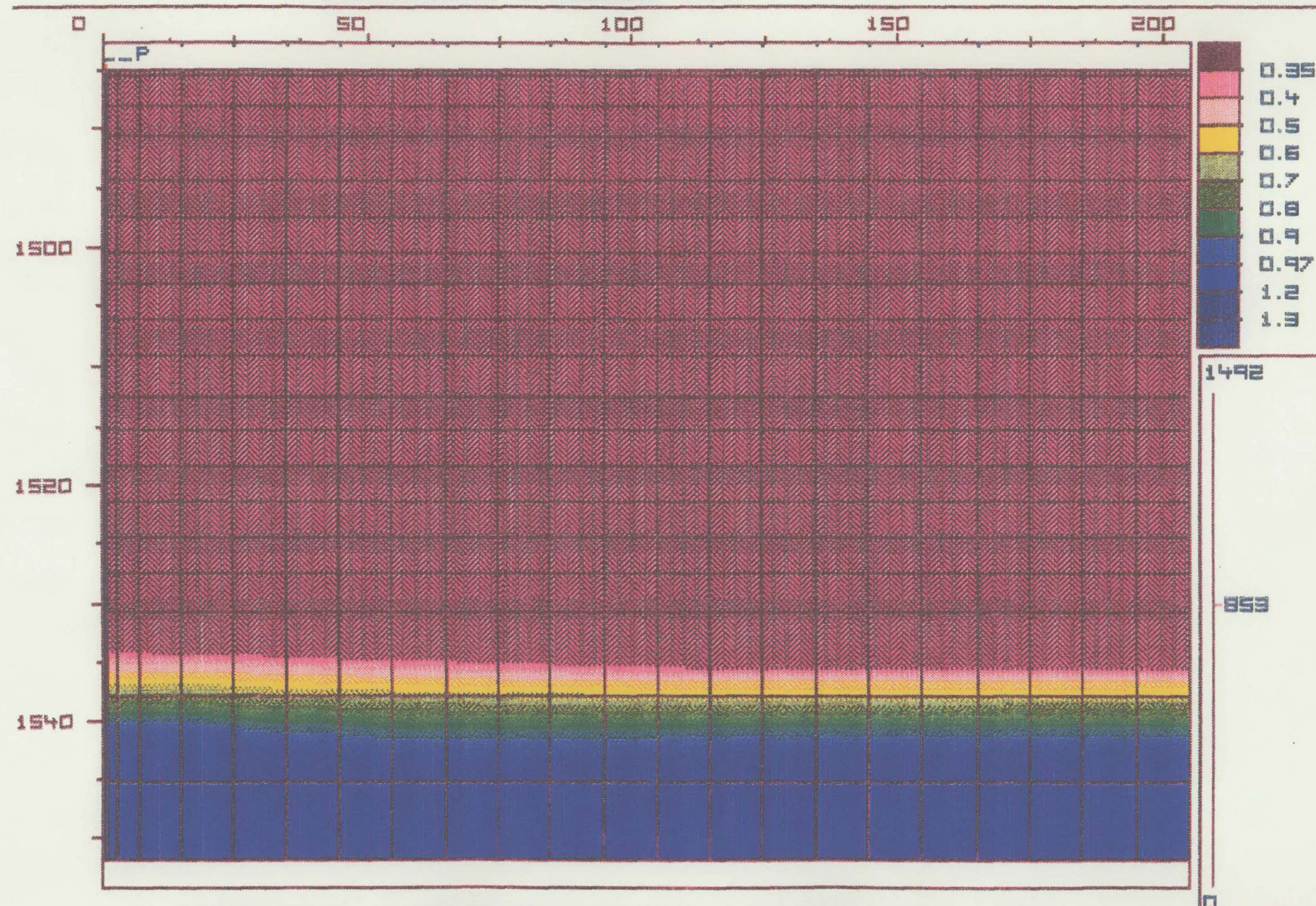


FIGURE 52 WATER SATURATION MATRIX-853 DAYS

PARAMOUNT CAMERON L47

PRED9

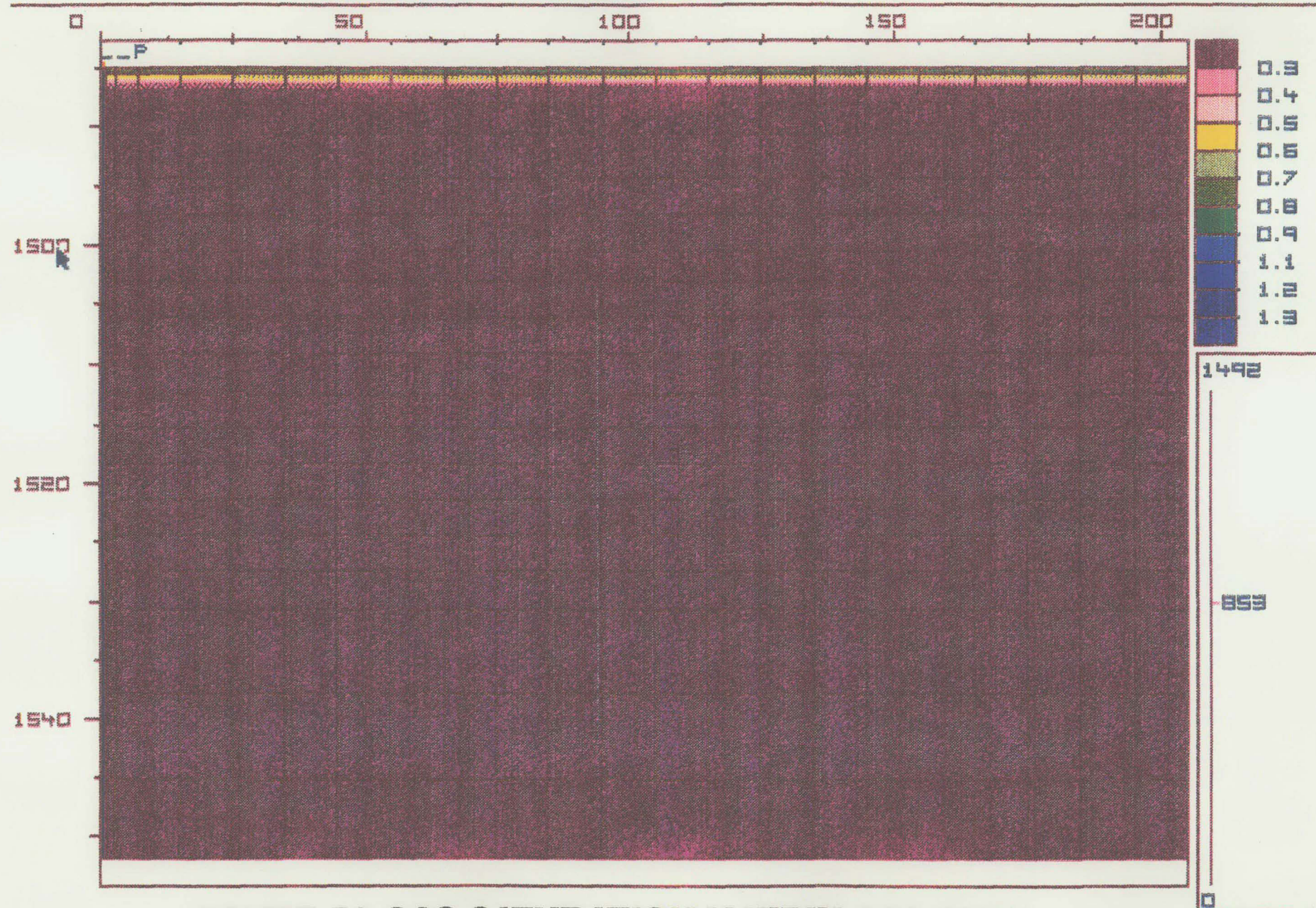


FIGURE 53 GAS SATURATION MATRIX-853 DAYS

PARAMOUNT CAMERON L47

PRED9

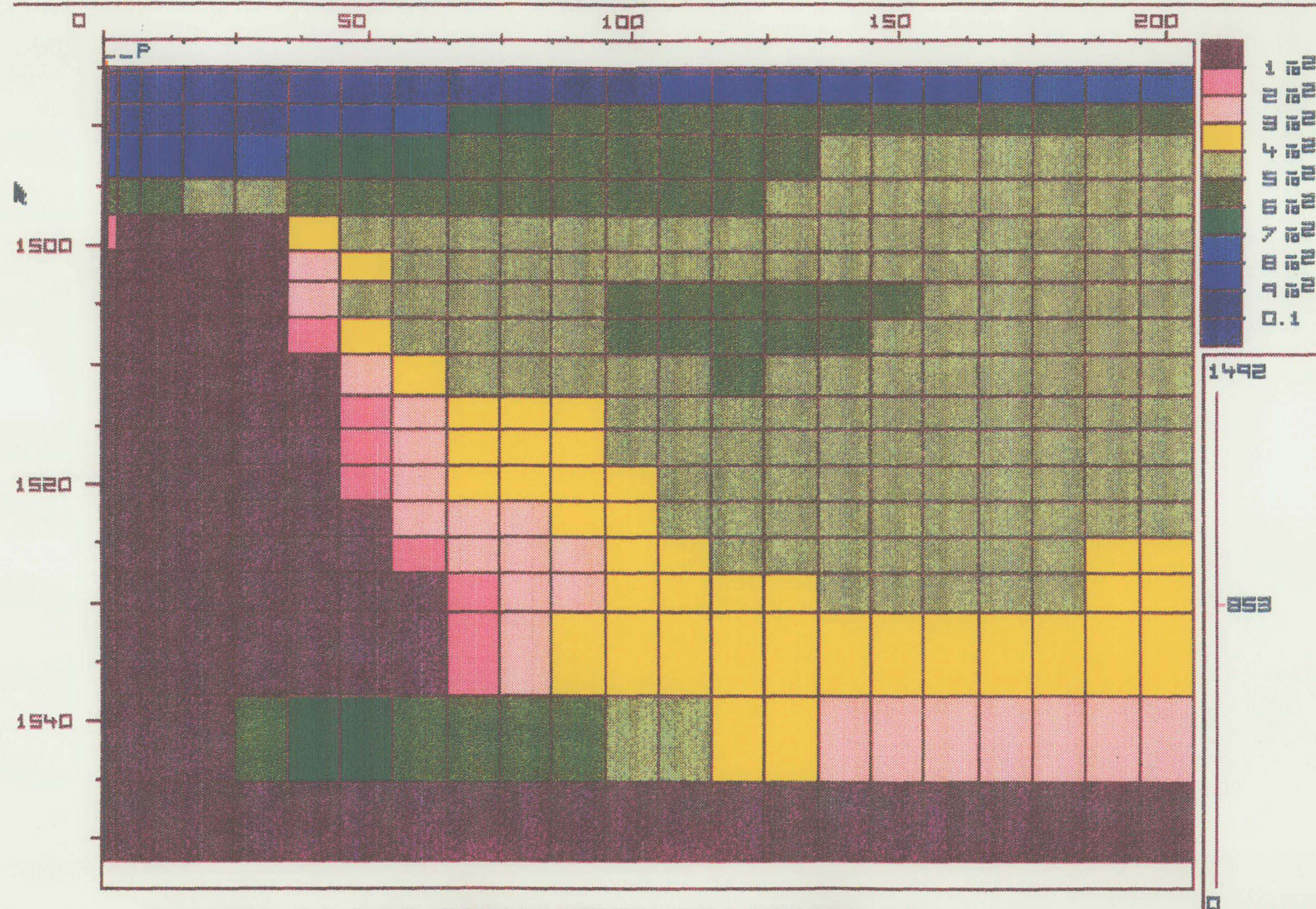


FIGURE 54 GAS SATURATION FRACTURE-853 DAYS

PARAMOUNT CAMERON L47

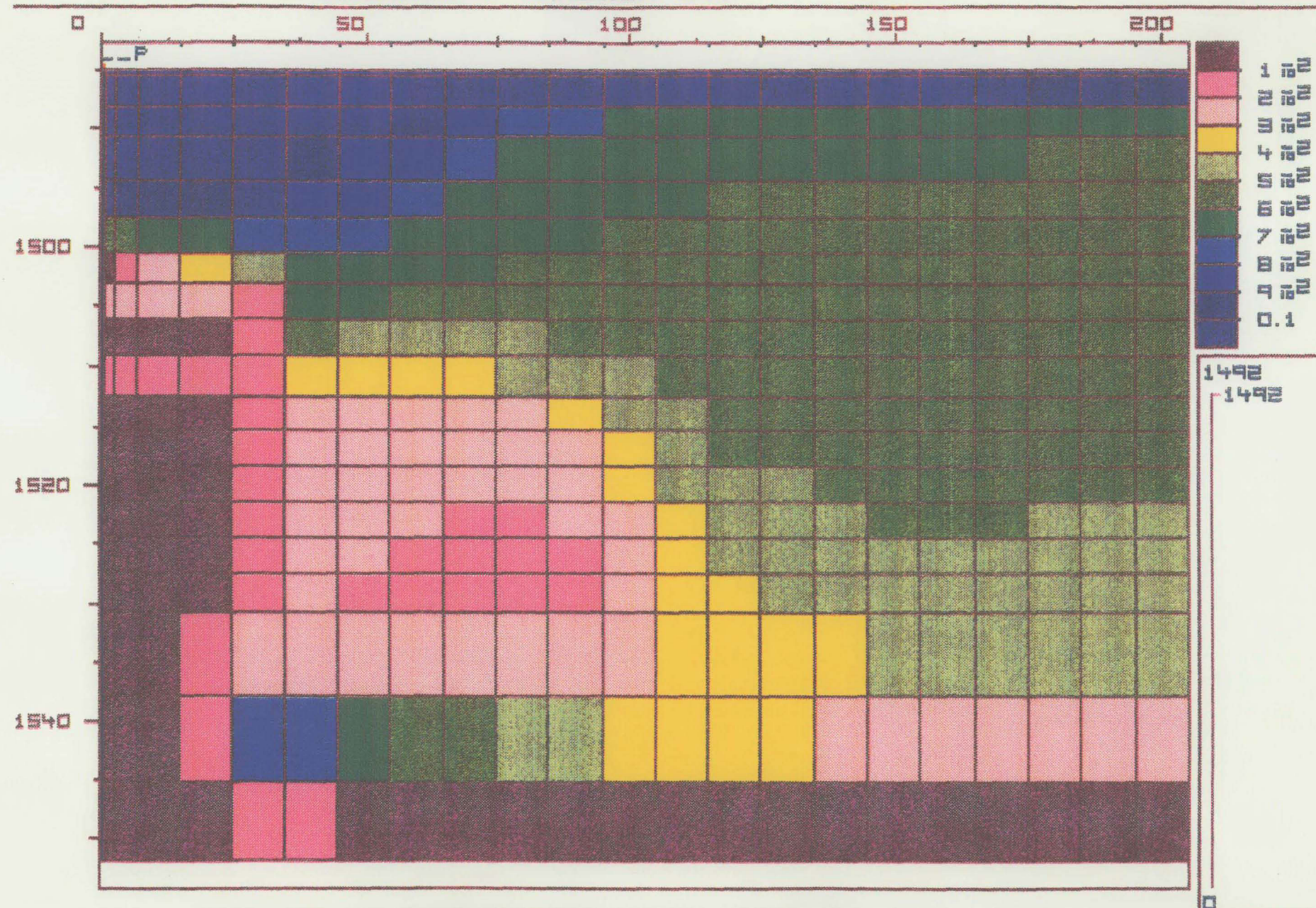


FIGURE 55 GAS SATURATION MATRIX-1492 DAYS

FIGURE 5o

COMPARISON OF CUMULATIVE OIL

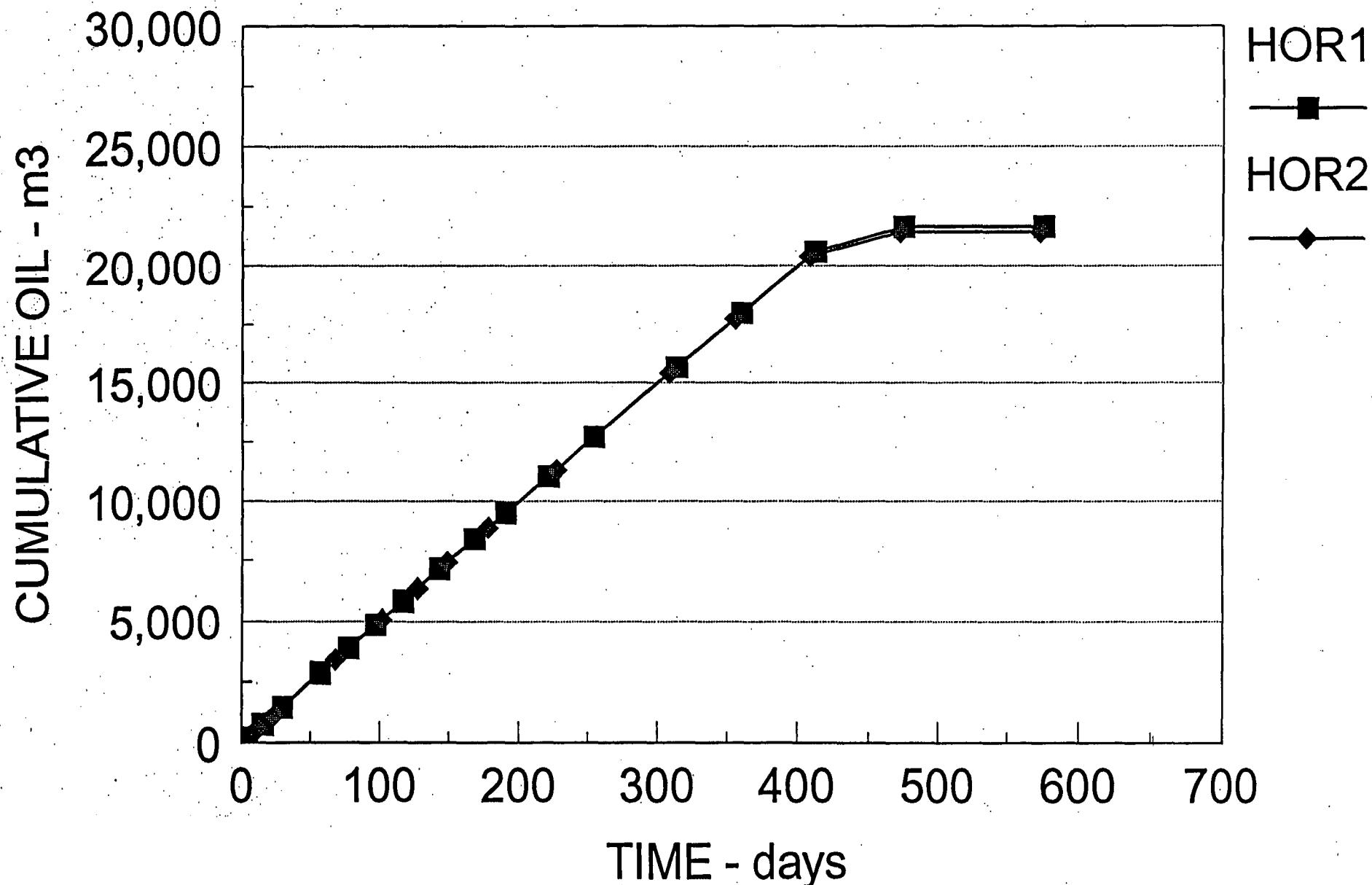


FIGURE 57

COMPARISON OF CUMULATIVE OIL

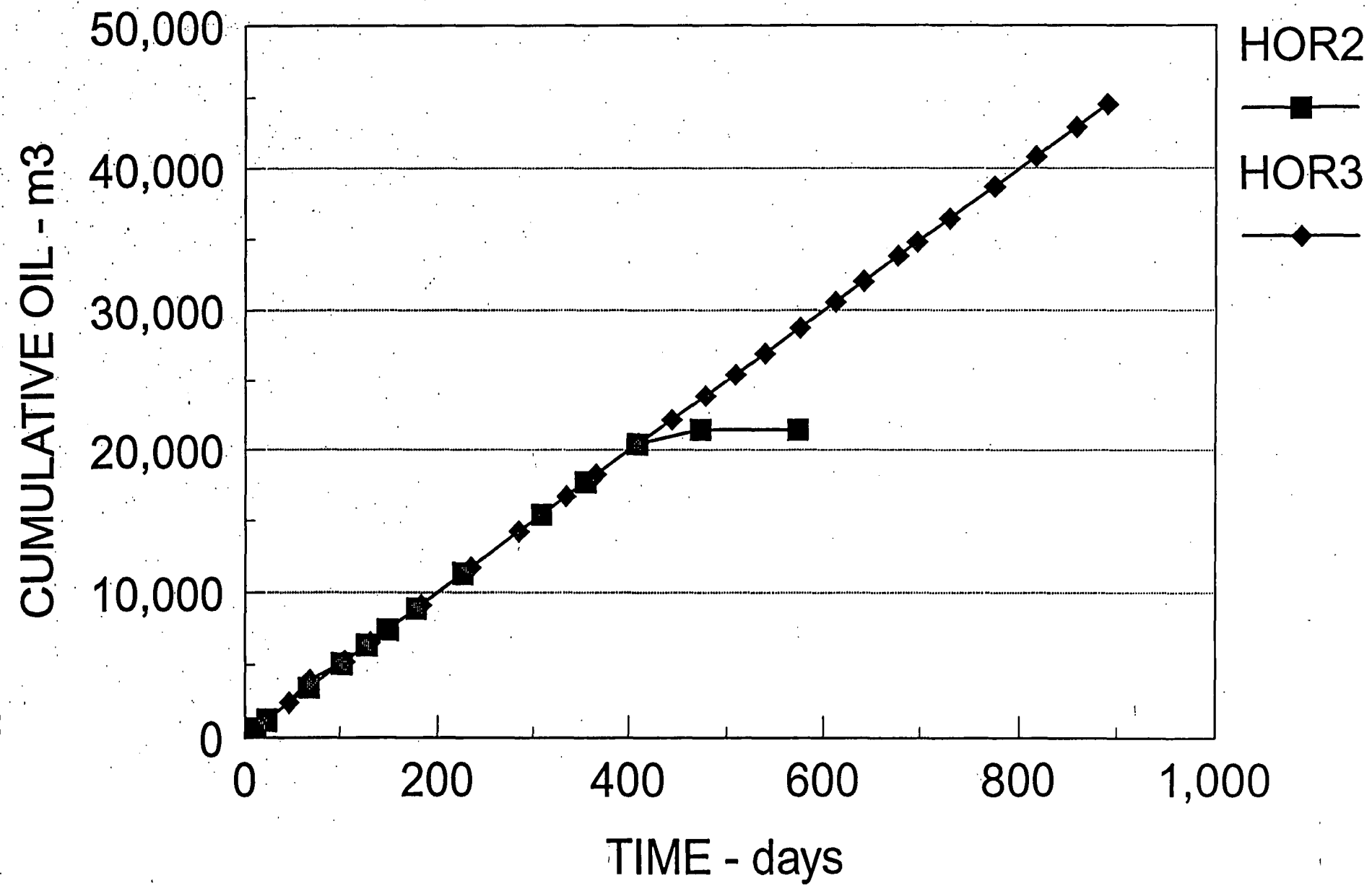


FIGURE 58

COMPARISON OF PRODUCING GAS OIL RATIOS

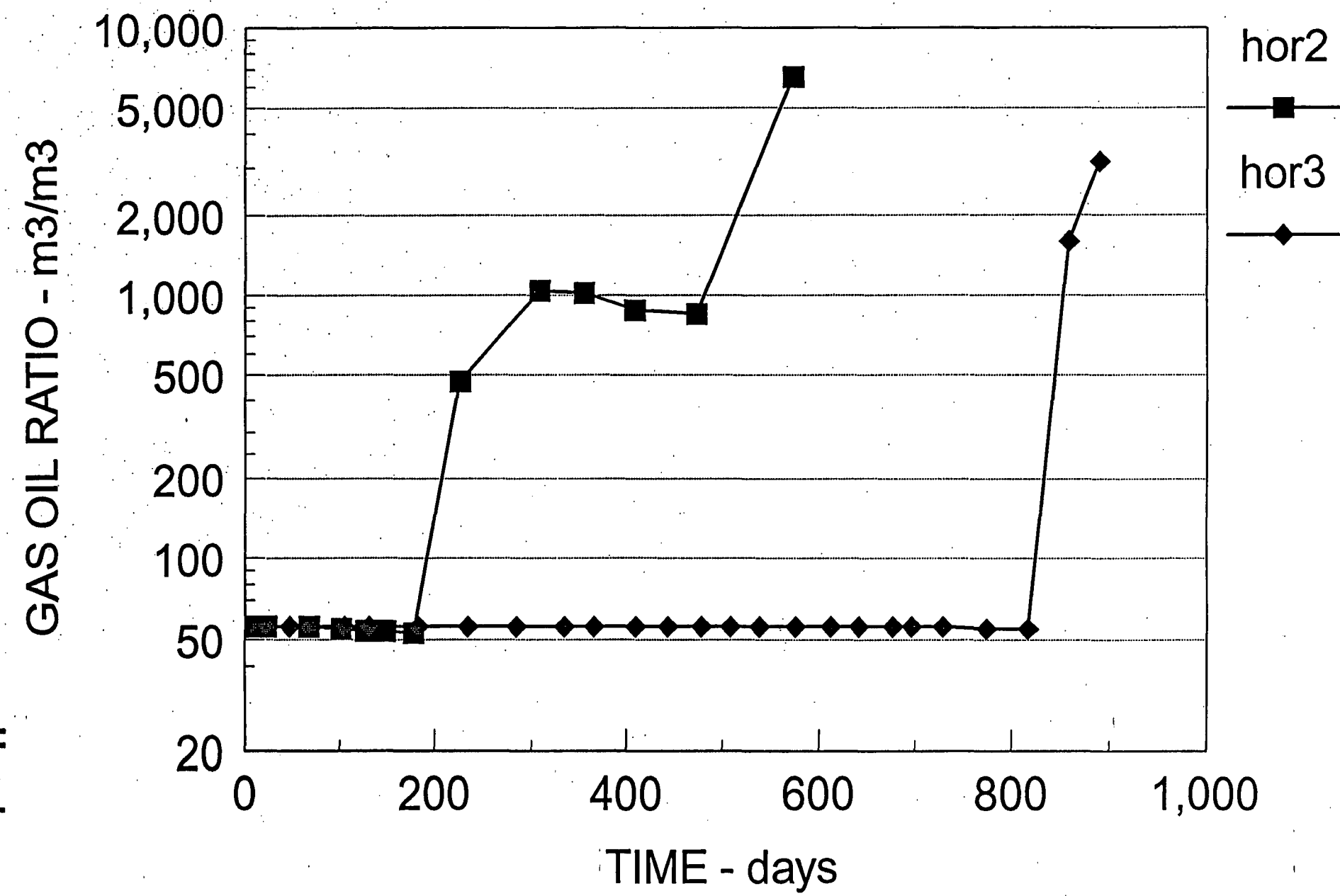
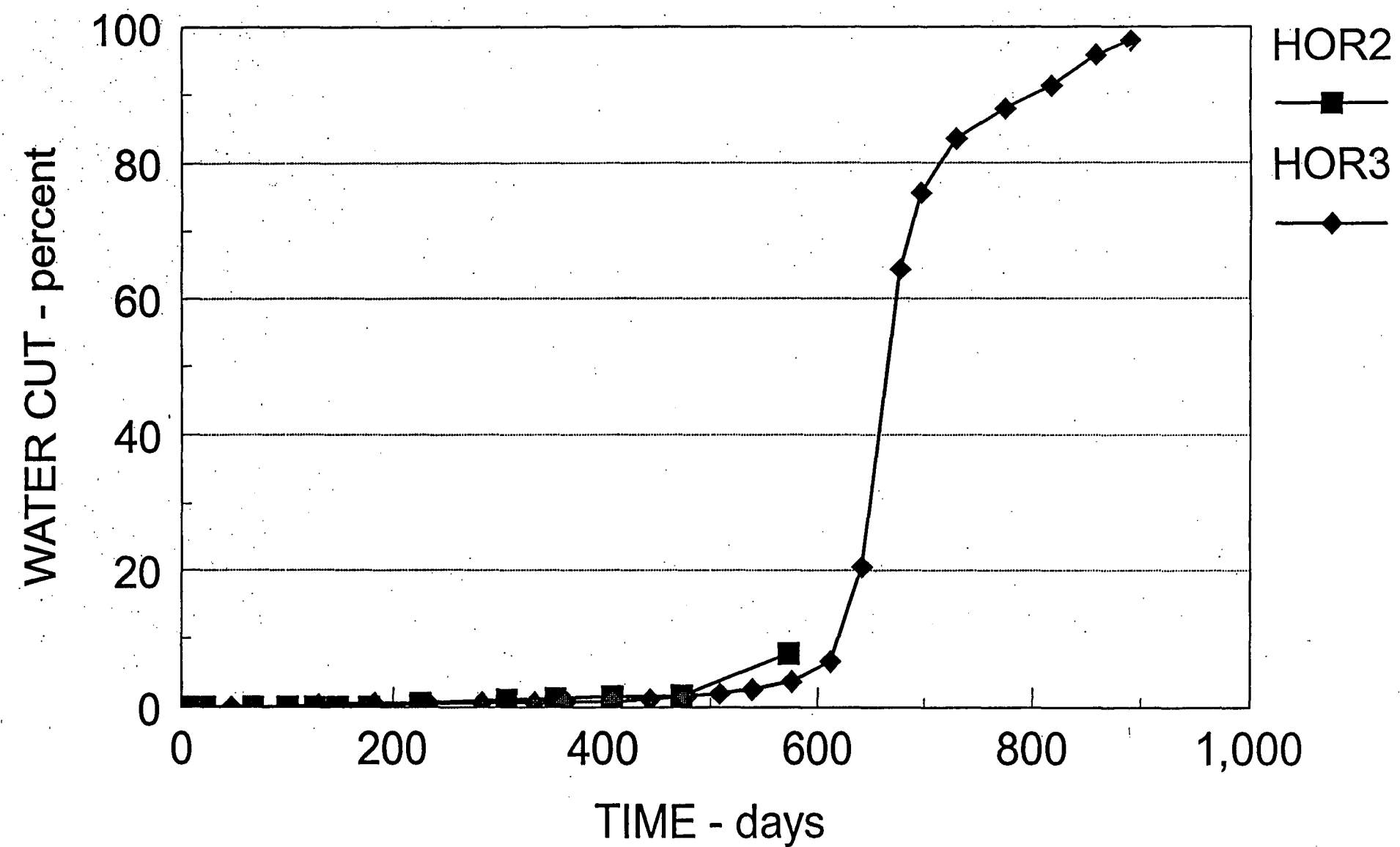


FIGURE 59

COMPARISON OF WATER CUT



PARAMOUNT CAMERON HORIZONTAL WELL

HOR2

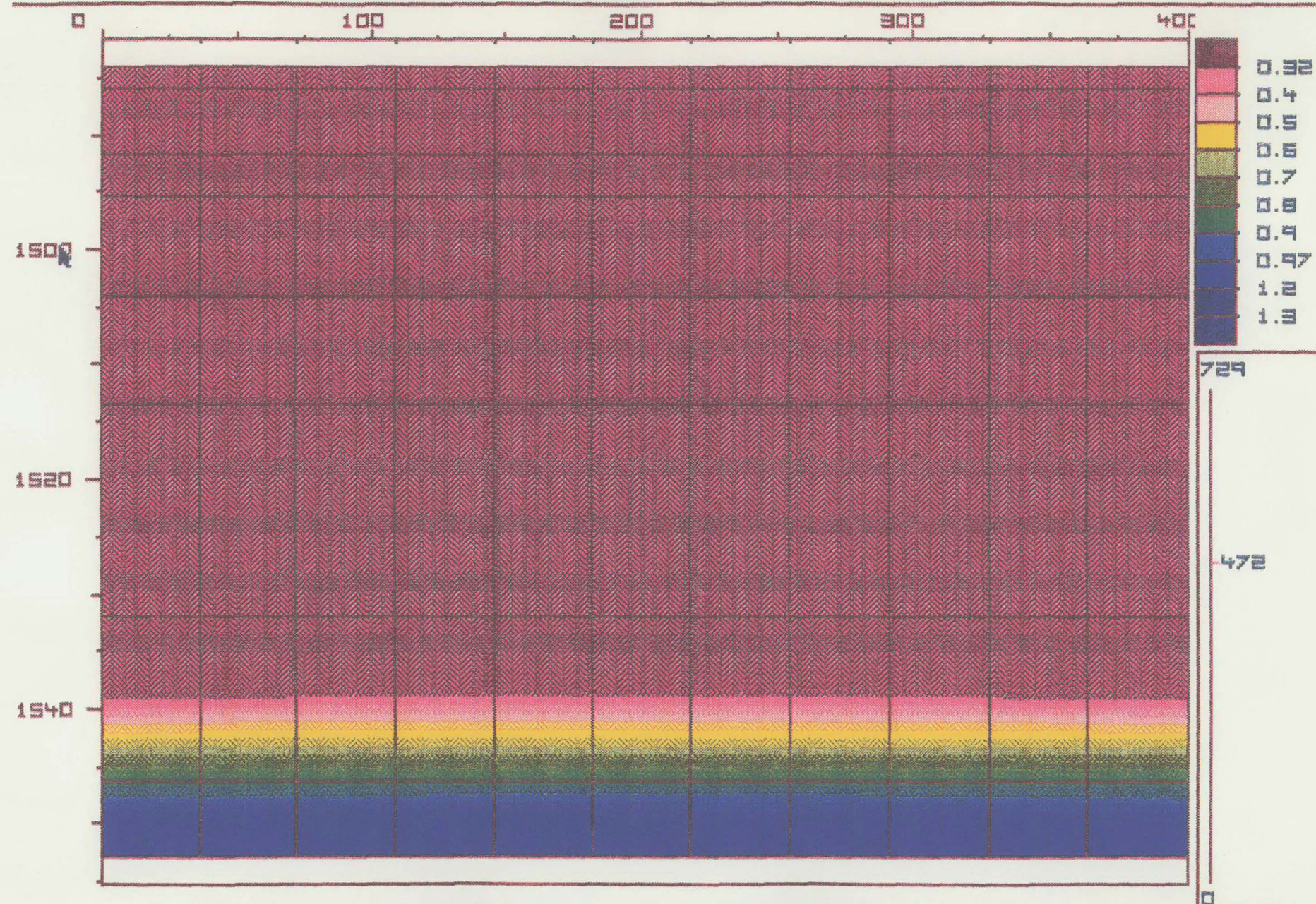


FIGURE 61 WATER SATURATION MATRIX-472 DAYS

PARAMOUNT CAMERON HORIZONTAL WELL

HOR2

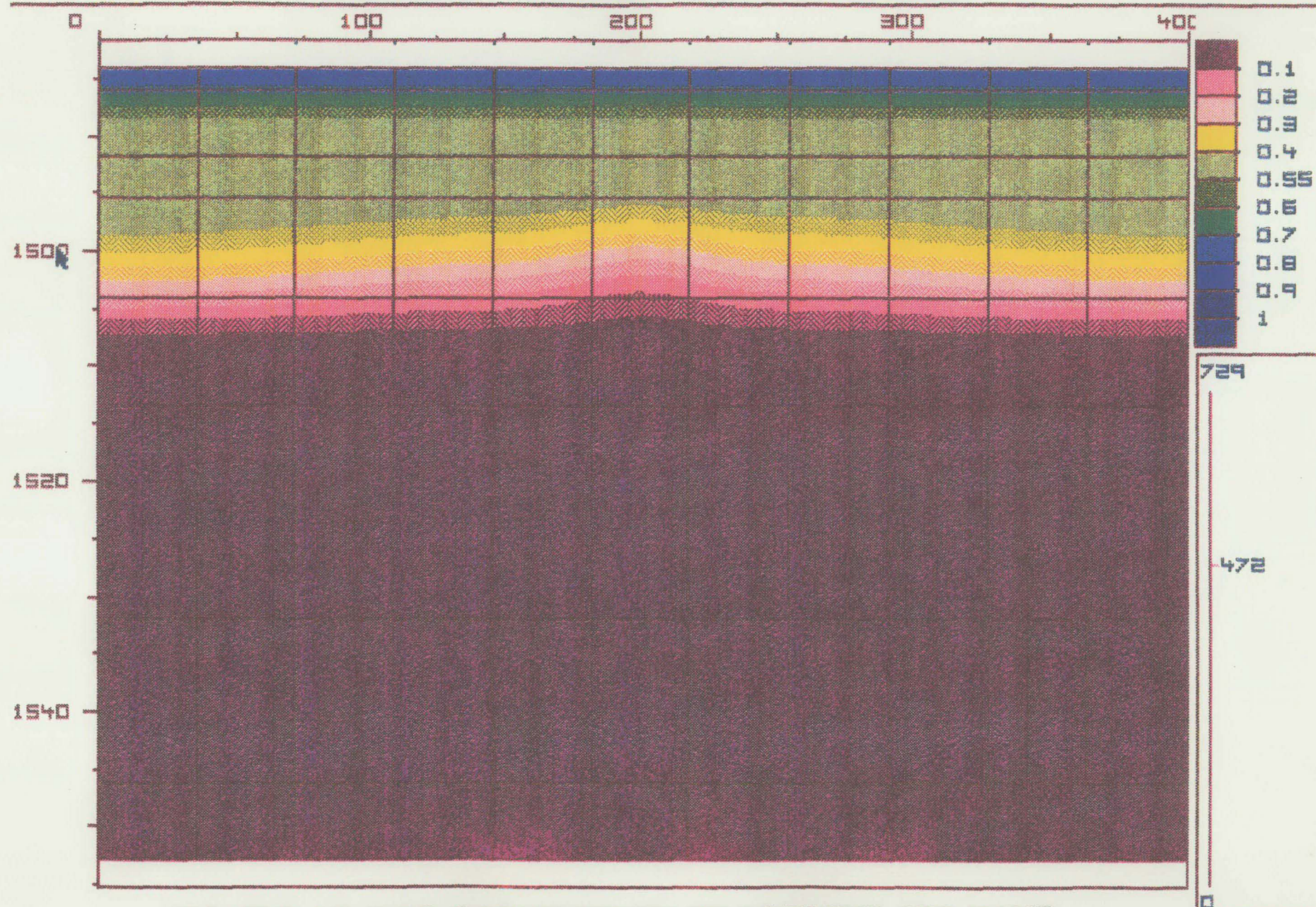


FIGURE 62 GAS SATURATION FRACTURE-472 DAYS

PARAMOUNT CAMERON HORIZONTAL WELL

HOR2

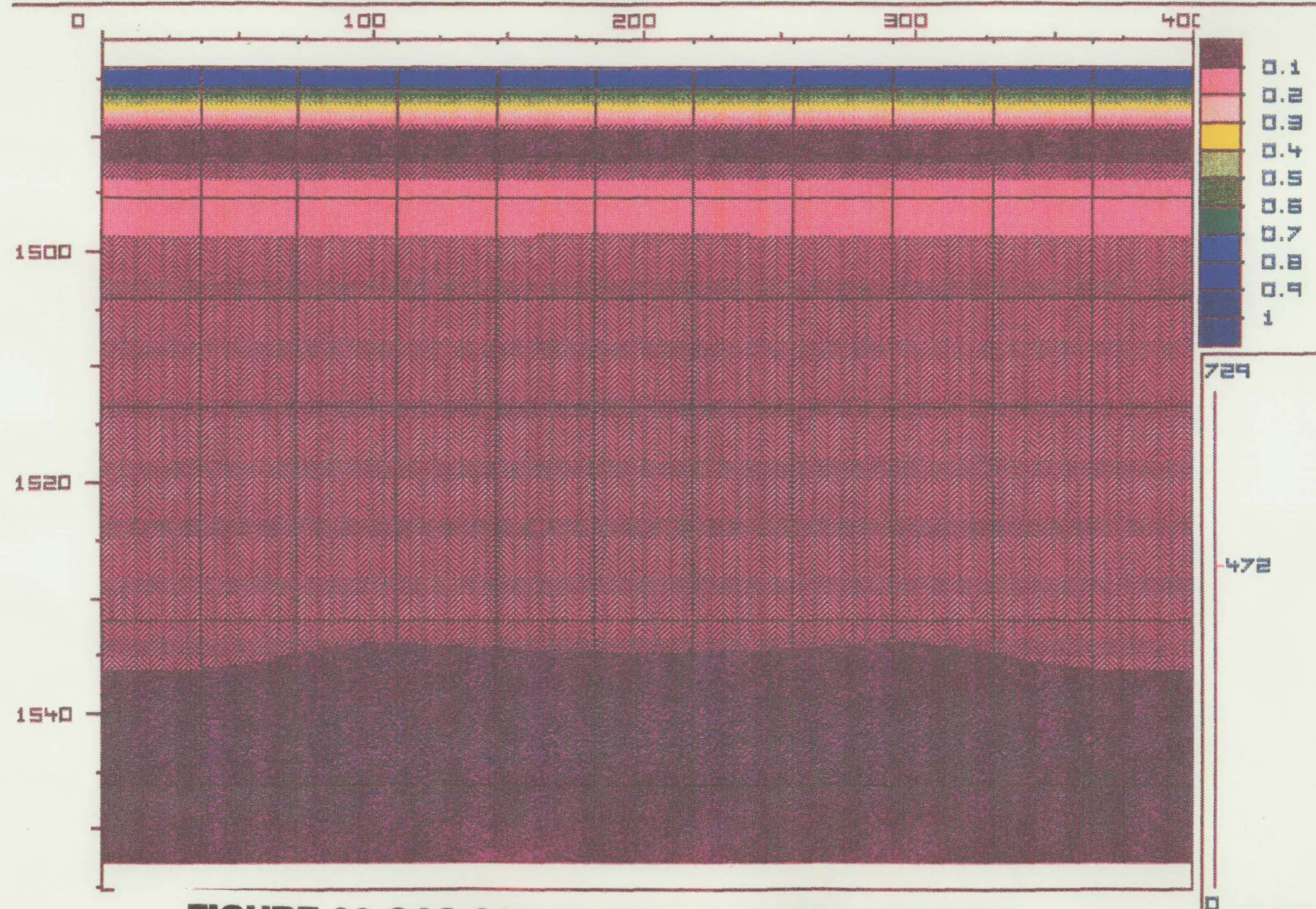


FIGURE 63 GAS SATURATION MATRIX-472 DAYS

HOR3

PARAMOUNT CAMERON HORIZONTAL WELL

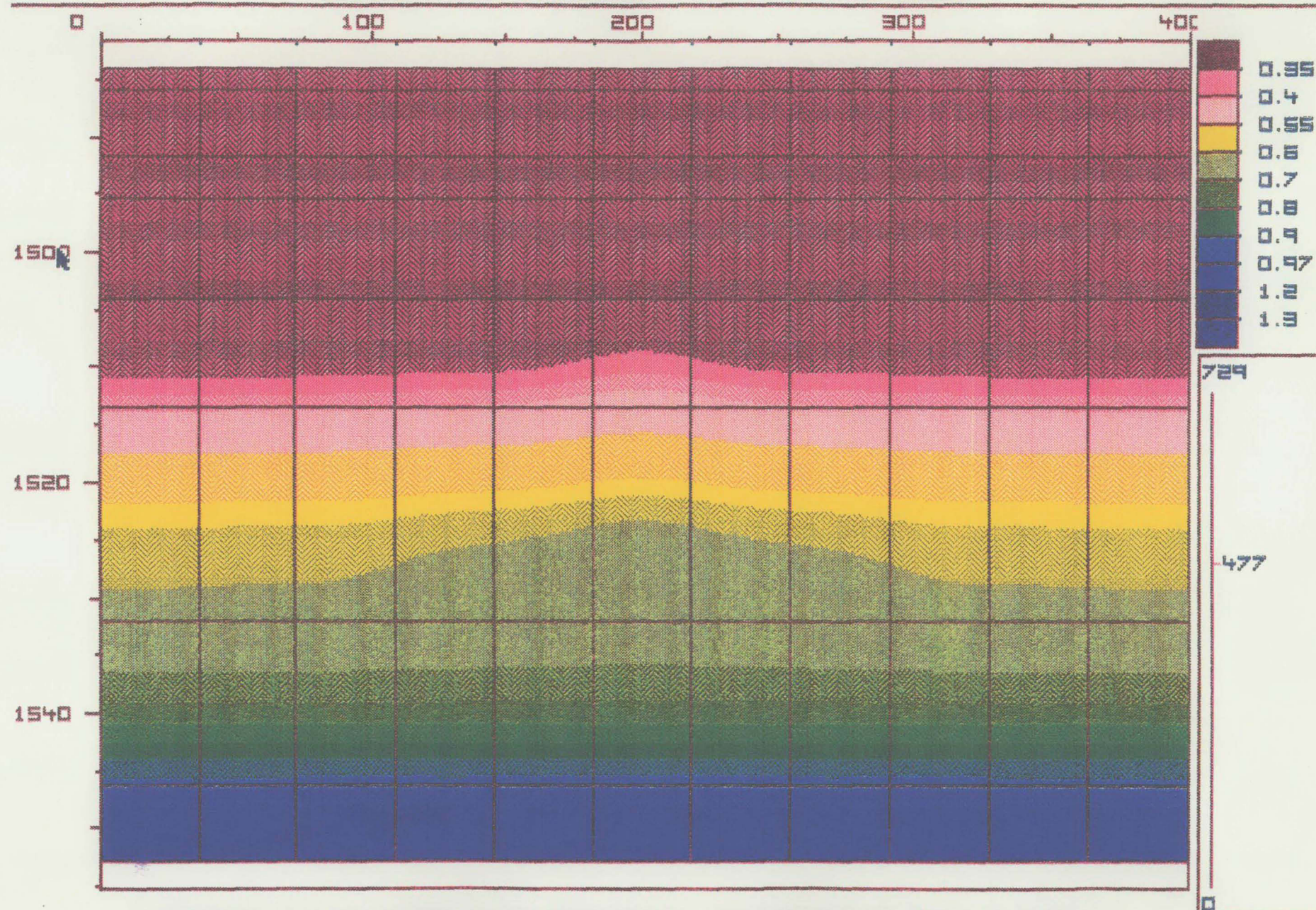


FIGURE 64 WATER SATURATION FRACTURE-477 DAYS

PARAMOUNT CAMERON HORIZONTAL WELL

HOR3

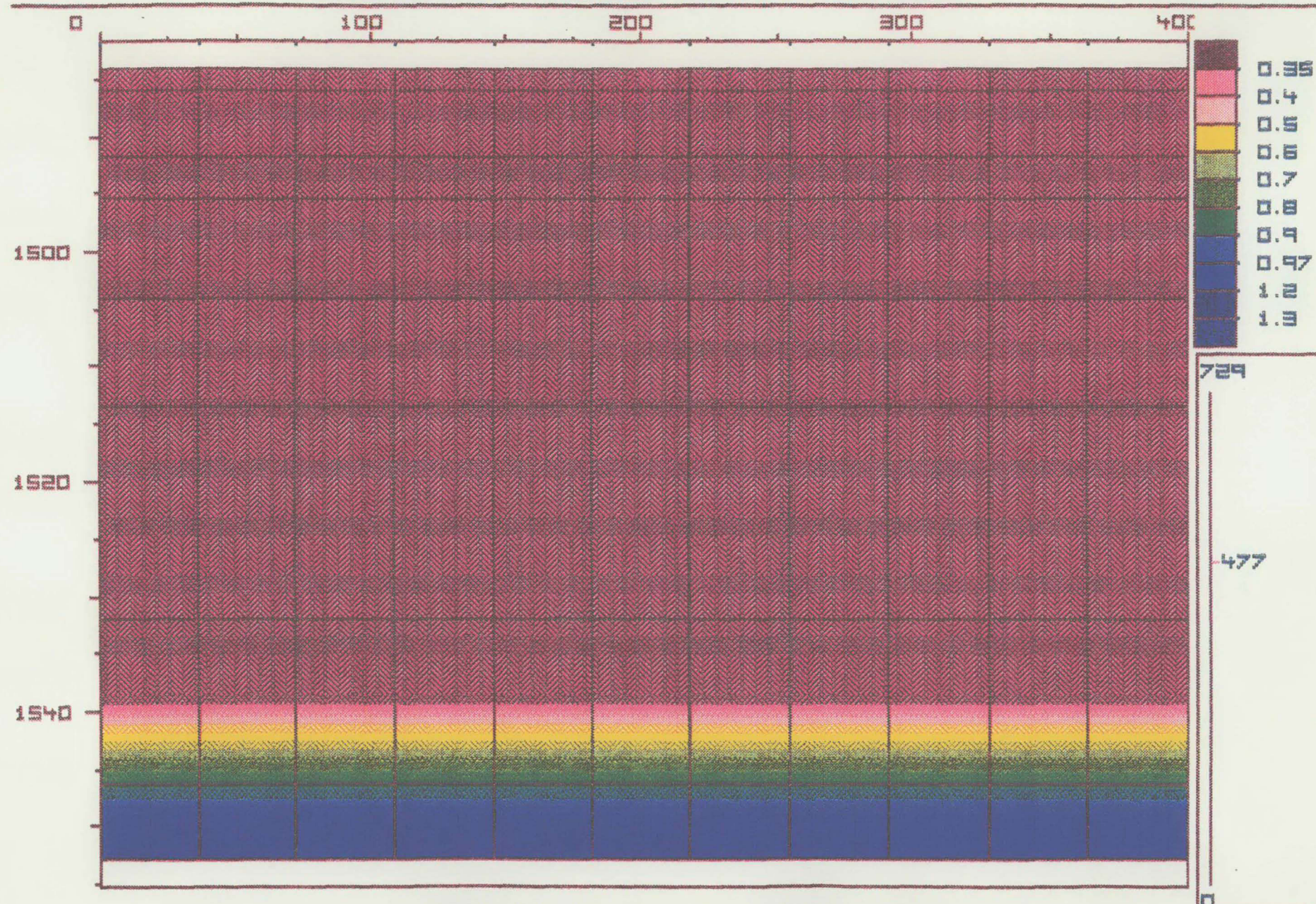


FIGURE 65 WATER SATURATION MATRIX-477 DAYS

ARAMOUNT CAMERON HORIZONTAL WELL

HOR3

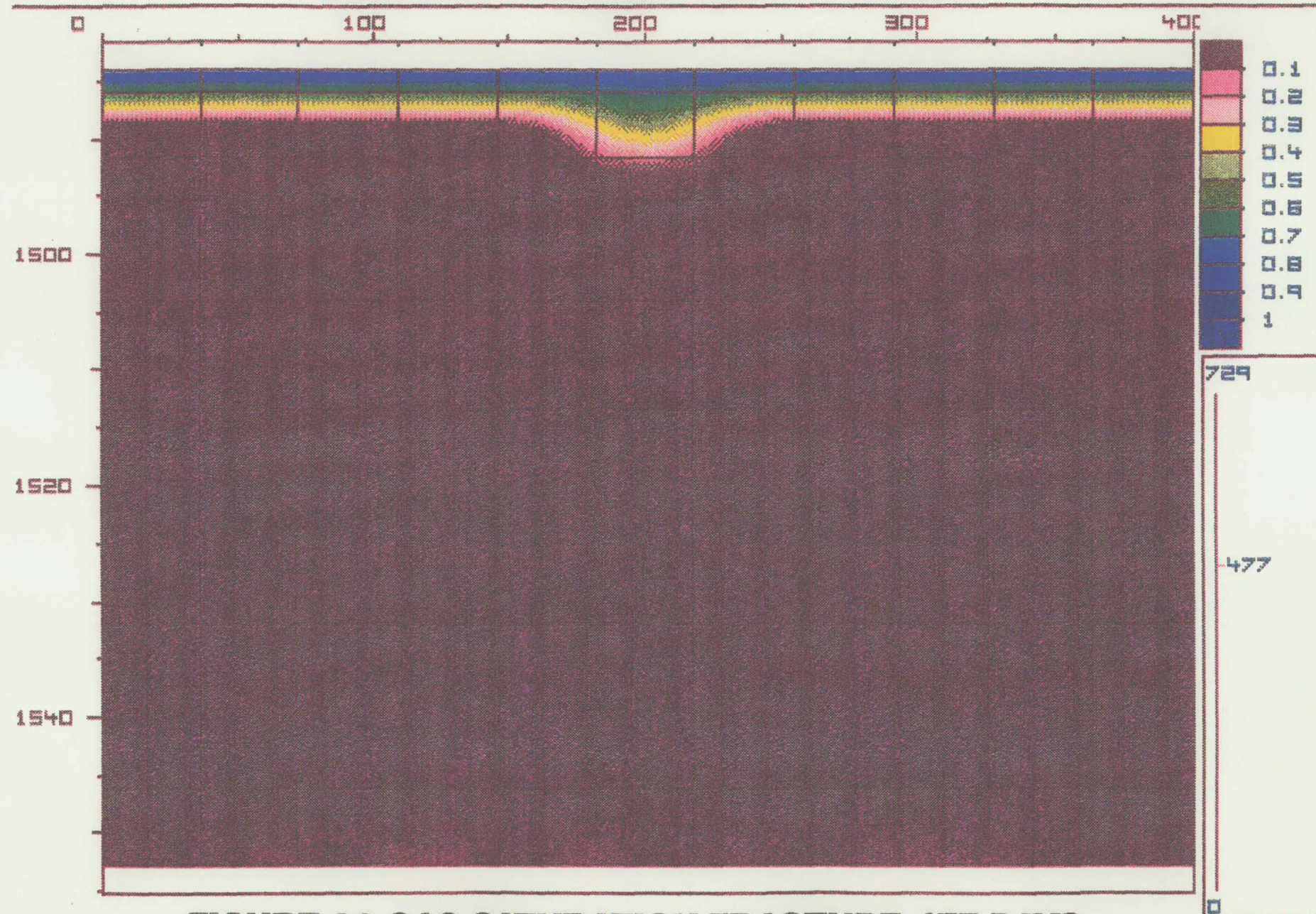


FIGURE 66 GAS SATURATION FRACTURE-477 DAYS

PARAMOUNT CAMERON HORIZONTAL WELL

HOR3

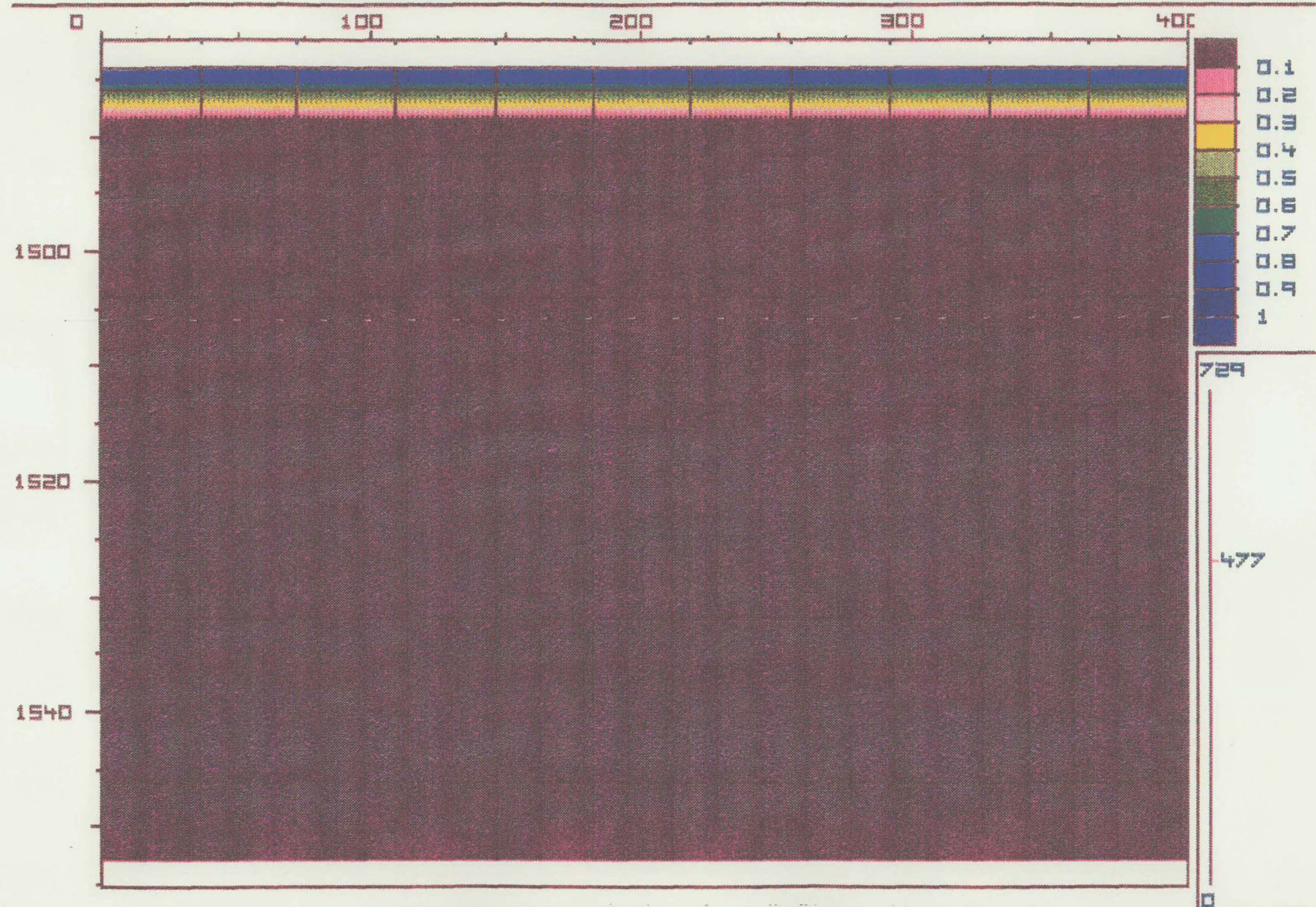


FIGURE 67 GAS SATURATION FRACTURE-477 DAYS

PARAMOUNT CAMERON HORIZONTAL WELL

HOR2

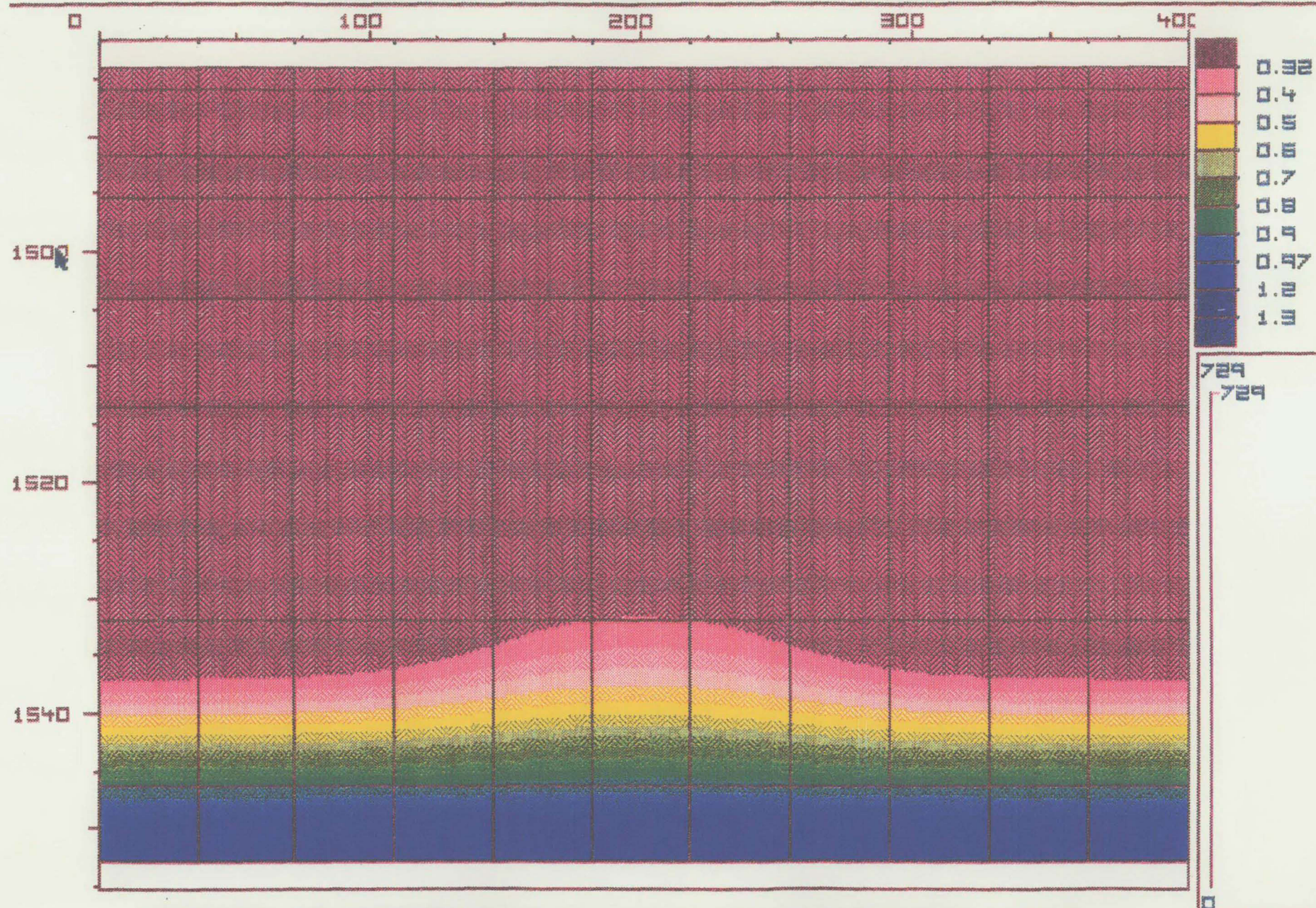


FIGURE 68 WATER SATURATION FRACTURE-729 DAYS

PARAMOUNT CAMERON HORIZONTAL WELL

HOR2

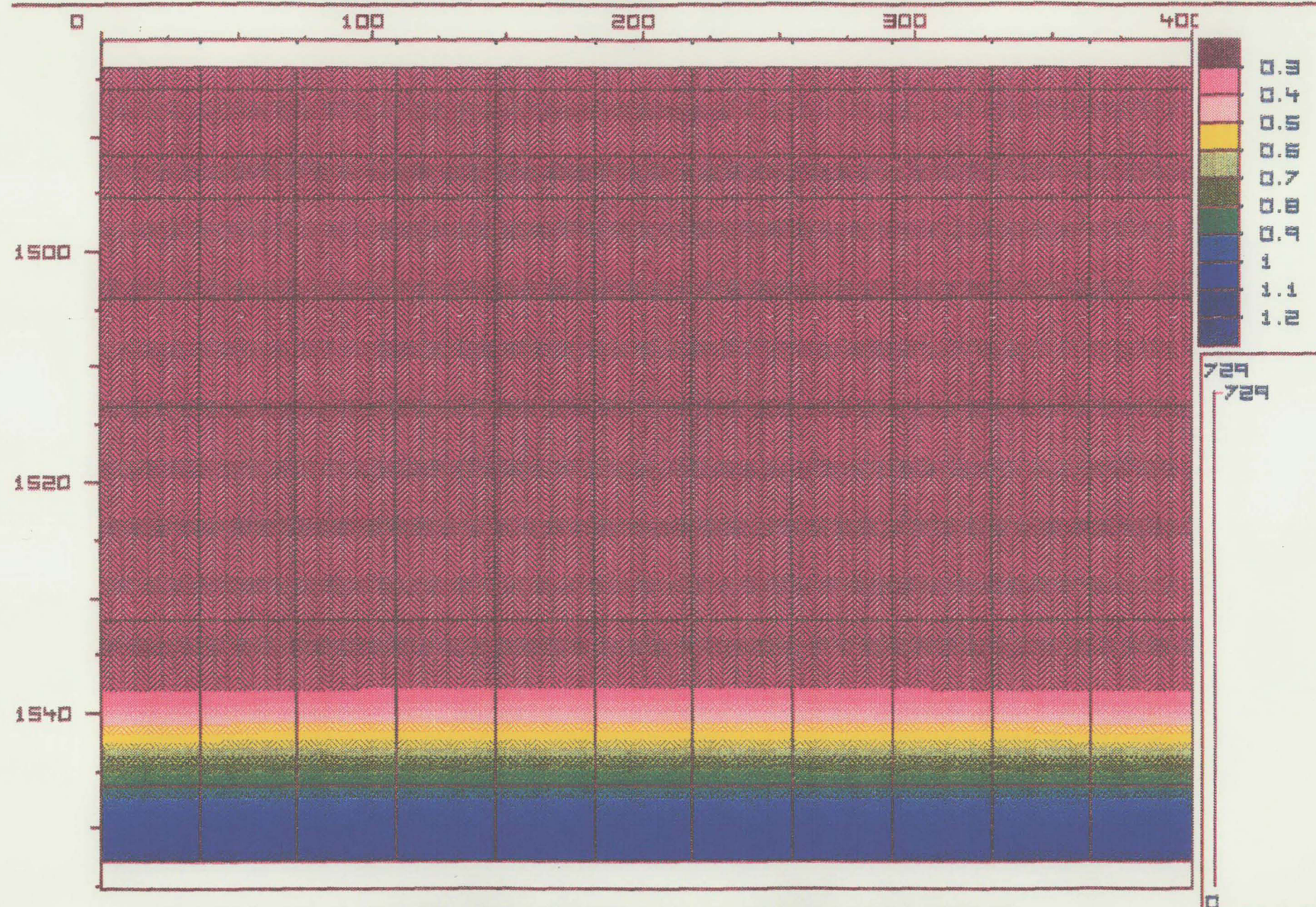


FIGURE 69 WATER SATURATION MATRIX-729 DAYS

PARAMOUNT CAMERON HORIZONTAL WELL

HOR2

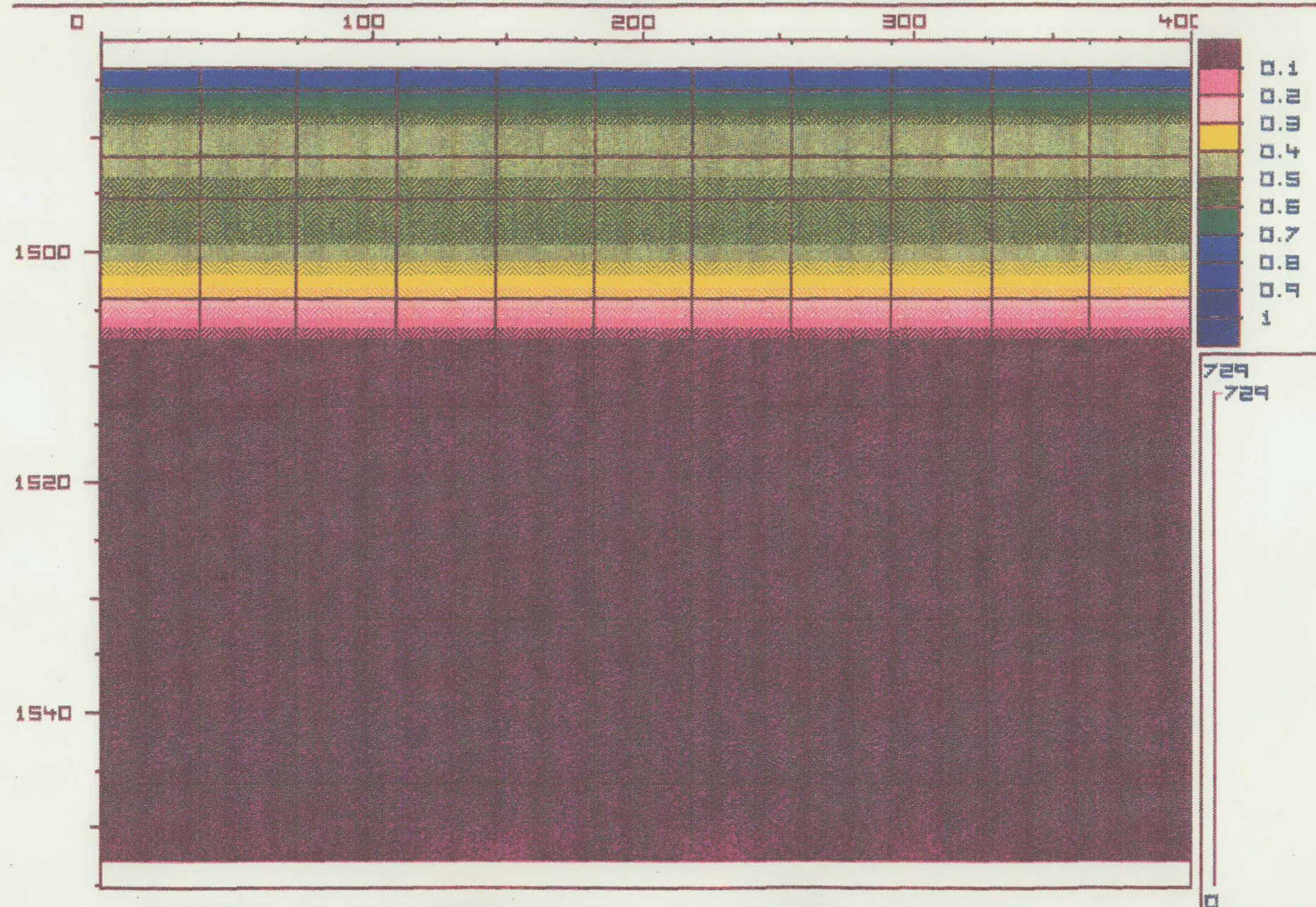


FIGURE 70 GAS SATURATION FRACTURE-729 DAYS

PARAMOUNT CAMERON HORIZONTAL WELL

HOR2

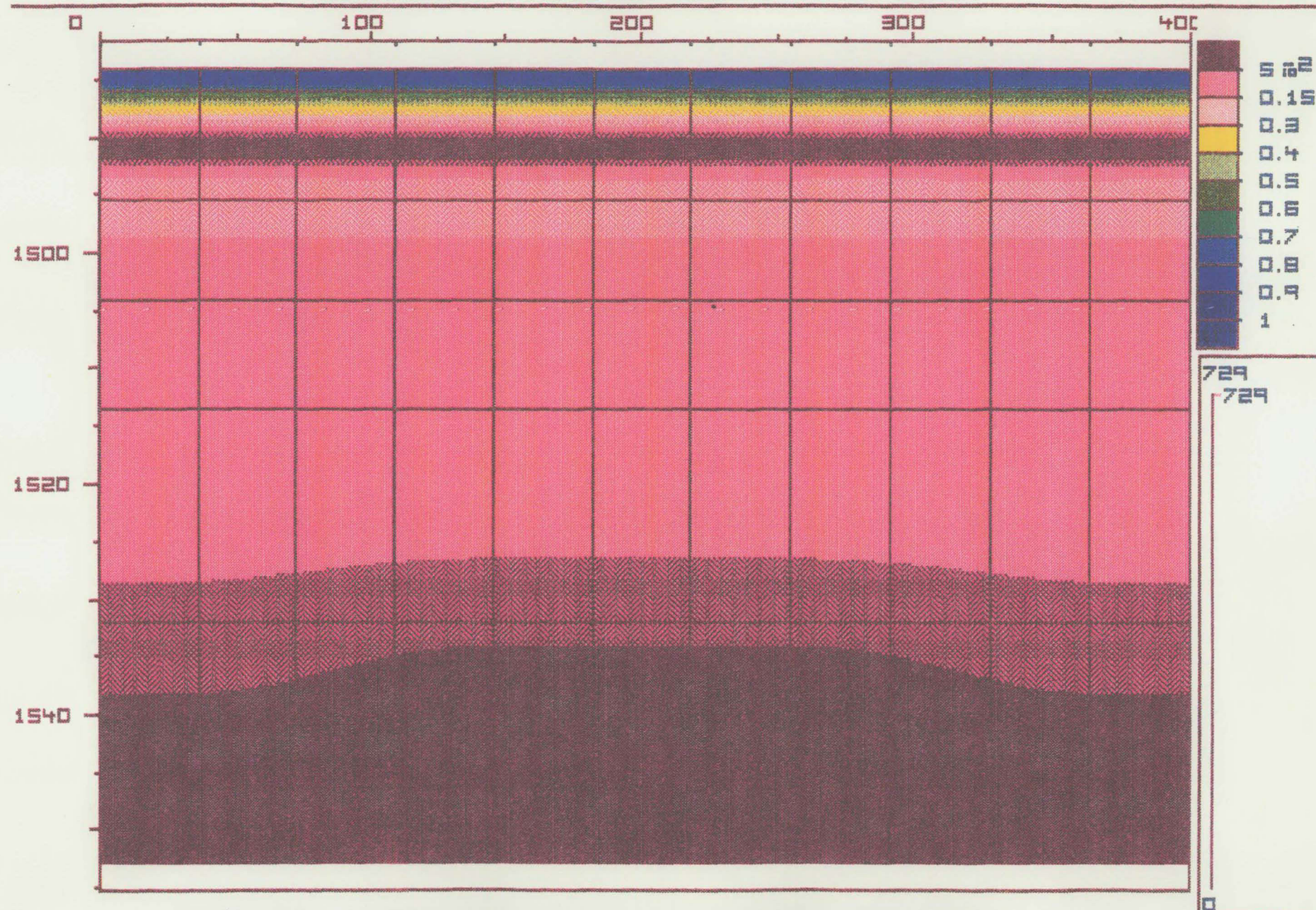


FIGURE 71 GAS SATURATION MATRIX-729 DAYS

PARAMOUNT CAMERON HORIZONTAL WELL

HOR3

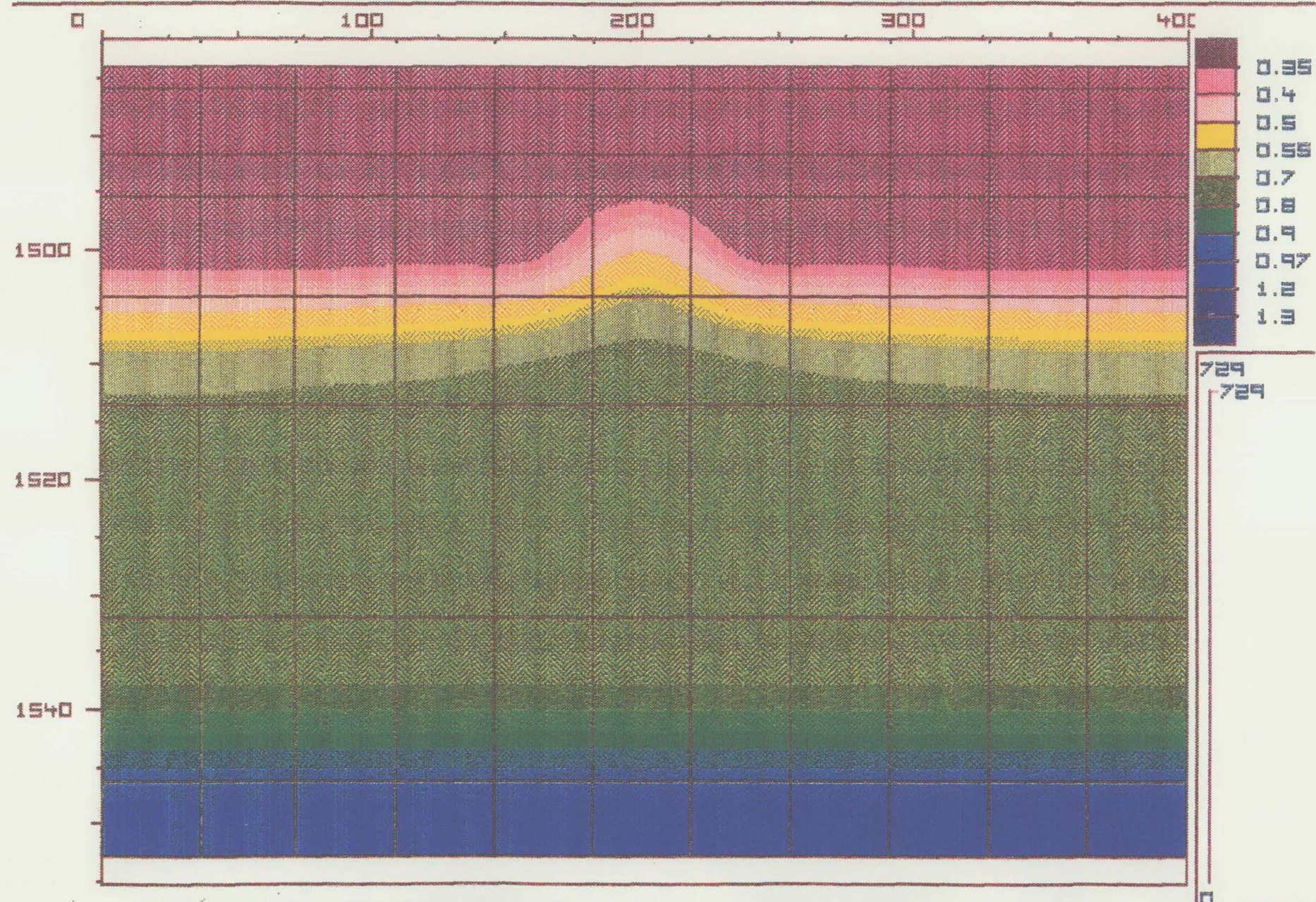


FIGURE 72 WATER SATURATION FRACTURE-729 DAYS

PARAMOUNT CAMERON HORIZONTAL WELL

HOR3

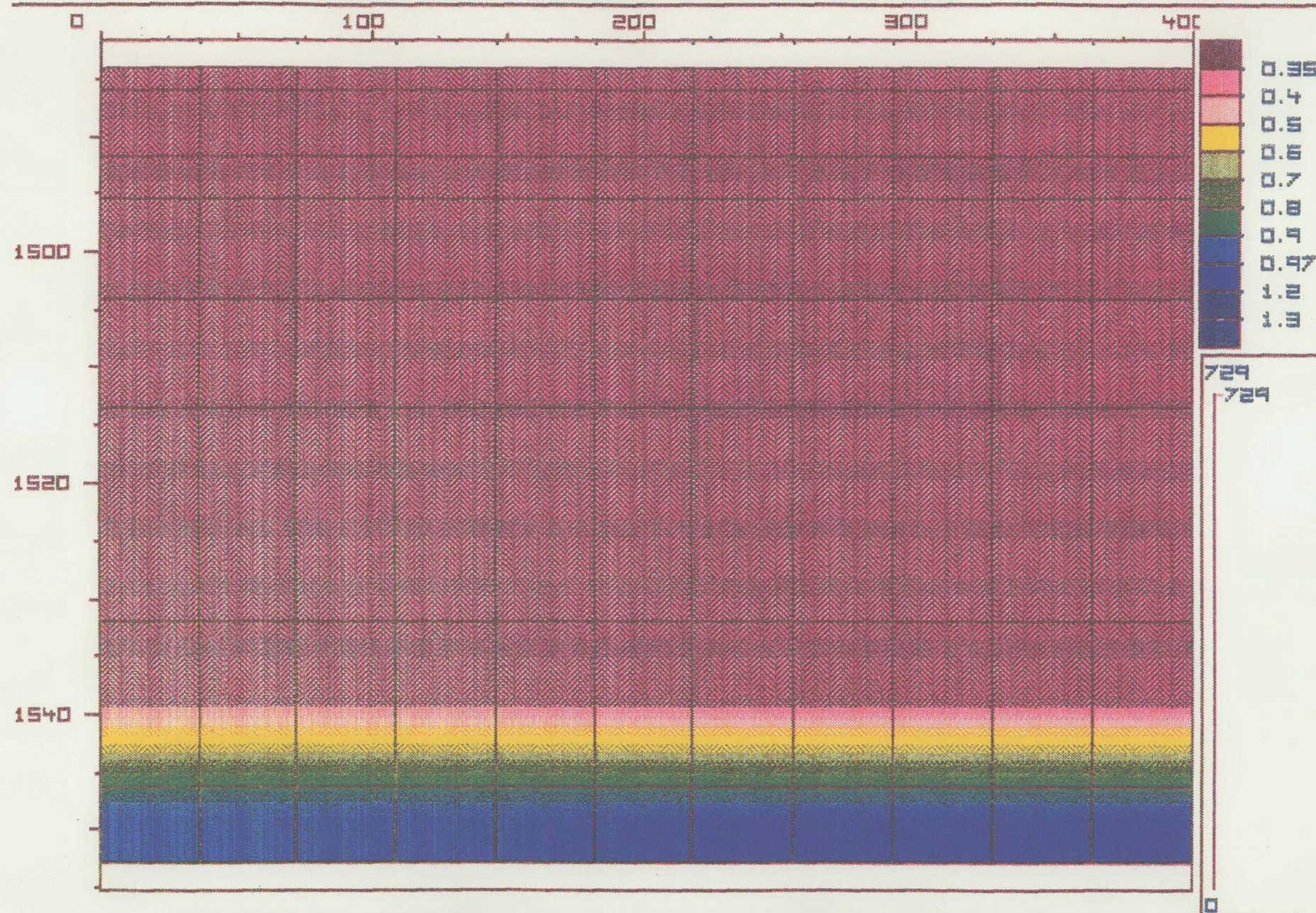


FIGURE 73 WATER SATURATION MATRIX-729 DAYS

PARAMOUNT CAMERON HORIZONTAL WELL

HOR3

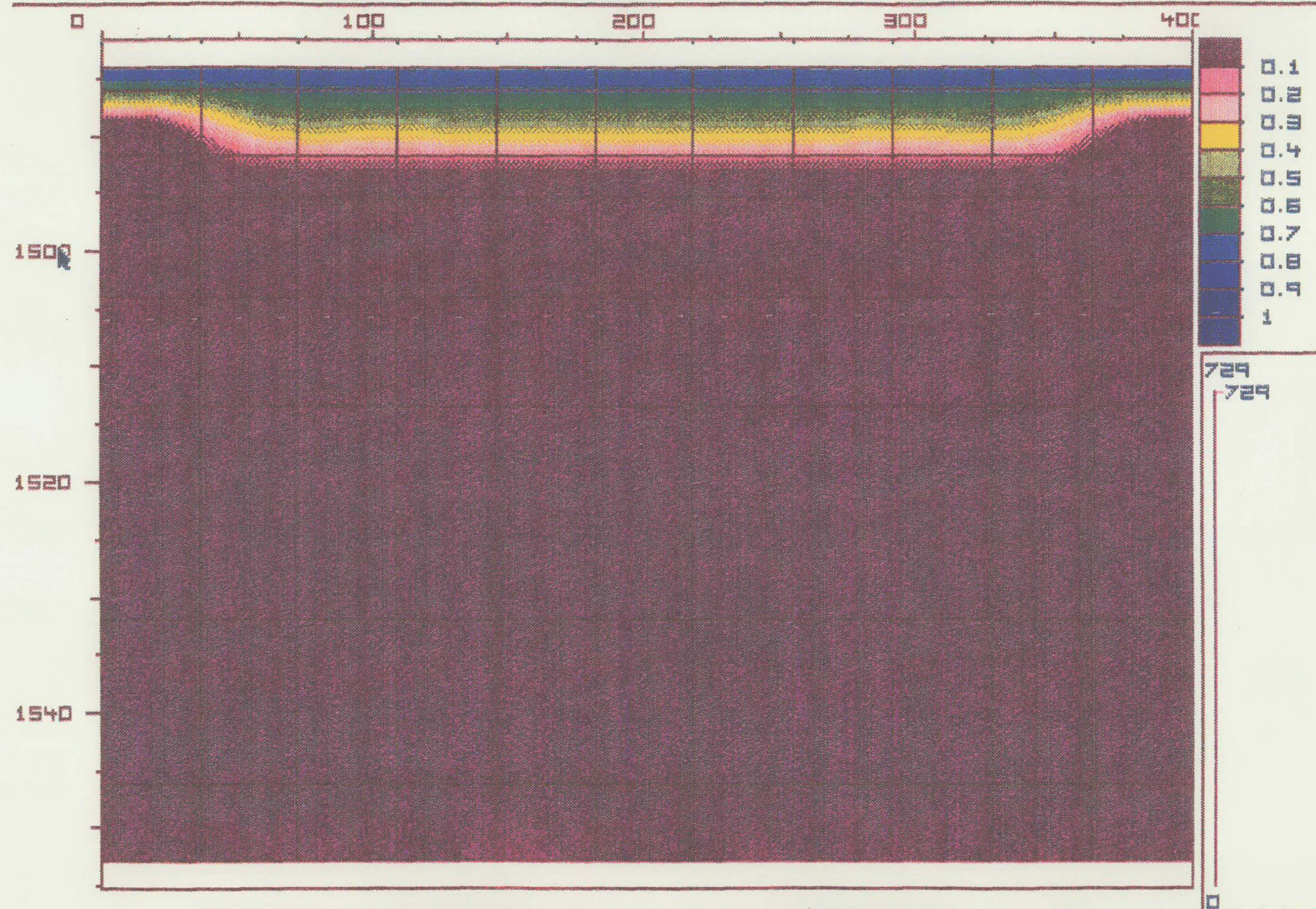


FIGURE 74 GAS SATURATION FRACTURE-729 DAYS

FIGURE 75

COMPARISON OF OIL RATES

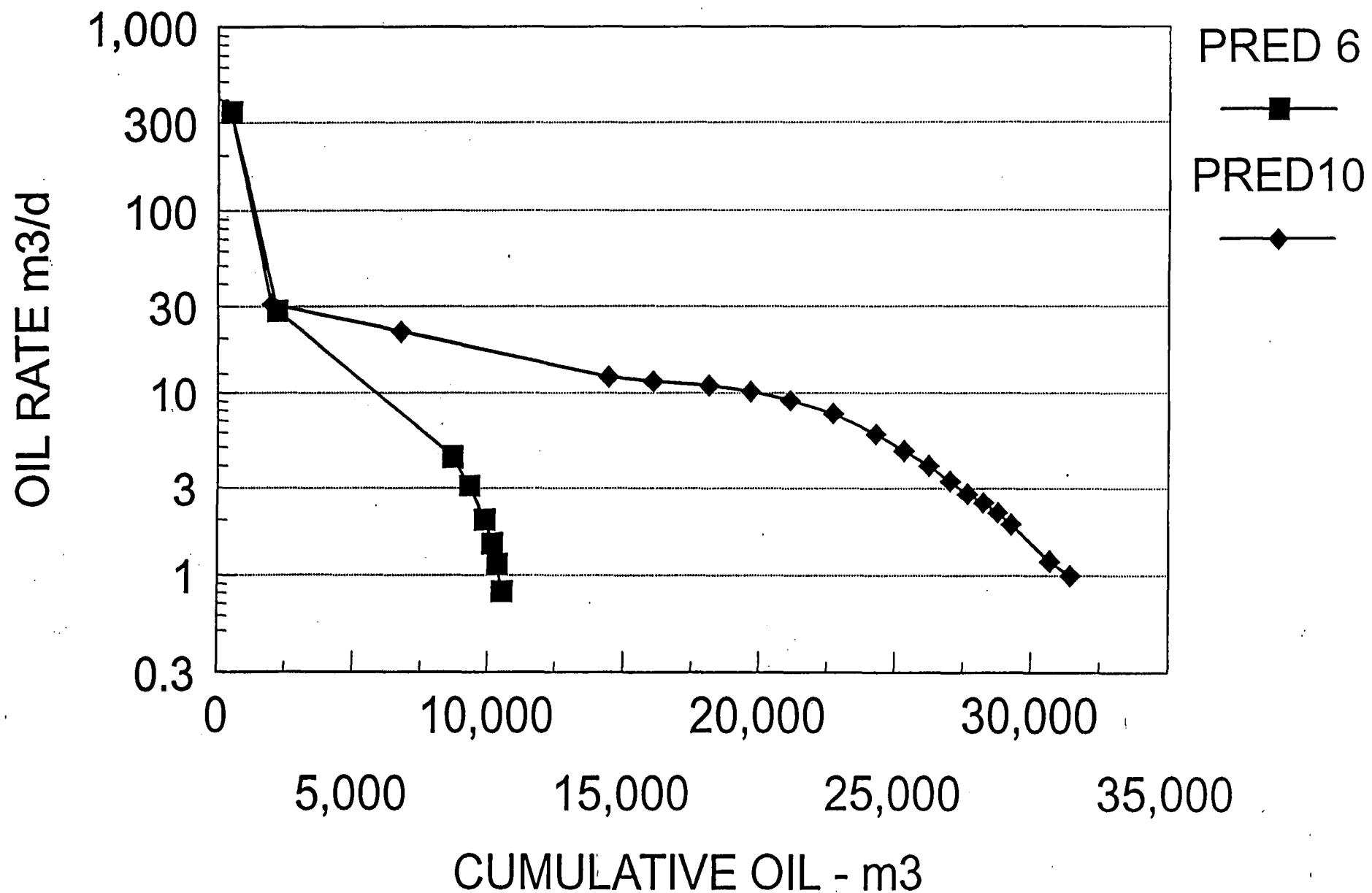
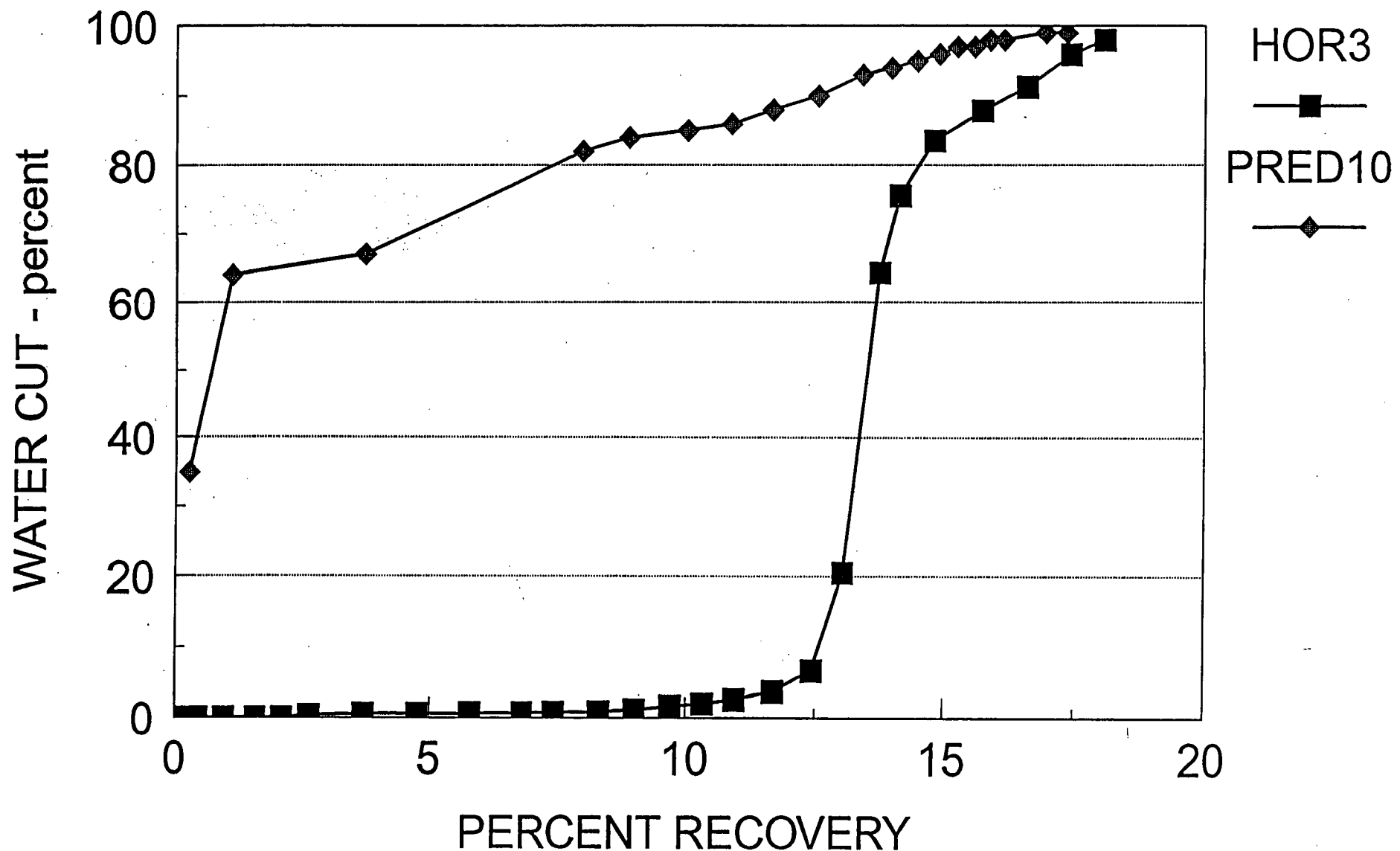


FIGURE 76

COMPARISON OF WATER CUT



COMPARISON OF OIL RATES

